PHENOMENOLOGICAL DUALITY

MASATAKA FUKUGITA
National Laboratory for High Energy Physics,
Tsukuba-gun, Ibaraki-ken, 300-32 Japan

and

KEIJI IGI
Department of Physics, University of Tokyo,
Tokyo, 113 Japan

NORTH-HOLLAND PUBLISHING COMPANY – AMSTERDAM

PHYSICS REPORTS (Section C of Physics Letters) 31, No. 4 (1977) 237–338. NORTH-HOLLAND PUBLISHING COMPANY

PHENOMENOLOGICAL DUALITY

MASATAKA FUKUGITA

National Laboratory for High Energy Physics, Tsukuba-gun, Ibaraki-ken, 300-32 Japan

and

KEIJI IGI*

Department of Physics, University of Tokyo, Tokyo, 113 Japan

Received September 1976

Contents:

Single orders for this issue

PHYSICS REPORTS (Section C of PHYSICS LETTERS) 31, No. 4 (1977) 237–338.

Copies of this issue may be obtained at the price given below. All orders should be sent directly to the Publisher. Orders must be accompanied by check.

Single issue price Dfl. 38.00, postage included.

*On sabbatical leave at Brookhaven National Laboratory and Fermi National Accelerator Laboratory.

1. Introduction

1.1. Duality in strong interaction

The purpose of this report is to discuss duality in strong interaction physics from the phenomenological view point.

Since the success of finite-energy sum rules (FESR) in two-body reactions the belief has been gaining ground that there exists a certain relation between two ways of describing scattering amplitude: the Regge-pole exchange at high energy and resonance dominance at low energy. The two descriptions appear to be quite different. Namely, the former corresponds to t-channel poles, while the latter corresponds to s-channel poles. The FESR tells us that these two descriptions are not independent but alternative expressions for the same amplitude. This leads to an interlocking of two descriptions generally called *duality*.

Duality can be regarded as a kind of bootstrap scheme for hadrons. This bootstrap is manageable due to its linear character, in contrast to the non-linear bootstrap dynamics (the N/D method) based on analyticity and unitarity. The old N/D method relies much on elastic unitarity which becomes useless with increasing energies, and it requires many-channel calculations inevitably. The new bootstrap scheme, however, closes within a single reaction by relating its direct and crossed channels.

The duality scheme produces very fruitful results when it is combined with the internal symmetry of hadron dynamics. One of the most important among them is the exchange degeneracy of Regge poles, which leads to qualitative understanding of hadron spectra as well as of high-energy phenomena. The exchange degeneracy correlates several multiplets of the internal symmetry. It leads, in particular, to the nonet scheme of the quark model when applied to mesons. Moreover, the scattering amplitude exhibiting duality can be expressed in terms of the rearrangement of quarks (duality diagram).

A solution of the duality bootstrap can be obtained in a compact form for meson–meson scattering within a certain approximation and it is known as the Veneziano model. The statement of duality is most explicit therein; an infinite sum of s-channel poles is equivalent to an infinite sum of t-channel poles.

Through the extension of the Veneziano model to an amplitude with any number of external lines (dual resonance model) the mathematical structure of such dual models could be clarified in great detail. In particular it turned out that a dual model has a spectrum such as that produced by an infinite number of harmonic oscillators. An operator formulation of the model then enabled us to decompose the amplitude into propagators and vertices and to calculate the dual amplitude perturbatively. Here the duality diagram appears in a new light as a "Feynman diagram" in the dual resonance model, although a line in the diagram has lost its meaning as a quark. Since the spectrum of the dual resonance model is realized by the oscillation of a finite string, people have reformulated the dual resonance model based on a string picture. In this picture the line of the duality diagram acquires a meaning as the end of the string.

From the phenomenological point of view, the Veneziano model itself is too idealized and it may not be suited to practical applications. The simple Veneziano model for meson systems, however, possesses many attractive properties, and it gives us many hints as to the properties of meson–baryon scattering, for which the construction of such a simple model meets difficulties due to the spin complexity (e.g., parity-doubling problem). Thus the Veneziano model furnishes a guide to our understanding of hadronic reactions.

Phenomenologically, duality is an approximate concept, based on a simple Regge expression at high energies and resonance saturation at low energies. The t-channel description in terms of several Regge poles often fails in explaining high-energy phenomena for $t < 0$, implying the necessity of Regge cuts for $t < 0$. Nevertheless the interlocking of the s-channel and the t-channel poles may persist to hold for $t > 0$ where the contributions of poles are expected to dominate. For $t < 0$, we can still see remnants of the pole–pole interlocking even in the presence of Regge cuts.

Furthermore duality enables us to take an alternative approach to give high-energy amplitudes in the circumstance of our ignorance of the prescription of Regge cuts: We can obtain a satisfactory description by employing the knowledge obtained in the direct channel, i.e., by replacing the Regge amplitude with the empirical s-channel (resonant) amplitude.

In this article we attempt to clarify the nature of the strong interaction in the framework of duality in the hope that it provides a coherent view of the hadron physics.

1.2. Outline of this article

As first discussed, the two assumptions of analyticity and asymptotic Regge behaviour for the scattering amplitude has led to finite-energy sum rules (FESR) of the form

$$\frac{1}{N}\int_0^N \mathrm{Im}\ f(\nu,t)\,\mathrm{d}\nu = \sum_i \beta_i \frac{N^{\alpha_i}}{\alpha_i+1}, \tag{1.1}$$

α_i and β_i being Regge parameters. This equation connects low energy amplitudes to high energy parameters (sections 2.1 and 2.2).

If one supplements the FESR with the assumption that the low energy side (left-hand side) of the FESR is saturated by the resonance contribution, eq. (1.1) implies

$$\langle \mathrm{Im}\, f(\mathrm{Res.})\rangle_{\mathrm{Ave}} = \sum \mathrm{Im}\, f(\text{Regge pole}), \tag{1.2}$$

showing that the description of the amplitude in terms of a sum of direct-channel resonances is equivalent to its description in terms of a sum of Regge exchanges in the crossed channel. This relationship is called duality (section 3.1).

When one considers an elastic process, however, one finds a substantial contribution to the low energy side besides that from resonances. This non-resonating background component is assumed to correspond to the pomeron at high energy,

$$\langle \mathrm{Im}\, f(\text{non-res. B. G.})\rangle_{\mathrm{Ave}} = \mathrm{Im}\, f(\text{pomeron}). \tag{1.3}$$

This two-component hypothesis – eqs. (1.2) and (1.3) – will allow us to treat the resonant and diffractive (non-resonating) components separately (section 3.2). In this article we shall concentrate upon the resonant or ordinary-Regge component.

The two-component hypothesis states that if there are no resonances in a certain reaction (e.g., $\pi^+\pi^+ \to \pi^+\pi^+$, $K^+p \to K^+p$; this condition is expected to be satisfied when the direct channel has exotic quantum numbers which cannot be associated with a three quark system if a baryon, or a quark–antiquark system if a meson), the imaginary part of the non-diffractive amplitude should vanish. We are then led to relations among Regge poles exchanged in the crossed channel (exchange degeneracy) (section 3.4),

$$\mathrm{Im}\,[\sum f(\text{Regge poles})] = 0. \tag{1.4}$$

In the case when we have two Regge poles with opposite signatures, we obtain

$$\alpha^{(+)} = \alpha^{(-)}, \qquad \beta^{(+)} = \beta^{(-)}, \tag{1.5}$$

where the superscript (+) or (−) refers to the signatures of the Regge poles. The Regge residue function is also restricted by eq. (1.5), which leads to the form $\beta(t) \sim \alpha(\alpha+1)(\alpha+2)\ldots$ With exchange degeneracy one can now understand several important systematics of two-body scattering at high energy.

In particular, in 0^-0^- scattering, eq. (1.5) reads

$$\alpha(1^-) = \alpha(2^+), \qquad \beta(1^-) = \beta(2^+). \tag{1.6}$$

This exchange degeneracy between vector and tensor mesons requires that they follow a nonet scheme with the ideal mixing (sections 3.4 and 3.5).

As for baryons, the simplest solutions of eq. (1.4) are given by the degeneracy of a $\underline{1} \oplus \underline{8}$ with one signature and an $\underline{8}$ with the opposite signature, and the degeneracy of an $\underline{8} \oplus \underline{10}$ and an $\underline{8}$. Although the realistic baryon spectrum is more complicated, these simple solutions lead us to a qualitative understanding of the SU(3) coupling patterns of observed parent baryon resonances (section 3.5). Furthermore it can be shown that the non-relativistic quark model (spectrum $SU(6) \times O(3)_L$: coupling $SU(6)_W$) is a solution of exchange degeneracy (sections 5.3 and 5.4). Exchange degeneracy in $0^- 1/2^+$ scattering also predicts that the t-channel Reggeon couplings have nonet coupling with a common F/D value for vector and tensor trajectories. The F/D value itself is fixed by the s-channel resonance through eq. (1.2).

One can then understand transparently the duality and symmetry structure of the scattering amplitude by representing a particle in terms of quark lines on the world sheet (duality diagram) (section 3.6). Exchange degeneracy allows only connected diagrams, since it leads to Reggeon couplings in which disconnected diagrams are forbidden (Okubo–Zweig–Iizuka rule). When a planar duality diagram is written for a certain two body reaction (we consider here meson–meson or meson–baryon scattering), the two non-exotic channels of the diagram are dual with respect to each other. Figure 1 shows an example of the s–t dual diagram.

On the other hand, it is impossible to draw a planar duality diagram for baryon–antibaryon scattering with only $q\bar{q}$ intermediate state in each channel; one must have $qq\bar{q}\bar{q}$ in either channel. Namely, one should introduce exotic states to maintain duality for baryon–antibaryon scattering (section 3.7).

If one considers a reaction in which two channels are identical, the FESR gives a linear bootstrap equation. The Veneziano amplitude which we consider next is a crossing symmetric solution of the equation in the narrow-resonance approximation (section 3.8). It has the form

$$V = \frac{\Gamma(-\alpha(s)\,\Gamma(-\alpha(t))}{\Gamma(-\alpha(s) - \alpha(t))}, \tag{1.7}$$

with $\alpha(s) = \alpha_0 + \alpha' s$, corresponding to the diagram in fig. 1. Here α' is an important parameter of the model and sets the energy scale for Regge pole asymptotics. This model provides us with an explicit manifestation of the pole–pole duality in its simplest form, viz.,

$$V = \sum \frac{R_n(t)}{n - \alpha(s)} = \sum \frac{R_n(s)}{n - \alpha(t)}, \tag{1.8}$$

exhibiting that the amplitude can be written either as a sum of s-channel poles or as a sum of

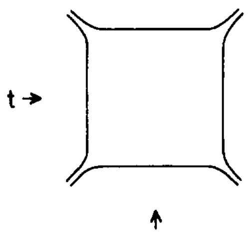

Fig. 1.

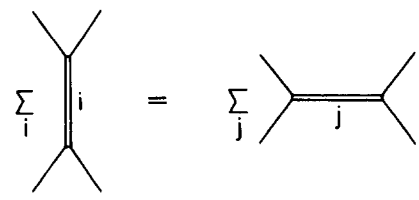

Fig. 2.

t-channel poles (fig. 2). This property clearly differs from conventional field theory, in which the t-channel poles should be added to the s-channel poles. The situation in the case of the dual model originates from the fact that the sum (1.8) is an infinite sum, i.e., a t-channel pole comes from the divergence of the infinite sum of s-channel poles and vice versa (section 3.8).

It is to be noted in eq. (1.7) that the double pole at the convergence of the two poles at $\alpha(s) = n$ and $\alpha(t) = m$ is avoided by the zero at $\alpha(s) + \alpha(t) = n + m$. This zero propagates into the physical region and produces dips in the angular distribution of cross-sections (section 5.1) which are characteristic of the dual model.

The Veneziano model is still plagued with several difficulties and it is far from a realistic theory of strong interactions. However, it is endowed with many desirable features in addition to its mathematical simplicity.

One of the fascinating properties of the Veneziano model is that it can readily be generalized to the N-point dual amplitude. The factorization property of multi-particle dual amplitude requires that pole–pole duality should hold not only for particle–particle scattering but also for particle–Reggeon or Reggeon–Reggeon scattering. Inclusive reactions have opened up the possibility of examining such duality properties through studies in a specific kinematical region (section 3.9). One can also study duality for scattering with pomeron as external lines. It presents us with an interesting problem on the nature of the pomeron and the role of twisted dual loops.

Regge–pole resonance duality, in the form we have presented it, is an idealized approximation of nature. Although the scheme enables us to grasp the global characteristics of two-body reactions, analyses of high energy data reveal that in some cases the high energy amplitude with a few Regge poles does not necessarily give a satisfactory description for $t < 0$ and that other J-plane singularities – possibly Regge cuts are necessary (section 4.1). In the presence of Regge cuts eq. (1.2) should be modified to

$$\langle \mathrm{Im}\, f(\mathrm{Res.})\rangle \simeq \sum \mathrm{Im}\, f(\text{Regge pole} + \text{possible cut}). \tag{1.9}$$

Although we have no correct prescription for the Regge cuts yet,† eq. (1.9) gives an important constraint on the scattering amplitude. Assuming eq. (1.9) in a semi-local form, one can construct a resonance model at high energies as an alternative to the t-channel description. We know empirically in $0^-1/2^+$ scattering that the imaginary part of the non-diffractive amplitude is dominated by peripheral partial waves centred at the impact parameter $b \approx 1$ fm (section 4.2). One can then readily understand this peripherality in the s-channel language by assuming that resonances with spin $l_R \approx m_R$ dominate, not only at low energy, but also at high energy (section 4.3). If the Regge pole amplitude has an imaginary part with dominant peripheral partial waves, Regge cut corrections

†The prescriptions of the Regge cut, proposed so far, have turned out to be inadequate (section 4.2).

should be small. But it does not always have a peripheral imaginary part and then it has to be corrected by a possible Regge cut. In such cases it is more convenient to use the s-channel picture to describe high energy phenomena (sections 4.3–4.5). Furthermore, the resonance model throws light on the mechanism of the reaction with an exotic crossed channel (section 4.6).

Duality does not say much directly about the diffractive component, the pomeron. The pomeron is usually understood as an inelastic shadow effect of multiparticle reactions. The duality idea, however, tells us what summation of the multiparticle states in the unitarity equation leads to the pomeron. In this article we only refer to the basic ideas of such attempts (section 5.6).

We have as yet no theory of the strong interactions, even at the level of weak-interaction theory. In this circumstance the present duality idea, although it is still underdeveloped and incomplete as a theoretical framework, provides us with a guide to future theories and at the same time gives us a grasp on the systematics of the enormous accumulation of experimental data.

2. Finite-energy sum rules (FESR)

2.1. Motivation for FESR

The idea of Regge pole was introduced to particle physics to systematize the description of high energy scattering as well as of hadron spectra in terms of Regge trajectories [113, 114, 115, 74, 203, 233].

The Regge pole hypothesis predicts that differential cross-sections have forward (backward) peaks at high energy if the t- (u-) channel of the reaction can communicate with observed resonances. A number of two-body scattering phenomena have been explained successfully in terms of several Regge poles [334, 407; see 40 and 299 for reviews].

Conventional Regge fits, however, were far from reliable, even if they explained the high energy $d\sigma/dt$ data. There were some ambiguities in the Regge-residue function due to the following facts:
(i) The sign of the residue function cannot often be determined.
(ii) Two independent amplitudes are involved due to the baryon spin and each amplitude has often more than one Regge-pole contribution. In order that the Regge fit obtains a full credit, additional restrictions on the amplitude were needed to resolve the ambiguities.

One of the powerful constraints on high-energy analyses is a sum rule which restricts Regge parameters in terms of low energy data by the use of fixed-momentum transfer dispersion relations and Regge asymptotic behaviours [275]. A motivation to obtain the sum rule was to check if there exists additional J-plane singularities with the vacuum quantum number except for the Pomeranchuk Regge pole, P. Under the assumption that there are no singularities with a real part between 1 and 0 in the J plane except for the P, we were led to the following sum rule for crossing-even amplitude of πN scattering,

$$(1+\mu/M)a^{(+)} = -\frac{f^2}{M}\frac{1}{1-(\mu/2M)^2} + \frac{1}{2\pi^2}\int_0^\infty dk'\,[\sigma_{\rm tot}^{(+)}(k') - \sigma_{\rm tot}^{(+)}(\infty)]$$

namely,

$$(1+\mu/M)a^{(+)} = -\frac{f^2}{M}\frac{1}{1-(\mu/2M)^2} + \frac{1}{2\pi^2}\int_0^N dk'\,[\sigma_{\rm tot}^{(+)}(k') - \sigma_{\rm tot}^{(+)}(\infty)] - \frac{\beta N^\alpha}{\alpha}. \tag{2.1}$$

Here $a^{(+)}$ is the s-wave scattering length of the crossing-even amplitude and α is a hypothetical secondary Regge trajectory ($\alpha < 0$) with residue β. This is the sum rule which correlates high-energy parameters with low-energy quantities, a kind of the so-called finite-energy sum rule (FESR). The consistency test of eq. (2.1) led us to the prediction of the second Pomeranchuk pole, P′ with $\alpha_{P'}(0) \approx 0.5$. (Later the f meson was found on the P′ trajectory.) Therefore, it was recognized that the FESR gives a powerful constraint on the Regge parameters in terms of low energy data.

We do not mention details of the Regge pole theory in the present report. We refer the reader to the other review articles [e.g., 67, 131, 130, 241].

2.2. Standard formula for FESR

The FESR can now be derived in the following way [280, 335, 163, 164]. Let us consider two-body scattering amplitude as a function of $\nu = (s - u)/4M$ and t.

Superconvergent relations

De Alfaro, Fubini, Rossetti and Furlan [148] observed that if an amplitude $F(\nu,t)$ satisfies a dispersion relation

$$F(\nu,t) = \frac{1}{\pi} \int_{-\infty}^{\infty} \mathrm{d}\nu' \, \frac{\mathrm{Im}\, F(\nu',t)}{\nu' - \nu} \tag{2.2}$$

and moreover, if $F(\nu,t)$ falls off faster than $1/\nu$ as $\nu \to \infty$, then it must be true that

$$\int_{-\infty}^{\infty} \mathrm{d}\nu \, \mathrm{Im}\, F(\nu,t) = 0. \tag{2.3}$$

This is called the superconvergent relation (SCR). If $F(\nu,t)$ is crossing odd in ν, eq. (2.3) reduces to

$$\int_{0}^{\infty} \mathrm{d}\nu \, \mathrm{Im}\, F(\nu,t) = 0. \tag{2.4}$$

FESR

As an illustration to derive FESR, let us consider a crossing-odd amplitude $f(\nu,t)$. Suppose that $f(\nu,t)$ is not superconvergent by itself, but we know its asymptotic form which is given by a sum of Regge poles,

$$f(\nu,t) \simeq \sum_i \beta_i(t) \, \frac{1 - \exp\{-\mathrm{i}\pi\alpha_i(t)\}}{\sin \pi\alpha_i(t)} \, \nu^{\alpha_i(t)} \tag{2.5}$$

for $\nu \geq N$ (N is sufficiently large). We can always define a superconvergent amplitude by subtracting the Regge poles as, $F(\nu,t) \equiv f(\nu,t) - \Sigma_i$ (Regge poles with $\alpha_i > -1$)†. Then we have

$$0 = \int_{0}^{\infty} \mathrm{d}\nu \, \mathrm{Im}\, F(\nu,t) = \int_{0}^{\infty} \mathrm{d}\nu \left[\mathrm{Im}\, f(\nu,t) - \sum_{\alpha_i > -1} \beta_i(t) \nu^{\alpha_i(t)} \right]$$

†If there is a pole at $\alpha_i = -1$, one can define them by taking the limit $\alpha_i \to -1$ after integration.

$$= \int_0^N d\nu \left[\mathrm{Im}\, f(\nu,t) - \sum_{\alpha_i > -1} \beta_i(t) \nu^{\alpha_i(t)} \right] + \int_N^\infty d\nu \sum_{\alpha_i < -1} \beta_i(t) \nu^{\alpha_i(t)}. \tag{2.6}$$

Notice that all integrals are now convergent. After the integration we obtain the FESR:

$$\int_0^N d\nu\, \mathrm{Im}\, f(\nu,t) = \sum_{\text{all } i} \beta_i(t) \frac{N^{\alpha_i(t)+1}}{\alpha_i(t)+1}. \tag{2.7}$$

(Note that all Regge terms enter in the same form, regardless of whether α happens to be above or below -1.) Similarly we can derive higher moment FESR as,

$$\int_0^N d\nu\, \nu^n \mathrm{Im}\, f(\nu,t) = \sum_i \beta_i(t) \frac{N^{\alpha_i(t)+n+1}}{\alpha_i(t)+n+1} \tag{2.8}$$

for *even* positive integer n, since $\nu^n f(\nu,t)$ is also crossing odd.

When the amplitude $f(\nu,t)$ is crossing even, eq. (2.8) also holds for *odd* positive integer n. One should work with the even- and the odd-moment sum rules according to whether the amplitude is crossing odd or even.

We can also derive negative-integer-moment FESR. However, the only significant FESR is a one for $f^{(+)}(\nu)/\nu$ corresponding to $n = -1$. All other cases reduce to conventional dispersion relations with subtractions. Given the crossing-even amplitude $f^{(+)}$ for πN scattering, let us define $F^{(+)}$ by $F^{(+)}(\nu) \equiv f^{(+)}(\nu) - \Sigma_i$ (Regge poles with the vacuum quantum number with $\alpha_i \geqslant 0$, say, P and P′). Then $F^{(+)}(\nu)/\nu$ is crossing odd and superconvergent, and we obtain

$$0 = F^{(+)}(0) - \frac{g_r^2}{4\pi} \frac{1}{M} - \frac{2}{\pi} \int_\mu^\infty d\nu \frac{\mathrm{Im}\, F^{(+)}(\nu)}{\nu}. \tag{2.9}$$

This relation is the sum rule [275] mentioned in section 2.1, which was used for deducing the P′ pole.

There is another derivation [464] of the FESR which starts from the Froissart-Gribov representation of the t-channel partial waves,

$$F_l(t) = \frac{1+(-1)^l}{2} a_l^+(t) + \frac{1-(-1)^l}{2} a_l^-(t), \tag{2.10}$$

$$a_l^\pm(t) = \frac{1}{\pi} \int_{z_0}^\infty dz_t A^\pm(z_t,t) Q_l(z_t) \tag{2.11}$$

with $A^\pm = \mathrm{Im}_s F \pm \mathrm{Im}_u F$. Here we have assumed $F(s,t) < O(1/s^N)$. Then $a_l^\pm(t)$ has fixed poles at $l = -1, -2, \ldots$ arising from $Q_l(z) \sim \pi \cot \pi l P_{-l-1}(z)$ in eq. (2.11), unless the residues vanish. Such poles must not be present in $a_l^\pm(t)$ at right-signature points, since otherwise they would conflict with the unitarity condition analytically continued in the angular-momentum plane. By equating to zero the corresponding residues, we get the SCR

$$\int^\infty \nu^n A^\pm(\nu,t)\, d\nu = 0 \tag{2.12}$$

for $n = 0,1,2, \ldots, (N-1)$, where the sign takes $(+)$ for n odd and $(-)$ for n even. This leads to the FESR eq. (2.8), following the previous procedure.

On the other hand, at the wrong-signature points $a_l^{\pm}$ could have fixed poles, so that the right-hand side of eq. (2.12) could include residues of wrong-signature fixed poles. When this wrong-signature fixed poles could be neglected,† eq. (2.12) holds for *arbitrary* positive integers. Then we have eq. (2.8) for any *arbitrary* positive integer [464].

FESR with continuous moment

The FESR can be generalized in the following way [333, 393]. Let us define $F(\nu,t) \equiv f(\nu,t)\,(\nu_0^2 - \nu^2)^{\gamma/2}$ where γ is a continuous real parameter (here ν_0 is a threshold value of ν). Then $F(\nu,t)$ is crossing odd in ν if $f(\nu,t)$ is. The factor $(\nu_0^2 - \nu^2)^{\gamma/2}$ is even in ν, and is real and positive for $-\nu_0 < \nu < \nu_0$, and has the phase $\exp(-i\pi\gamma/2)$ just above the cut for $|\nu| > \nu_0$. Using the same technique as before, we obtain a continuous family of sum rules, dropping terms of $O(\nu_0/N)^2$,

$$\int_0^N d\nu\,(\nu^2 - \nu_0^2)^{\gamma/2}\left[\cos\frac{\pi\gamma}{2}\,\mathrm{Im}\,f(\nu,t) - \sin\frac{\pi\gamma}{2}\,\mathrm{Re}\,f(\nu,t)\right]$$

$$= \sum_i \beta_i(t)\,\frac{N^{\alpha_i(t)+\gamma+1}}{\alpha_i(t)+\gamma+1}\left[\cos\frac{\pi}{2}(\alpha_i(t)+\gamma)/\cos\frac{\pi}{2}\alpha_i(t)\right]. \tag{2.13}$$

This is often called the continuous-moment sum rule (CMSR).

When γ is equal to an odd integer, the integral on the left-hand side involves the real part of amplitude $f(\nu,t)$ and the right-hand side includes $\mathrm{Re}\,f(N,t)$, while when γ is an even integer we recover the integer-moment FESR. The use of FESR with continuous moment makes a full use of informations of low-energy data in principle.

If we replace $(\nu_0^2 - \nu^2)^{\gamma/2}$ by an appropriate analytic function, we can obtain a FESR which emphasizes such specific energy regions that have reliable informations of low-energy data. This is called an optimized FESR [180].

2.3. *Application of FESR*

The FESR relates the low-energy data to the high-energy parameters expressed in terms of Regge poles. Thus the FESR gives fruitful constraints on Regge parameters.

A straightforward application of FESR is made at $t = 0$. One can use the total cross-section σ_{tot} to estimate the integrand on the left-hand side and choose the value N sufficiently large such as e.g., $p_N = 5$ GeV/c at which energy σ_{tot} already shows the Regge behaviour (p_N is a laboratory momentum corresponding to the value N). The FESR can be used as a quantitative restriction to determine precise Regge parameters [280, 335].

More fruitful results are obtained when FESR is applied to $t < 0$, [163, 164; for a review, see 299]. A big advantage of FESR is that it relates directly to a particular amplitude itself (helicity-flip or -nonflip) rather than to a quadratic function of amplitudes, as in the case of scattering data.‡ Therefore, the FESR gives a powerful constraint to the Regge-pole analysis. In order to estimate Im f on

†The dip at the wrong-signature point of the ρ trajectory ($t \simeq -0.6$ (GeV/c)^2) in πN charge-exchange scattering is regarded as an evidence for the absence of the wrong-signature fixed pole.

‡Using only the differential cross-section and polarization data, we cannot determine the amplitude even if we assume the Regge phase [144].

the left-hand side of FESR, one must rely either on the resonance-dominance approximation or on phase-shift solutions. We cannot take the cut-off N at sufficiently large value in this case. The resonance-dominance approximation is valid only when the value p_N does not exceed 2 GeV/c. In the case of phase-shift solutions, the value p_N is also limited to at most 2 GeV/c. Although the FESR, evaluated using such a low cut-off value, is less reliable, it gives qualitative or even semi-quantitative restriction on high-energy amplitudes. It is an important question where the Regge behaviour begins. The exotic reaction such as K^+p seems to be Regge behaved down to $p_L \simeq 1$ GeV/c. The amplitudes such as $B^{(-)}(\pi N)$ or $A'^{(+)}(\pi N)$, where all prominent resonances enter with the same sign adding up constructively, show fairly regular behaviours already for $p_L = 1 \sim 1.5$ GeV/c particularly as the t-dependence is concerned.

In such a case, one can safely take low values for p_N.† On the contrary, for amplitudes like $A'^{(-)}(\pi N)$ or $B^{(+)}(\pi N)$, where resonances contribute with alternating signs and tend to cancel, we have to take a high cut-off value because of large fluctuation. Otherwise, the results could include large errors.‡ One must pay much attention in the estimation of errors due to the cut-off value N (or p_N) in the FESR analysis.

Let us consider the application to πN charge-exchange scattering. Using the low-energy data (phase shifts) on the left-hand side of FESR, one obtains the Regge parameters which can reproduce the qualitative feature of high-energy amplitude. Furthermore, one can determine the sign of Regge residue as well as the t-dependence of the residue function which were not uniquely determined from the high-energy data alone (fig. 3) [163]. The main results are:

(i) $[\nu B^{(-)}/A'^{(-)}]_{t=0} \approx +10$. This explains the dip at $t = 0$ in the forward peak of πN charge-exchange scattering. High-energy analysis gives us

$$[\nu B^{(-)}/A'^{(-)}]_{t=0}$$

$\simeq$ 9.5 (Arbab and Chiu [15]: ρ-Regge pole)
$\simeq$ 10.8 (Höhler, Baacke and Eisenbeiss [262]: ρ-Regge pole)
$\simeq$ +11.5 (Halzen and Michael [239]: amplitude analysis)
$\simeq$ +14 (Cozzika et al. [134]: amplitude analysis).

(ii) Im $A'^{(-)}$ has a zero* at $t \simeq -0.2$ (GeV/c)^2. This is the so-called cross-over zero which has been expected from the cross-over phenomenon in π^-p and π^+p elastic scattering.

(iii) Im $B^{(-)}$ has a nonsense zero* at $t \simeq -0.5$ (GeV/c)^2. This zero together with the property (i) explains the famous dip at $t \simeq -0.5$ (GeV/c)^2 observed in the angular distribution of πN charge-exchange. Im $B^{(-)} \approx -$Im $A^{(-)}/\nu$ has also zeros at $t \simeq -1.5$ and -2.5 (GeV/c)^2, [178].§ This supports the residue function to be of the form, $\beta \sim \alpha(\alpha+1)(\alpha+2)\ldots \sim 1/\Gamma(\alpha)$.¶

One can also determine a t-channel trajectory, using the FESR with two different moments as

$$\frac{S_n}{S_m} = \frac{1}{N^n}\int_0^N \nu^n \,\mathrm{Im}\, f(\nu,t)\,\mathrm{d}\nu \Big/ \frac{1}{N^m}\int_0^N \nu^m \,\mathrm{Im}\, f(\nu,t)\,\mathrm{d}\nu = \frac{\alpha(t)+m+1}{\alpha(t)+n+1}. \tag{2.14}$$

†In a kind of resonance model such as the Veneziano (B_4) model, the left-hand-side integral with low cut-off value (including only one or two resonances) predicts a high-energy amplitude in a good approximation (see section 3.8). Nature appears to satisfy this property.

‡In an extreme case of the B_4 model, the integral with low cut-off would give an appreciable contribution on the left-hand side of integral even when the imaginary part of high-energy amplitude is to vanish on the right-hand side (see section 3.8).

* This zero has been verified by the amplitude analysis at $p_L = 6$ GeV/c [239, 134].

§A structure at the second wrong-signature point ($t \simeq -2.5$ (GeV/c)^2) seems to be seen in the $\pi^-p \to \pi^0 n$ angular distributions [85, 86].

¶Dips at $t \simeq -1.5$ (GeV/c)^2 ($\alpha = -1$) and $t \simeq -3.5$ (GeV/c)^2 ($\alpha = -3$) in the $\pi^-p \to \eta n$ angular distributions also support this type of residue function [252, 315].

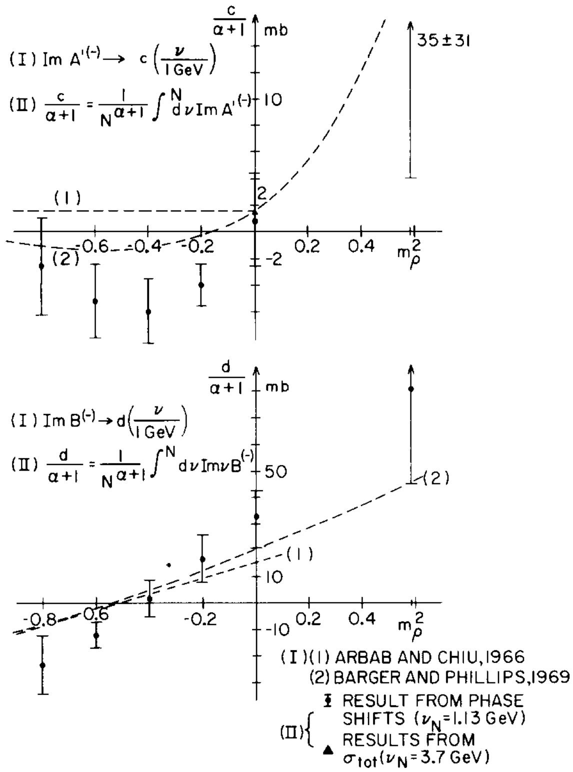

Fig. 3. Regge-residue functions of the ρ exchange from the FESR under the one-pole assumption ($\alpha_\rho = 0.57 + 0.96t$) compared with those from high-energy fits (from Dolen, Horn and Schmid [163]).

The FESR with a continuous moment turns out the most effective method for this purpose. We list the ρ trajectory obtained by various methods in table 1.

An important result, in the analysis of crossing-even amplitude (where the P and the f are exchanged), is $\nu B^{(+)} \simeq A'^{(+)}$† [53]. This implies that that the P and f exchanges are decoupled from $A^{(+)}$ amplitude, as was originally suggested by the dispersion-relation analysis [266]. Actually, the analysis of the $A^{(+)}$ amplitude in terms of CMSR indicates $\alpha_{\mathrm{eff}}(0) \approx -0.5$, [389, 481], which implies the s-channel helicity conservation of the pomeron and f [226, 251, 418, 215, 43]. We also list the P and the f trajectories obtained by various methods in table 2.

Thus, the FESR is used as a fruitful constraint on Regge parameters for high-energy Regge-pole analysis. The analysis of πN scattering amplitude by Barger and Phillips [54] is a good example which employs the FESR most extensively. Their results have been verified by the later amplitude analysis, and have a great advantage as a model amplitude of πN scattering [239, 44]. The Barger–Phillips solution showed a predictive power also from fairly low energy region [e.g., 90, 258] to the Serpukhov–FNAL energy regions.

Applications of FESR to KN and $\bar{\mathrm{K}}$N scattering so far have not been so fruitful like the πN case. The reason is mainly due to the difficulties in estimating low-energy parameters below threshold such as $Y_1^*(1385)$, $Y_0^*(1405)$ as well as the Born terms, and also due to the lack of reliable phase-shift data for K^+N ($I = 0$). Moreover, systematic uncertainties appearing, when one constructs the

†Amplitude analysis at $p_L = 6$ GeV/c gives us $\nu B^{(+)}/A'^{(+)} \simeq 0.8$ (Halzen and Michael [239]) $\simeq 0.9$ (Cozzika et al. [134]).

Table 1

The ρ trajectory

	$\alpha(0)$	$\alpha'(\mathrm{GeV}/c)^{-2}$	
Höhler et al. [263]	0.575 ± 0.01	0.91 ± 0.06	high energy analysis
Höhler et al. [262]	0.57	0.96	high energy analysis
Arbab, Chiu [15]	0.56 ± 0.03	0.81 ± 0.08	high energy analysis
Barger et al. [51]	0.54 ± 0.01		high energy analysis
Barger [33]	0.53	0.83	high energy analysis (up to $p_{\mathrm{L}} \approx 100\mathrm{GeV}/c$)
Dolen et al. [164]	0.4 ± 0.2	0.9	FESR
Olsson [393]	0.57 ± 0.01		CMSR
Della Selva et al. [150]	0.550 ± 0.015		CMSR
Ferro Fontán et al. [191]	0.58	0.96	CMSR
Chew–Frautschi plot	0.500	0.895	ρ, f and g
Chew–Frautschi plot	0.468	0.897	ρ and g
Lovelace [337]	0.483	0.885	$\alpha(m_\rho^2) = 1$ and $\alpha(m_\pi^2) = 1/2$
Barger, Phillips [54]	0.55	1.0	CMSR + high energy fit ($\rho + \rho'$ fit)
Lyberg [342]	0.6	1.0	CMSR + high energy fit ($\rho + \rho'$ fit)

Table 2

The pomeron (P) and the f trajectories

	α_{P}	α_{f}	
von Dardel et al. [501]	1.	0.7	total cross section
Foley et al. [197]	1.	0.31 ± 0.1	total cross section
Barger et al. [51]	1.	0.51 ± 0.03	total cross section
Olsson [394]	1.	0.49 ± 0.02	CMSR
Della Selva et al. [151]	1.	0.60	CMSR
Ferro Fontán et al. [190]	1.00 ± 0.02	0.62 ± 0.05	CMSR
Restignoli et al. [419]	1.	0.66 ± 0.03	FESR + total cross section
Miyamura, Takagi [372, 373]	1.	$0.61\ {}^{+0.11}_{-0.15}$	FESR + total cross section
Barger, Phillips [54]	$1. + 0.36t$	$0.56 + 0.86t$	CMSR + high energy fit (5-pole fit)
Lyberg [342]	$0.98 + 0.4t$	$0.54 + 0.90t$	CMSR + high energy fit (5-pole fit)

amplitude from K^+p (and K^+N, $I = 0$) phase-shift data, make the obtained results unreliable. This is caused by the ambiguity among various phase-shift solutions, which give the same $d\sigma/dt \sim |f_{++}|^2 + |f_{+-}|^2$ and $P \cdot d\sigma/dt \sim [f_{++} \times f_{+-}]$, but give the quite different $f_{++} \cdot f_{+-} \sim \tilde{R} \cdot d\sigma/dt$ (here $\bar{f}_{+\pm} = (\mathrm{Re}\, f_{+\pm}, \mathrm{Im}\, f_{+\pm})$, see eq. (A.10)). (On the contrary a gross feature of the amplitude in non-exotic channel is well determined by dominating parent resonances and is not so much affected by unreliable daughter resonances. It should be noted that the first application of FESR to πN charge exchange gave correct results, though it was based on the phase-shift solutions at the preliminary stage.)

Table 3 contains a list of most of the FESR analyses which have been made.

The FESR for $t > 0$ provides another interesting example [163, 164, 445]. Let us observe how the t-channel pole is built in the FESR. Though the discontinuity of the Regge-pole amplitude in the direct channel, $\mathrm{Im}_s f_{\mathrm{Regge}}(s,t)$, is regular at $t = m_{\mathrm{res}}^2$ like,

$$\mathrm{Im}_s f_{\mathrm{Regge}}(s,t) \sim \mathrm{Im}_s \frac{\beta(t) P_{\alpha(t)}(-z_t)}{m_{\mathrm{res}}^2 - t} \sim \mathrm{Im}_s \frac{\beta(t)(-\nu)^{\alpha(t)}}{\sin \pi\alpha(t)} \sim \beta(t)\nu^{\alpha(t)},$$

the t-channel pole of $f(s,t)$ is built through the divergence of the fixed-t dispersion integral in the s-channel. In the FESR, once a discontinuity function, $\mathrm{Im}_s f(s,t)$, is known for $\nu \leqslant N$, the t-channel

Table 3
Summary of FESR analyses

$\pi\pi$ scattering	KN *scattering*
Schmid [445]	Matsuda, Igi [360]
Schmid, Yellin [458]	Dass, Michael [143]
Kaiser [307]	Di Vecchia et al. [161]
Ukawa et al. [489]	Ferro Fontán et al. [190]
Pennington [519]	Elvekjaer, Martin [179]
	Lyberg [343]
πN scattering	
Igi [275, 276]	$\bar{\mathrm{K}}\mathrm{N} \to \pi\Lambda(\Sigma)$, $\pi\mathrm{N} \to \mathrm{K}\Lambda(\Sigma)$
Restignoli et al. [419]	Field, Jackson [194]
Scanio [442]	Hirshfeld [260]
Logunov et al. [335]	Devenish et al. [157]
Igi, Matsuda [280]	Vanryckeghem [490]
Igi, Matsuda [281]	
Dolen et al. [163, 164]	$\pi\mathrm{N} \to \pi\Delta$
Gatto [219]	Froggatt, Parsons [208]
Liu, Okubo [333]	
Della Selva et al. [150]	*baryon exchange*
Della Selva et al. [151]	Chiu, der Sarkissian [122]
Olsson [393]	Barger et al. [49]
Olsson [394]	Liu, McGee [332]
Ferro Fontán et al. [191]	Kayser [310]
Gilman, Harari, Zarmi [224]	Peterson, Sollin [404]
Miyamura, Takagi [372]	
Miyamura, Takagi [373]	*photoproduction*
Barger, Phillips [53, 54]	Chu, Roy [126]
Ferrari, Violini [188]	Vasavada, Raman [491]
Phillips, Ringland [409]	Di Vecchia et al. [162]
Elvekjaer, Pietarinen [180]	Jackson, Quigg [301]
Worden [508]	Worden [507]
Lyberg [342]	Barker et al. [57]
Gabarro, Pajares [218]	
Elvekjaer et al. [178]	*electroproduction*
	Creutz et al. [136]
	Damashek, Gilman [138]
	Dominguez et al. [165]
	Matsumoto et al. [361]
	Biyajima [73]

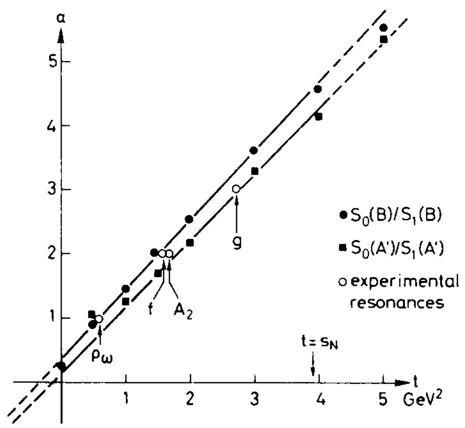

Fig. 4. Determination of the meson trajectory, $\alpha = \alpha_\rho = \alpha_{A_2} = \alpha_\omega = \alpha_f$, from the Y_0^* resonances ($1/2^+$, $3/2^-$, $5/2^+$) through the FESR (see eq. (2.14)), (from Schmid [449]).

pole is produced through the assumption that the asymptotic behaviours are controlled by the Regge pole. Equation (2.14) is essentially a formula to obtain m_{res}^2 of t-channel pole by the s-channel discontinuity. The residue function, when extrapolated to $t = m_{\text{res}}^2$, is directly connected to the coupling strength of t-channel pole to the external particles. Fig. 4 is an example of the output t-channel meson trajectory (assuming $\alpha_\rho = \alpha_{A_2} = \alpha_f = \alpha_\omega$)using the Y_0^* resonances as the s-channel inputs [449]. If one considers the reaction where the s- and t-channels are identical and employs the resonance approximation to evaluate the s-channel discontinuity for $\nu \leqslant N$, one obtains linear bootstrap equations which are called, the FESR bootstrap [347, 236, 445, 359]. This FESR bootstrap gave us an important key to find the Veneziano model [2, 492].

3. Duality and exchange degeneracy

3.1. FESR duality

As was explained in the preceding section, the assumption of analyticity as well as Regge asymptotic behaviours for two-body scattering amplitudes immediately leads to the FESR. If we further assume that the low-energy amplitude is dominated by s-channel resonances, we are led to the concept of duality.

As a simple illustration of duality, let us consider the FESR with $n = 0$ for the crossing-odd amplitude of πN scattering at $t = 0$. Equation (2.8) can be re-written as,

$$\int_0^N d\nu \, \mathrm{Im}\,[f(\nu,0) - f_{\rho\text{-Regge}}(\nu,0)] = 0. \tag{3.1}$$

Here

$$\mathrm{Im}\, f(\nu,0) = \frac{1}{4\pi}(\nu^2 - \mu^2)^{1/2}\{\sigma_{\pi^- \mathrm{p}}(\nu) - \sigma_{\pi^+ \mathrm{p}}(\nu)\}$$

and

$$\mathrm{Im}\, f_{\rho\text{-Regge}}(\nu,0) = \beta_\rho(0)\nu^{\alpha_\rho(0)}.$$

Fig. 5 shows that the ρ-Regge-pole amplitude extended all the way down to elastic threshold, far below the energy where we think of asymptotic behaviours as setting in, provides a good average description of the imaginary part of low-energy scattering amplitude. On the other hand, the *imaginary part* of low-energy amplitude is known to be well approximated† by a sum of direct-channel resonances in such a combination of scattering amplitudes without pomeron. The success of the FESR as is illustrated in fig. 5 implies that the *imaginary part* of s-channel resonances are, in an average sense, equivalent to that of t-channel Regge-pole exchanges, i.e.,

$$\langle \text{Res.} \rangle_{\text{Ave.}} = \text{Regge pole.} \tag{3.2}$$

This is the so-called duality [111] between direct-channel and crossed-channel descriptions, in the weakest form. It is often called the global duality or FESR duality. This hypothesis has been explicitly stated by Dolen, Horn and Schmid [163, 164] through detailed studies of the t-dependence of the ρ-Regge residues and of the properties of the dominant s-channel resonances in πN charge-exchange scattering in terms of the FESR.

3.2. The two-component hypothesis

When the scattering amplitude includes the contribution from pomeron exchange (diffraction), the imaginary part of low-energy amplitude cannot be approximated by a sum of resonances alone but includes a large non-resonating background. Freund [204] and Harari [244] made a conjecture that the ordinary Regge trajectories are built by the direct-channel resonances alone in the sense of FESR, while the pomeron is associated with the non-resonating background,‡ i.e.,

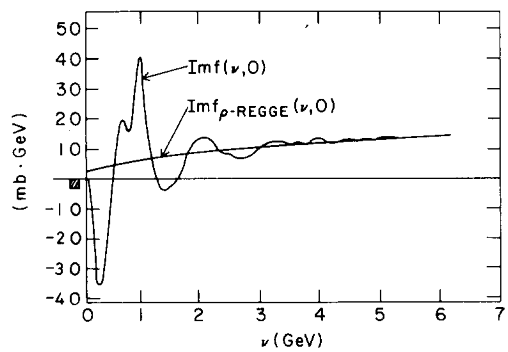

Fig. 5. The integrands for the FESR, eq. (3.1), for the crossing-odd amplitude in πN scattering at $t = 0$ (from Igi and Matsuda [280]).

†The resonance-dominance assumption cannot be justified for the real part of scattering amplitude since the real part at a given energy may show substantial contributions from distant resonances which has long-range tails as $\sim 1/s$. However, *the resonances do dominate the imaginary part in a local way.*

‡This hypothesis explicitly claims that the imaginary part of the inelastic amplitude is given by a sum of resonances alone and does not include the non-resonating background.

$$\langle \text{Res.} \rangle_{\text{Ave.}} = \text{ordinary Regge pole}$$
$$\langle \text{Non-resonating background} \rangle_{\text{Ave.}} = \text{pomeron.} \tag{3.3}$$

This enables us to construct the P and the f exchange amplitudes separately through the FESR† [224]. This hypothesis has been supported by the analysis of πN scattering [250] and $\bar{\text{K}}$N scattering (see fig. 6) [217, 325].

The idea of duality runs counter to the assumption of the interference model [34] which assumes that the amplitude is given by the *sum* of s-channel resonance contribution and t- or u-channel Regge-pole contribution, i.e.,

$$f = f_{\text{Res.}} + f_{\text{Regge}} . \tag{3.4}$$

Here, it is assumed that f_{Regge} include the pomeron term as well as ordinary Regge term. Then the use of FESR

$$\int_0^N \mathrm{d}\nu \, \mathrm{Im}\, [f - f_{\text{Regge}}] = 0 \tag{3.5}$$

together with eq. (3.4) should give

$$\int_0^N \mathrm{d}\nu \, \mathrm{Im}\, f_{\text{Res.}} = 0. \tag{3.6}$$

For forward elastic scattering, eq. (3.6) essentially means $\Sigma_i g_i^2 = 0$, which cannot be satisfied unless each resonance coupling g_i vanishes. This is a contradiction of the interference model.

3.3. Schmid circle

In the previous section, we have seen that the direct-channel resonances build the ordinary Regge trajectories through FESR. Let us consider here the behaviour of partial waves of the Regge-pole amplitude [446].

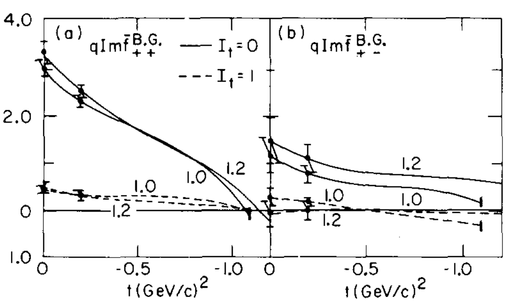

Fig. 6. Imaginary parts of the background part of $\bar{\text{K}}$N scattering amplitude at p_{L} = 1.0 and 1.2GeV/c. A diffraction-like t-dependence can be seen in the I_t = 0 amplitudes, especially in Im f_{++}, whereas the I_t = 1 amplitudes are quite small (from Fukugita, Inami and Kimura [217]).

†Thus it is found that (i) β_{f} has a zero at $t \simeq -0.25$ (GeV/c)^2 for the $A'^{(+)}$ amplitude and (ii) $\beta_{\text{f}} \sim \alpha(t)$ for the $B^{(+)}$ amplitude, resembling to the ρ-Regge residues [224; see also 217].

We take the typical residue function β to be of a form $\lambda/\Gamma(\alpha)$ (λ is a constant). Then, we have

$$f_{\mathrm{Regge}}(s,t) = \frac{\lambda}{\Gamma(\alpha)} \frac{\mp 1 - \mathrm{e}^{-\mathrm{i}\pi\alpha}}{\sin \pi\alpha} \left(\frac{s}{s_0}\right)^{\alpha} = \frac{\lambda}{\pi} \Gamma(1-\alpha)(\mp 1 - \mathrm{e}^{-\mathrm{i}\pi\alpha}) \left(\frac{s}{s_0}\right)^{\alpha}. \tag{3.7}$$

The factor $1/\Gamma(\alpha)$ kills the poles which could otherwise appear at right-signature points (ghost-killing factor) and produces zeros in f_{Regge} at wrong-signature points. The latter zeros are observed as dips in $\mathrm{d}\sigma/\mathrm{d}t$ as was seen in section 2.3. Here let us make a partial-wave analysis of $f_{\mathrm{Regge}}(s,t)$ in the direct channel as,

$$f_l(s) = \tfrac{1}{2} \int_{-1}^{1} \mathrm{d}z\, P_l(z) f_{\mathrm{Regge}}(s,t). \tag{3.8}$$

In order to see qualitative behaviours of $f_l(s)$, we approximate $f_{\mathrm{Regge}}(s,t)$ as $\sim(1 - \mathrm{e}^{-\mathrm{i}\pi\alpha})(s/s_0)^{\alpha}$, since $\Gamma(1-\alpha)$ is a smooth function in the above integrand. The partial-wave projection of the second term is then

$$\left(\mathrm{e}^{-\mathrm{i}\pi\alpha} \frac{s}{s_0}\right)^{\alpha_0 - 2\alpha' q^2} \mathrm{e}^{\mathrm{i}\pi l/2} j_l \left[-2q^2\alpha' \left(\ln \frac{s}{s_0} - \mathrm{i}\pi\right)\right]. \tag{3.9}$$

In the region for $s \gg l$, eq. (3.9) involves a factor $\sim\exp[\mathrm{i}\pi(\alpha' s - \alpha_0 + l)]$, rotating counterclockwise as s increases. This implies that f_l describes circles on the Argand diagram. Such circles are identified with direct-channel resonances [446]. If we define the resonance mass by $\delta_l \sim \frac{1}{2}(\alpha' s - \alpha_0 + l) = n + \pi/2$, we have resonances every $\Delta s = 2/\alpha'$ for each l, [436, 171].

We make a partial-wave analysis of the ρ-Regge amplitude for πN charge-exchange scattering with helicity-flip, $B^{(-)}(s,t)$, of the form of eq. (3.7) which fits the experiments. Then its partial wave draws a circle as in fig. 7a, and the predicted leading resonances lie approximately linearly on the Chew–Frautschi plot (fig. 7b), though they are slightly deviated from the observed N* trajectories [446; see also 467].

Whether these circles really correspond to resonance circles is in suspect, since eqs. (3.7) and (3.8) are regular at $s = m^2_{\mathrm{res}} - \mathrm{i}(m\Gamma)_{\mathrm{res}}$ and do not contain s-channel poles. The Veneziano model gives us a guide to clarify this situation. The Veneziano amplitude itself contains poles at $\alpha(s) = n$, but its asymptotic form (Regge-pole expression) does not contain s-channel poles. We note here that the asymptotic form is a good approximation only outside a wedge $|\arg(s)| > \epsilon$, and it breaks down if we penetrate into the wedge. (It is known empirically that the Schmid circle of this asymptotic expression gives the resonance at mass near the original pole position.)

We expect similar situation for f_{Regge}: The Regge asymptotic form f_{Regge} is a good approximation to the full amplitude f for real s. Both amplitudes contain the resonance circles. But if we go below the physical axis, especially for $\mathrm{Im}\, s \sim -(m\Gamma)_{\mathrm{res}}$, the approximation breaks down.

In order to discuss second-sheet poles (the poles of $f_l(s)$ at $s = m^2_{\mathrm{res}} - \mathrm{i}(m\Gamma)_{\mathrm{res}}$), we have to know the behaviour of $f(s,t)$ for $t \to \infty$, since the pole of $f_l(s)$ ($s = m^2_{\mathrm{res}} - \mathrm{i}(m\Gamma)_{\mathrm{res}}$, l = integer) arises from the divergence of the integral

$$f_l(s) = \frac{1}{\pi} \int_{t_0}^{\infty} \frac{\mathrm{d}t}{2q^2} Q_l \left(1 + \frac{t}{2q^2}\right) \mathrm{Im}_t f(s,t).$$

Thus the Regge expression for f, which is valid only for $s \to \infty$ with t fixed, becomes useless when we deal with the resonance pole itself, but it may give useful approximation to study the behaviour off the pole [448].

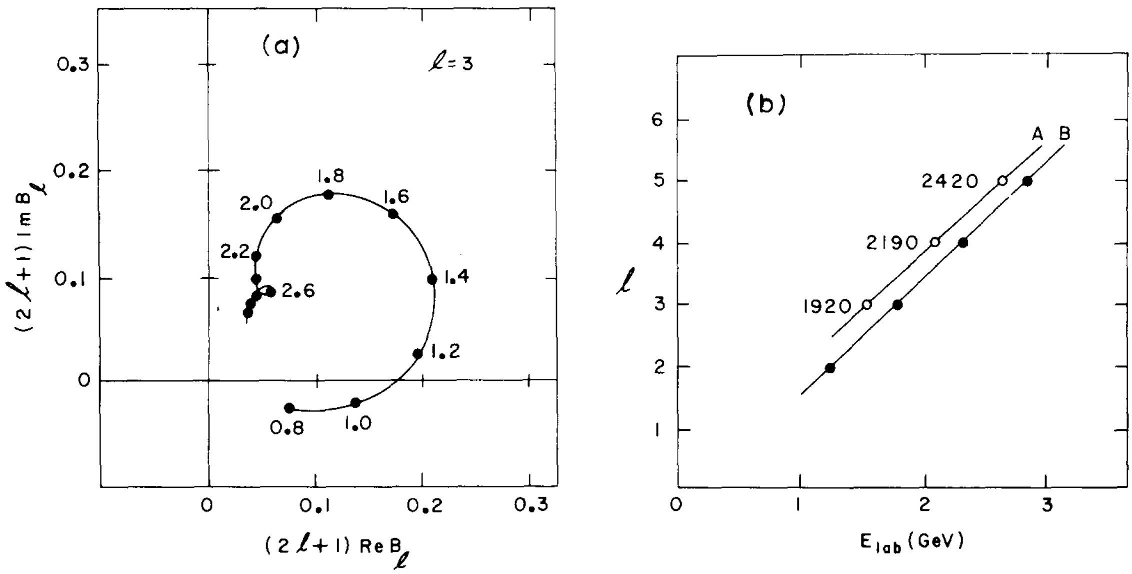

Fig. 7. (a) A typical partial wave of the Regge-pole amplitude

$$B^{(-)} = \frac{\beta}{\Gamma(\alpha)}\,\frac{1-e^{-i\pi\alpha}}{\sin\pi\alpha}\left(\frac{\nu}{\nu_0}\right)^{\alpha-1}$$

with $\alpha = 0.57 + 1.08t$, β = const. = 60.3mb and ν_0 = 0.7GeV, which fits the forward peak of $\pi^- p$ charge exchange. The numbers along the circle are the values of p_L. (b) Chew–Frautschi plot of leading N* resonances from the partial-wave analysis of the ρ Regge exchange (B), compared with that of observed ones (A) (after Schmid [446]).

3.4. Exchange degeneracy (I)

As is well known in potential scattering, there are two kinds of forces, i.e., the ordinary and the Majorana forces. Since the latter changes the sign according as l is even or odd, the presence of the two kinds of the forces gives two distinct families of bound states or resonances. This was the origin of signature in the Regge pole model. The absence of the Majorana force implies that states with even and odd l values belong to the same family.

In particle physics the mechanism is essentially the same. Consider two-particle scattering with exotic s channel† (e.g., $K^+p \to K^+p$). In exotic channels no resonance is observed. According to the two-component hypothesis of duality, the imaginary part of the non-diffractive amplitude (we denote it merely as $f(\nu,t)$) should vanish:

$$\mathrm{Im}\, f(\nu,t) \simeq \beta_{\mathrm{even}}(t)\nu^{\alpha_{\mathrm{even}}(t)} - \beta_{\mathrm{odd}}(t)\nu^{\alpha_{\mathrm{odd}}(t)} \simeq 0. \tag{3.10}$$

Therefore we obtain

$$\begin{aligned}\alpha_{\mathrm{even}}(t) &= \alpha_{\mathrm{odd}}(t) = \alpha(t)\\ \beta_{\mathrm{even}}(t) &= \beta_{\mathrm{odd}}(t) = \beta(t).\end{aligned} \tag{3.11}$$

†By "exotic" we mean the following. All resonances so far known can be considered to be composed of $q\bar{q}$ for mesons and qqq for baryons. This corresponds to SU(3) multiplets $\underline{1}$ and $\underline{8}$ for mesons and $\underline{1}$, $\underline{8}$ and $\underline{10}$ for baryons. All other sets of quantum numbers are called "exotic". There is also another kind of exoticity in connection with charge conjugation. Particles with abnormal C-parity states that cannot come from $q\bar{q}$ model (e.g., $J^{PC} = 0^{--}; 0^{+-}, 1^{-+}, 2^{+-}, \ldots$) are called "exotics of the second kind".

This is the exchange degeneracy (EXD),† which was first proposed by Arnold [17]. In this case, therefore, the amplitude $f(\nu,t)$ at high energy becomes real as,

$$f(\nu,t) \sim -\beta(t)\,\frac{1}{\sin\pi\alpha(t)}\,\nu^{\alpha(t)}. \tag{3.12}$$

The absence of $e^{-i\pi\alpha(t)}$ is evident if one remembers that the first term of the signature factor $1 - e^{-i\pi\alpha(t)}$ comes from the left-hand cut and the second from the right-hand cut. In the line-reversed reaction (e.g., $K^-p \to K^-p$), the amplitude takes the form (rotating phase)

$$f(-\nu,t) \sim -\beta(t)\,\frac{e^{-i\pi\alpha(t)}}{\sin\pi\alpha(t)}\,\nu^{\alpha(t)}. \tag{3.13}$$

Thus, the differential cross section of line-reversed reaction should be equal to that of the original one.

It is important to notice that the exchange degeneracy gives a further restriction to the form of residue function. The positive- and negative-signature-residue functions should vanish at their right-signature points, i.e., $\alpha(t) = 0, -2, -4, \ldots$ and $\alpha(t) = -1, -3, -5, \ldots$ respectively, to avoid poles in the scattering region. The exchange degeneracy tells us $\beta_{\rm even}(t) = \beta_{\rm odd}(t)$, so that both residue functions should vanish at also wrong-signature points, without any further assumption of particular mechanism such as wrong-signature-nonsense zeros. Thus, the residue function $\beta(t)$ must vanish at $\alpha(t) = 0, -1, -2, \ldots$, the simplest form being $\beta(t) \sim 1/\Gamma(\alpha(t))$.

Examples of the exchange degeneracy

(1) meson–meson scattering. Consider $\pi^+\pi^+$ scattering. The s-channel is exotic and hence has no resonances. Since we have the Regge poles ρ and f in the t-channel, we get

$$\mathrm{Im}\, f^{\pi^+\pi^+}(\nu,t) \simeq \beta_{f\pi^+\pi^-}(t)\,\nu^{\alpha_f(t)} - \beta_{\rho\pi^+\pi^-}(t)\,\nu^{\alpha_\rho(t)} \simeq 0.$$

Thus it follows that

$$\alpha_f(t) = \alpha_\rho(t), \qquad \beta_{f\pi^+\pi^-}(t) = \beta_{\rho\pi^+\pi^-}(t). \tag{3.14}$$

Similarly, we obtain the ρ–f and K^*–K^{**} exchange degeneracy in $K^+\pi^+ \to K^+\pi^+$, and the ρ–A_2, ω–f and ϕ–f′ exchange degeneracy in $K^+K^+ \to K^+K^+$.‡ Hence we have

†In order to derive the exchange degeneracy we shall have to go a little bit beyond FESR duality. Assuming the absence of wrong-signature fixed pole, we have the nth moment FESR

$$\frac{1}{N^{n+1}}\int_0^N d\nu\,\nu^n\,\mathrm{Im}\, f^{\rm even}(\nu,t) = \beta_{\rm even}(t)\,\frac{N^{\alpha_{\rm even}(t)}}{\alpha_{\rm even}(t)+n+1}$$

$$\frac{1}{N^{n+1}}\int_0^N d\nu\,\nu^n\,\mathrm{Im}\, f^{\rm odd}(\nu,t) = \beta_{\rm odd}(t)\,\frac{N^{\alpha_{\rm odd}(t)}}{\alpha_{\rm odd}(t)+n+1}$$

for both even and odd positive integers n. (One of the above FESR is the Schwarz sum rule.) Thus, for an amplitude $f \equiv f^{\rm even}(\nu,t) - f^{\rm odd}(\nu,t)$, we obtain

$$\frac{1}{N^{n+1}}\int_0^N d\nu\,\nu^n\,\mathrm{Im}\, f(\nu,t) = \beta_{\rm even}(t)\,\frac{N^{\alpha_{\rm even}(t)}}{\alpha_{\rm even}(t)+n+1} - \beta_{\rm odd}(t)\,\frac{N^{\alpha_{\rm odd}(t)}}{\alpha_{\rm odd}(t)+n+1}.$$

If we take an exotic amplitude for f, the vanishing of the left-hand side gives eq. (3.11). It should be noted that we have not invoked local form of eq. (3.10).

‡The absence of second-kind exotics leads to another kind of exchange degeneracy. Consider $\pi^0\eta$ scattering. The combination $f(s,t) - f(s,u)$ involves only the partial waves of the second-kind exotic states ($J^{PC} = 1^{-+}, 3^{-+}, 5^{-+}, \ldots$). The absence of these exotic resonances gives the f–A_2 exchange degeneracy [466].

$$\alpha_{f} = \alpha_{A_2} = \alpha_{\omega} = \alpha_{\rho}, \qquad \alpha_{K^*} = \alpha_{K^{**}}, \qquad \alpha_{f'} = \alpha_{\phi} \tag{3.15}$$

and

$$\beta_{K^+K^-\omega} = \beta_{K^+K^-f}, \qquad \beta_{K^+K^-\rho} = \beta_{K^+K^-A_2}, \qquad \beta_{K^+K^-\phi} = \beta_{K^+K^-f'} \tag{3.16}$$

and so on.† Equation (3.15) implies the mass degeneracy of ρ and ω and of f and A_2, which was first proposed by Okubo [390].

(2) Kaon–nucleon scattering. Both K^+p and K^+n channels are exotic and no prominent resonances are observed. The Regge poles are f, ω, ρ and A_2 in the t-channel, and Y_0^*'s and Y_1^*'s in the u-channel. Thus, exchange degeneracy is required for the following pairs: ρ–A_2, f–ω, Y_0^* pair (Λ_α–Λ_γ) and Y_1^* pair (Σ_δ–Σ_β).

We mention here how the exchange degeneracy is supported by experiments. The Chew–Frautschi plot gives an evidence for the ρ–A_2 and for the f–ω exchange degeneracies in the region for $t > 0$. The fact that $\sigma_{tot}(K^+p) = \sigma_{tot}(K^+n)$ = constant for wide range of s also supports the exchange degeneracies at $t = 0$. For $t \leq 0$, we have the following evidences for the ρ–A_2 exchange degeneracy.

(i) Forward amplitude of $K^-p \to \bar{K}^0n$ is predominantly imaginary, while that of $K^+n \to K^0p$ is almost purely real [e.g., 20, 195].

(ii) The dip observed in the forward direction of $\pi^-p \to \eta n$ implies $[\nu B/A']_{A_2} \approx 10$, [408]. The agreement of this value with $[\nu B/A']_\rho \approx 10$ for $\pi^-p \to \pi^0n$ indicates that $A_2N\bar{N}$ vertex and $\rho N\bar{N}$ vertex have the same helicity structure in accord with the exchange-degeneracy requirement. (A simultaneous analysis of the $\pi^-p \to \pi^0n$ and ηn gives $[\nu B/A']_\rho \simeq 11.2$ and $[\nu B/A']_{A_2} \simeq 10.2$, and that of K^-p and K^+n charge exchanges gives $[\nu B/A']_\rho \simeq 11.0$ and $[\nu B/A']_{A_2} \simeq 9.8$, [336].

(iii) The approximate equality $d\sigma/dt(K^-p \to \bar{K}^0n) \simeq d\sigma/dt(K^+n \to K^0p)$ holds for $P_L \gtrsim 5$GeV/c [128, 159; see also 20, 195, 238]. Especially at $t = 0$, the agreement is extremely good. This seems to hold true also at fairly low energy (such as $P_L \approx 1$GeV/c) [128].

(iv) The trajectories determined from the s dependences of differential cross sections (up to 100GeV/c) for $\pi^-p \to \pi^0n$ and $\pi^-p \to \eta n$ indicate that the exchange degeneracy holds to an extent of $\alpha_\rho(t) - \alpha_{A_2}(t) \approx 0.1$, [33, 520, 521]. The slightly higher ρ trajectory implies $d\sigma/dt(K^+n \to K^0p) \gtrsim d\sigma/dt(K^-p \to \bar{K}^0n)$ as is actually observed in low energy regions.

(v) Assume the pomeron amplitude to be purely imaginary and to conserve the s-channel helicity (i.e., $A_{pomeron} \approx 0$). Since it has a structure smooth in t, the polarization of elastic scattering shows qualitative features of Re A_{meson}, or equivalently $-$Re B_{meson} when $\nu B/A' \gg 1$. The phases of the B_{meson}, $-e^{-i\pi\alpha}$ for K^-p and -1 for K^+p, lead to

$$P(K^+p \to K^+p) \sim \sqrt{-t} \times \text{(smooth function)}$$

$$P(K^-p \to K^-p) \sim \sqrt{-t} \cos\pi\alpha \times \text{(smooth function)}.$$

This correctly predicts the elastic polarization of $K^\pm p$ (see fig. 8), [12, 81]. This structure remains unchanged qualitatively down to the resonance region such as $P_L \approx 1$GeV [5,60]. (In the non-exchange-degenerate cases, $\sqrt{-t}$ Re $B_\rho \sim \sqrt{-t}(1 - \cos \pi\alpha)$, giving a well-known double zeros for $P d\sigma/dt(\pi^-p) - P d\sigma/dt(\pi^+p)$ at $\alpha = 0$ [183, 80].)

On the other hand, evidence for the f–ω exchange degeneracy is poor for $t < 0$. We only know the helicity conservation of ω together with that of f, i.e., $[\nu B/A']_\omega \approx [\nu B/A']_f \approx 1$, [389].

†These equations are not satisfied simultaneously, if both vector and tensor mesons belong to octet; since the vector coupling has to be of pure F type while the tensor coupling should be of pure D type. Mixing with (at least) a singlet tensor is required [457].

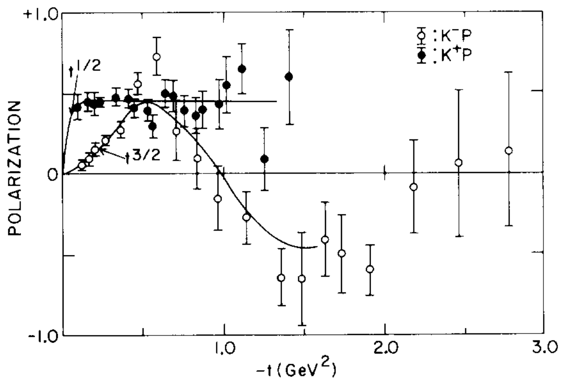

Fig. 8. Polarization of $K^{\pm}p$ elastic scattering at 2.74 GeV/c (Andersson et al. [12]). The curve expected from the exchange degeneracy of ρ and A_2 is drawn to guide the eye.

As for baryon Regge poles, fig. 9 shows the exchange degeneracy of Y_0^*'s and of Y_1^*'s for $t > 0$, [447]. It should be noted that not only the trajectories but the couplings of resonances exhibit clear exchange-degenerate pattern for leading $\Lambda_\alpha - \Lambda_\gamma$ and $\Sigma_\delta - \Sigma_\beta$ resonances.

The exchange degeneracy of $\Sigma_\delta - \Sigma_\beta$ implies that of the decuplet δ and the octet β series, i.e., $\underline{10}_\delta - \underline{8}_\beta - \underline{10}_\delta - \ldots$, for the Σ_δ belongs to $\underline{10}$ and the Σ_β to $\underline{8}$. Thus, in order to hold the exchange-degeneracy condition for the $I_u = 0$ combination of the KN amplitude (u-channel: $\bar{K}N$), the Λ_β should decouple from $\bar{K}N$ system, since decuplet Reggeon cannot couple to the $I_u = 0$ channel. This implies the $\underline{8}_\beta$ to have $F/D = -1/3$. (Experimentally Λ_β (1830) couples to $\bar{K}N$ only weakly.) As for the $\Lambda_\alpha - \Lambda_\gamma$ series, Λ_α belongs to $\underline{8}$ and Λ_γ to dominantly $\underline{1}$; we have thus the exchange degeneracy $\underline{8}_\alpha - \underline{1}_\gamma - \underline{8}_\alpha \ldots$. (We ignore $\underline{8}_\gamma$ here for simplicity.) The exchange degeneracy condition for the $I_u = 1$ combination of the $\bar{K}N$ amplitudes leads to $\Sigma_\alpha \not\to \bar{K}N$, since $\underline{1}_\gamma$ does not couple to $I_u = 1$, i.e., we have $[F/D]_{8\alpha} = 1$. What we argued here is only qualitative, and it is necessary to take into account more multiplets in order to satisfy the exchange-degeneracy conditions imposed by the exoticity in the t-channel as well as those in the u-channel. This will be discussed in more detail in the next section.

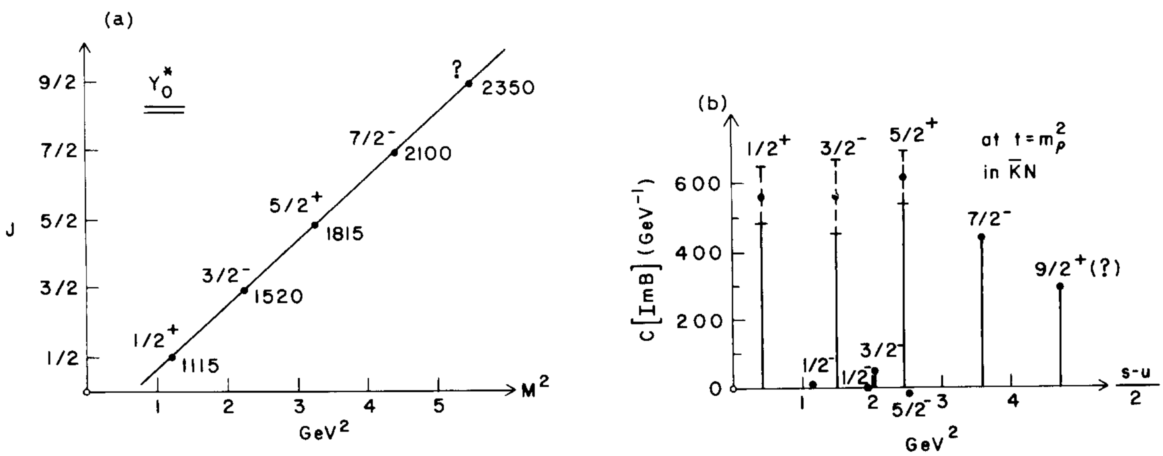

Fig. 9. (a) The exchange-degeneracy sequence $\Lambda_\alpha - \Lambda_\gamma$. (b) The contribution of Y_0^* resonances to Im B at $t = m_\rho^2$. The figure shows that those resonances which do not fit into the exchange-degeneracy pattern give very small contributions while those included in (a) have not only exchange-degenerate masses but also exchange-degenerate couplings (from Schmid [447]).

On the other hand, resonances coupled only weakly to the $\bar{K}N$ system as well as low-partial-wave resonances do not appear to fit in the exchange-degenerate pattern so well. The exchange-degeneracy condition, in general, imposes strong restrictions to peripheral-partial-wave resonances, but not too strong to low-partial-wave resonances. The stronger the resonance couplings are, the more severe the restrictions become (see [447]).

The exchange degeneracy of Y*'s in the scattering region makes the phase of K^+p backward scattering amplitude to be real. In fact, the polarization of K^+p backward scattering which is consistent with zero [60, 399] is regarded as an evidence for the Y^* exchange degeneracy in the region for $u < 0$.

In summarizing, we have the following systematics in the presence of the exchange degeneracy.

KN		$\bar{K}N$
no resonance in the s-channel	$\longleftrightarrow$	rapid decrease of the 180° cross section
real phase in the backward region	$\longleftrightarrow$	Y_0^*, Y_1^* exchange degeneracy in s-channel
real phase in the forward region	$\longleftrightarrow$	rotating ($e^{-i\pi\alpha}$) phase in the forward region

(3) Wrong-signature sense zeros. One of the interesting predictions of the exchange degeneracy is a wrong-signature-sense zero of Δ_δ (or Σ_δ) trajectory at $\alpha(u) = \frac{1}{2}$ [48]. This was originally introduced [282] so that the extrapolation to $\alpha = \frac{3}{2}$ of the Regge residue function in $\pi^- p$ backward scattering should give the correct elastic width for $\Delta_\delta(3/2^+)$.

In the reaction $K^- p \to \Sigma^- \pi^+$ which is exotic in the t-channel, the N_β and the Δ_δ should be exchange degenerate. (Note that the N_α and the N_γ are decoupled from ΣK systems if $[F/D]_{8\alpha} = 1$.) Since the N_β is missing at $\alpha = \frac{1}{2}$, the Δ_δ Regge residue should have a zero at $\alpha(u) = \frac{1}{2}$. This exchange degeneracy holds also in $\pi^+ p \to p\pi^+$ scattering through factorization of the reactions $K^- p \to \Sigma^- \pi^+$, $K^- \Sigma^- \to \Sigma^- K^-$ and $\pi^+ p \to p\pi^+$. Then the vanishing of Δ_δ residue at $\alpha = \frac{1}{2}$ leads to the zero of the $\pi^- p \to p\pi^-$ amplitude at that point. Phenomenological arguments will be presented in section 4.7.

3.5. Exchange degeneracy (II)

Algebraic solutions of exchange degeneracy

Most fruitful results are obtained when the exchange-degeneracy arguments are combined with internal symmetry. Using the SU (3) crossing matrices X_{st} and X_{ut} [154, 417], eq. (3.10) can be rewritten as,

$$\sum_b [X_{st}]^{ab} \sum_i \beta_i^b(t) \nu^{\alpha_i^b(t)} = 0 \tag{3.17a}$$

for the exotic s-channel and

$$\sum_b [X_{ut}]^{ab} \sum_i \tau_i \beta_i^b(t) \nu^{\alpha_i^b(t)} = 0 \tag{3.17b}$$

for the exotic u-channel. Here a and b denote SU (3) quantum numbers in each channel. The non-trivial way for eq. (3.17) to be satisfied is to have

$$\alpha_i^b(t) \equiv \alpha(t) \text{ for all } (i,b)$$

$$\sum_b [X_{st}]^{ab} \sum_i \beta_i^b(t) = 0, \qquad \sum_b [X_{ut}]^{ab} \sum_i \tau_i \beta_i^b(t) = 0. \tag{3.18}$$

(1) In $0^-{-}0^-$ scattering [123, 352], taking the $\underline{8} \times \underline{8} \to \underline{8} \times \underline{8}$ crossing matrix for X_{st} and X_{ut} (eqs. (B.3) and (B.4) in Appendix B), we have eq. (3.17) for $a = \underline{10}$, $\underline{10^*}$ and $\underline{27}$. (In this case the t-channel and u-channel constraints give the same equations.) Denoting couplings of 0^- mesons to the octet vector, octet tensor and singlet tensor trajectories as γ_{V_8}, γ_{T_8} and γ_{T_1} respectively ($\gamma_i^2 \equiv \beta_i$)† (the vector singlet does not couple at all), we obtain

$$\begin{aligned} &\text{no } \underline{10}, \underline{10}^*; \quad && \gamma_{T_1}^2 - \gamma_{T_8}^2 = 0 \\ &\text{no } \underline{27} \quad ; && \gamma_{T_1}^2 + \tfrac{1}{2}\gamma_{T_8}^2 - \tfrac{3}{2}\gamma_{V_8}^2 = 0 \end{aligned} \tag{3.19}$$

or

$$\gamma_{V_8}^2 = \gamma_{T_1}^2 = \gamma_{T_8}^2. \tag{3.20}$$

This implies the exchange degeneracy between octet vector and nonet tensor trajectories.

The exchange degeneracy still holds even if there are mass breakings as in the actual world. In this case, we have the ideally mixed nonet, i.e., $|f\rangle = |f_1\rangle \cos\theta + |f_8\rangle \sin\theta$ with $\tan\theta = 1/\sqrt{2}$, so that $\gamma_{f\pi^+\pi^-} = \gamma_{\rho\pi^+\pi^-}$ and $\gamma_{f'\pi^+\pi^-} = 0$. Similarly, ideal mixing ($\tan\theta = 1/\sqrt{2}$) is required also for the vector nonet ($|\omega\rangle = |\omega_1\rangle\cos\theta + |\omega_8\rangle\sin\theta$). These results are just the eqs. (3.14)–(3.16) and they imply ω, f $\sim (\bar{p}p + \bar{n}n)/\sqrt{2}$ and ϕ, f$' \sim -\bar{\lambda}\lambda$ in terms of the quarks.

Similar arguments for $0^-{-}1^-$ scattering [353, 142] lead to the analogous conclusion not only for the vector and tensor mesons, but also for all other meson multiplets, whereas the 0^- seems to be much more like an octet ($\tan\theta \approx -0.2$).‡ Table 4 is a summary of the patterns of the meson exchange degeneracies.

(2) $0^-{-}1/2^+$ scattering [352, 48]: Let us consider baryon–Regge-pole exchanges in the s-channel. We then have the following set of duality constraints for the $\tau P = +(\alpha{-}\gamma$ series) and $-(\beta{-}\delta$ series) Regge sequences separately,

Table 4
The patterns of the exchange degeneracies for meson–meson scattering

reactions	exchange-degeneracy pattern	quark model
$0^-{-}0^-$	$\underline{8}(1^{--})-\underline{9}(2^{++})$	${}^3L_{L+1}-{}^3(L+1)_{L+2}$
	$\underline{9}(1^{--})-\underline{8}(2^{++})$	${}^3L_{L+1}-{}^3(L+1)_{L+2}$
$0^-{-}1^-$	$\underline{8}(1^{++})-\underline{9}(2^{--})$	${}^3(L+1)_{L+1}-{}^3(L+2)_{L+2}$
	$\underline{8}(0^{-+})-\underline{9}(1^{+-})$	${}^1L_L-{}^1(L+1)_{L+1}$
$1^-{-}1^-$	$\underline{9}(1^{++})-\underline{8}(2^{--})$	${}^3(L+1)_{L+1}-{}^3(L+2)_{L+2}$
	$\underline{9}(0^{-+})-\underline{8}(1^{+-})$	${}^1L_L-{}^1(L+1)_{L+1}$

†These couplings are so normalized as $\Gamma_{VMM} \equiv -i\gamma_{V_8} f_{\alpha\beta\gamma}\phi_\alpha\phi_\beta V_{8\gamma}$, $\Gamma_{TMM} \equiv \gamma_{T_8} d_{\alpha\beta\gamma}\phi_\alpha\phi_\beta T_{8\gamma} + \gamma_{T_1} d_{\alpha\beta 0}\phi_\alpha\phi_\beta T_1$, so that they are related to the reduced matrix elements (γ_1, γ_{8F}, γ_{8D}) of the Wigner–Eckart formula for SU (3) [153] as, $(1/\sqrt{3})\,\gamma_{8F} = \gamma_{V_8}$, $\sqrt{(3/5)}\,\gamma_{8D} = \gamma_{T_8}$, $-(\sqrt{3}/4)\,\gamma_1 = \gamma_{T_1}$.

‡One must remember here that the validity of these equations depend upon the compatibility of the two different approximations, Regge-pole dominance and resonance saturation. Presumably resonance saturation is not so good an approximation for the $0^-{-}1^-$ case because of the high threshold. Thus the results obtained there may not be so reliable as in the $0^-{-}0^-$ case.

$$\sum [X_{ts}]^{ab} \sum \beta_i^b t^{\alpha_i^b} = 0 \text{ for } a = \underline{10},\ \underline{10}^*,\ \underline{27},$$
$$\sum [X_{us}]^{ab} \sum \tau_i \beta_i^b u^{\alpha_i^b} = 0 \text{ for } a = \underline{10}^*,\ \underline{27}, \tag{3.21}$$

since Regge-exchange contributions are separable according to τP as t or $u \to \infty$.

These equations cannot be satisfied with fewer than three trajectories. The simplest solutions satisfying the positivity of residues are,

$$\begin{aligned}
&\text{(i)}\ \underline{8}_1 \longleftrightarrow \underline{1} \oplus \underline{8}_1 \\
&\text{(ii)}\ \underline{8}_{-1/3} \longleftrightarrow \underline{8}_{-1/3} \oplus \underline{10} \\
&\text{(iii)}\ \underline{8}_\infty \longleftrightarrow \underline{1} \oplus \underline{8}_0 \\
&\text{(iv)}\ \underline{8}_0 \longleftrightarrow \underline{8}_\infty \oplus \underline{10}\ .
\end{aligned} \tag{3.22}$$

Here suffixes to the octets denote their F/D ratios and the double arrow means that multiplets in both sides form an exchange-degenerate pair with opposite signatures. These solutions except for (iii) satisfy factorization of MB → MB, MB → MΔ and MΔ → MΔ. The solutions (i) and (ii) are the particular cases of a four-trajectory solution $(\underline{1} \oplus \underline{8}) \leftrightarrow (\underline{8}' \oplus \underline{10})$. In this more general solution, one F/D ratio (e.g., that of $\underline{8}$) is arbitrary and the relative couplings are determined in terms of it (e.g., the F/D ratio of another octet $\underline{8}'$ is given as $F'/D' = (D/F + 2)/3$). Specific choices of F/D ($F/D = 1$ and $-1/3$) decouple the decuplet and singlet and reduce the solution to (i) and (ii), respectively. The other four-trajectory solutions are $(\underline{1} \oplus \underline{8}) \leftrightarrow (\underline{1}' \oplus \underline{8}')$ with $F/D \cdot F'/D' = 1$ and $(\underline{8} \oplus \underline{10}) \leftrightarrow (\underline{8}' \oplus \underline{10}')$ with $F/D \cdot F'/D' = 1/9$, which contain the solutions (iii) and (iv) as the special case. Many solutions exist when more than four trajectories are included.

Exchange degeneracy for baryons

Some of the solutions of exchange degeneracy, eq. (3.22), gives us a qualitative understanding of the SU(3) coupling patterns of the observed leading baryon resonances.

The natural parity resonances (τP = +, the α–γ series) can be associated with the solution (i). A good example of an exchange degeneracy for the α–γ series is

$$\Lambda_\alpha(1/2^+) - \Lambda_\gamma(3/2^-, 1520) - \Lambda_\alpha(5/2^+, 1815) - \Lambda_\gamma(7/2^-, 2100) - \ldots$$

where the Λ_α are octet and Λ_γ dominantly singlet. Here the $\Lambda_\gamma(3/2^-, 1520)$ accompanies the dominantly octet $\Lambda_\gamma(3/2^-, 1690)$ which couples rather weakly to $\bar{\text{K}}$N. (Another $\Lambda_\gamma(7/2^-)$, belonging to the dominantly octet, might have a mass too high to have been observed.) For the Σ the exchange degeneracy

$$\Sigma_\alpha(1/2^+) - \Sigma_\gamma(3/2^-, 1670) - \Sigma_\alpha(5/2^+, 1915) - \Sigma_\gamma(7/2^-, 2100) - \ldots$$

holds within $\Delta\alpha \simeq 0.25$. The expected pattern

$$\text{N}_\alpha(1/2^+) - \text{N}_\gamma(3/2^-, 1520) - \text{N}_\alpha(5/2^+, 1688) - \text{N}_\gamma(7/2^-, 2190) - \ldots$$

holds only within $\Delta\alpha \simeq 0.4$. It is to be noted, however, that this exchange degeneracy is not required directly from the condition of no exotics but only through the SU (3) symmetry. The F/D ratios in the solution (i), $[F/D]_{8\alpha} = [F/D]_{8\gamma} = 1$ (which implies $\Sigma \not\to \bar{\text{K}}$N), corresponds to our observation that the Λ_α–Λ_γ couples more strongly to $\bar{\text{K}}$N than the Σ_α–Σ_γ (e.g., $g^2_{\text{KN}\Sigma} \ll g^2_{\text{KN}\Lambda}, g^2_{\pi\text{NN}}$ [e.g., 413, 410]; $\Gamma[\Lambda(5/2^+, 1815) \to \bar{\text{K}}\text{N}]/\Gamma[\Sigma(5/2^+, 1915) \to \bar{\text{K}}\text{N}] \simeq 5$, [397]).

It is of interest to compare the F/D values with those obtained by the SU (3) fittings to the decay widths of octet baryons [486, 328, 411, 364, 166, 32, 440, 317] some of which are listed in table 5. This table shows that the F/D ratios of the octets, $1/2^+$, $3/2^-$, $5/2^+$, ... , alternate around one (see also fig. 10).

The unnatural-parity resonances ($\tau P = -$, the δ–β series) can be associated with the solution (ii). The exchange degeneracies

$$\Sigma_\delta(3/2^+, 1385) - \Sigma_\beta(5/2^-, 1765) - \Sigma_\delta(7/2^+, 2030) - \dots,$$

$$\Delta_\delta(3/2^+, 1232) - N_\beta(5/2^-, 1670) - \Delta_\delta(7/2^+, 1950) - \dots,$$

hold within $\Delta\alpha \simeq 0.1$. These are the degeneracies required only by the condition of no exotics. The Σ_δ and the Δ_δ belong to $\underline{10}$, while the Σ_β and the N_β to $\underline{8}$. At $J = 7/2^+$ the Δ_δ accompanies the wanted $\underline{8}$, $N_\delta(7/2^+, 1990)$, and there is also a candidate for the Λ_δ, $\Lambda_\delta(7/2^+, 2020)$.(An octet Σ_δ has not been found yet, however.) The exchange degeneracy requires the Regge residue of $\underline{10}_\delta$ to have a zero at $\alpha = 1/2$ corresponding to the absence of $1/2^-$ octet. The solution, $(\underline{8}_{-1/3})_\beta \leftrightarrow (\underline{8}_{-1/3} \oplus \underline{10})_\delta$, correctly predicts that the Σ_δ and the Σ_β dominate over the Λ_β in the $\bar{K}N$ channel ($F/D = -1/3$ implies $\Lambda \not\to \bar{K}N$; experimentally we have $\Gamma[\Sigma_\beta(5/2^-, 1765) \to \bar{K}N]/\Gamma[\Lambda_\beta(5/2^-, 1830) \to \bar{K}N] \simeq 5$) [397]. The F/D ratio of $\underline{8}(5/2^-) = -0.1 \sim -0.2$ in table 5 is near to the predicted value $F/D = -1/3$. (Note that $F/D = -1/3$ is also the quark model value.)

There has been, however, a trouble with the solution (ii): One had to introduce an unobserved $3/2^+$ octet. To overcome this difficulty, one should rely on a particular mechanism [350, 427] (in which one can eliminate the $\underline{8}(3/2^+)$ without breaking the duality; see section 5.4 for details), or one must break duality either (a) by neglecting the constraints imposed by exoticity in the t-channel [93, 353, 354] or (b) by fulfilling all constraints only approximately [451]. (In the case (a), we have solutions, $\underline{8}_{-1/3} \leftrightarrow \underline{10}$ and $\underline{1} \leftrightarrow \underline{8}_1$. These are the exchange degeneracy in example (2) in the preceding section.) We mention here that the unwanted $3/2^+$ octet of the exact solution couples only weakly; an expected contribution of $N(3/2^+)$ is only 1/32 of that of $\Delta_\delta(3/2^+)$ in the $A^{(\pm)}(\pi N)$ or $B^{(\pm)}(\pi N)$ amplitude.

Table 5
The F/D ratios for the coupling of parent baryon octets to $0^-1/2^+$

		$1/2^+$	$3/2^-$	$5/2^+$	$7/2^-$	$5/2^-$
(1)	Plane et al. [411] Meyer and Plane [364][a]		2.33 ± 0.56	0.82 ± 0.10	4.0 ± 5.5	−0.19 ± 0.04
(2)	Ebenhöh et al. [166][b]	0.58 ± 0.03				
(3)	Barbaro-Galtieri [32][a]		1.99 ± 0.28	0.61 ± 0.09		−0.11 ± 0.04
(4)	Samios et al. [440][a]	0.43 ~ 0.67†	$2.57^{+4.1}_{-1.25}$	1.17 ± 0.30‡	4.88 ± 0.70	−0.14 ± 0.01
(5)	Kleinknecht [317][b]	0.52 ± 0.06				
	SU (6)$_W$ value	2/3	5/3	2/3	5/3	−1/3

[a] Fit to the baryon decay widths (or partial-wave amplitudes). (In these analyses (1) and (4) use the barrier factor of type p^{2l}, and (3) uses that of Blatt and Weisskopf [75].)
[b] The value obtained from hyperon leptonic decay using the PCAC [91].
† The value from $g^2_{\pi NN}$, $g^2_{KN\Lambda}$ and $g^2_{KN\Sigma}$.
‡ This value ($F/D > 1$) contradicts with the observed sign of $\bar{K}N \to \Sigma \to \pi\Lambda$.

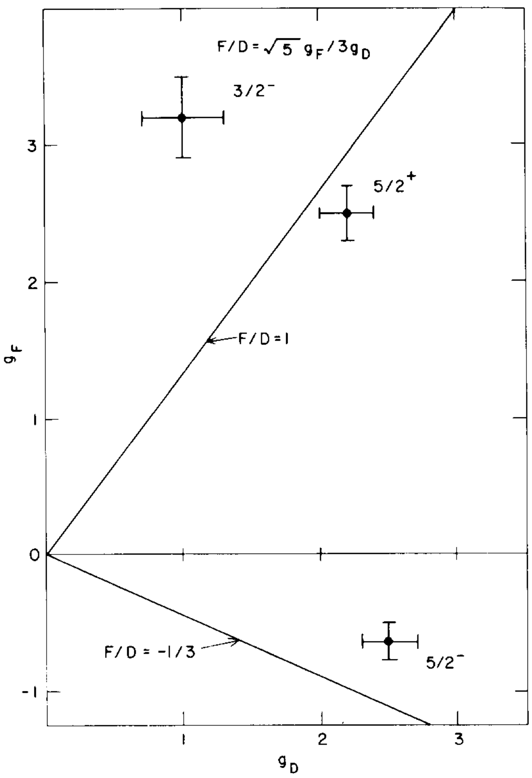

Fig. 10. Typical values of g_F and g_D ($F/D = \sqrt{5}g_F/3g_D$) for the decay of the baryon octets ($3/2^-$, $5/2^+$, $5/2^-$) into $0^-\,1/2^+$. The data are taken from Plane et al. [411] (from Schmid [451]).

In this way the coupling patterns of the parent baryon resonances can be understood by exchange-degeneracy arguments. The stronger the resonance couplings to the external particles are, the better the exchange degeneracy between the two trajectories is. On the other hand, larger deviations are observed for the trajectories with weaker couplings, particularly when the exchange degeneracy is required only through the symmetry. Conversely, even a large deviation from exchange degeneracy in such a case will not break the duality constraints so much. The exchange-degeneracy patterns for baryons are summarized in table 6.

The t-channel Reggeon couplings

Equation (3.21) together with eq. (3.20) gives the following relation for the t-channel Reggeon couplings [430];

$$\gamma^2_{V_8 B\bar{B}} = \gamma^2_{T_8 B\bar{B}} = \gamma^2_{T_1 B\bar{B}}; \qquad [F/D]_{VB\bar{B}} = [F/D]_{TB\bar{B}}. \tag{3.23}$$

If there are mass breakings in the t-channel Reggeons, we have the ideal-mixing nonet, and the $\phi(f')$ decouples from $N\bar{N}$ [480]. This decoupling is supported by the Regge-pole analysis at $t = 0$ [52], as well as by the absence of backward peaks in the reaction $\bar{K}N \to (\Lambda, \Sigma)\phi$ [e.g., 152, 444, 149].

The F/D ratio of the t-channel Reggeon coupling is, however, left arbitrary since the relative contributions from $\tau P = +$ and $\tau P = -$ baryon resonances are still left to be free. Experimentally it has different values for the s-channel helicity nonflip and flip amplitudes. We list in table 7 the

Table 6

Observed patterns of baryon exchange degeneracies. Horizontal: exchange degeneracy. Vertical: SU (3) multiplets.

$\tau P = +$ series

J^P	$1/2^+$		$3/2^-$		$5/2^+$		$7/2^-$		$9/2^+$		
	$\underline{8}_1$		$\underline{1} \oplus \underline{8}_1$		$\underline{8}_1$		$\underline{1} \oplus \underline{8}_1$		$\underline{8}_1$		
Λ	Λ_α	$\leftrightarrow$	$\begin{Bmatrix} \Lambda_\gamma(1520) \\ \Lambda_\gamma(1690) \end{Bmatrix}$	$\leftrightarrow$	$\Lambda_\alpha(1815)$	$\leftrightarrow$	$\begin{Bmatrix} \Lambda_\gamma(2100) \\ ? \end{Bmatrix}$	$\leftrightarrow$	$\Lambda_\alpha(2350)$?	$\leftrightarrow \ldots$	$\Delta\alpha \simeq 0$
Σ	Σ_α	$\leftrightarrow$	$\Sigma_\gamma(1670)$	$\leftrightarrow$	$\Sigma_\alpha(1915)$	$\leftrightarrow$	$\Sigma_\gamma(2100)$	$\leftrightarrow$	?	$\leftrightarrow \ldots$	$\Delta\alpha \simeq 0.25$
N	N_α	$\leftrightarrow$	$N_\gamma(1520)$	$\leftrightarrow$	$N_\alpha(1688)$	$\leftrightarrow$	$N_\gamma(2190)$	$\leftrightarrow$	$N_\alpha(2220)$	$\leftrightarrow \ldots$	$\Delta\alpha \simeq 0.4$
F/D	$0.5 \sim 0.6$		~ 2		$0.6 \sim 0.8$		~ 4				

$\tau P = -$ series

J^P	$3/2^+$		$5/2^-$		$7/2^+$		$9/2^-$		
	$\underline{10}(\oplus \underline{8}_{-1/3})$		$\underline{8}_{-1/3}$		$\underline{10} \oplus \underline{8}_{-1/3}$		$\underline{8}_{-1/3}$		
Σ	$\Sigma_\delta(1385)$	$\leftrightarrow$	$\Sigma_\beta(1765)$	$\leftrightarrow$	$\begin{Bmatrix} \Sigma_\delta(2030) \\ ? \end{Bmatrix}$	$\leftrightarrow$	$\Sigma_\beta(2250)$?	$\leftrightarrow \ldots$	$\Delta\alpha \simeq 0.1$
Δ, N	$N_\delta(1232)$	$\leftrightarrow$	$N_\beta(1670)$	$\leftrightarrow$	$\begin{Bmatrix} \Delta_\delta(2050) \\ N_\delta(1990) \end{Bmatrix}$	$\leftrightarrow$	?	$\leftrightarrow \ldots$	$\Delta\alpha \simeq 0.1$
Λ			$\Lambda_\beta(1830)$	$\leftrightarrow$	$\Lambda_\delta(2020)$?	$\leftrightarrow$	?	$\leftrightarrow \ldots$	?
F/D			$-0.1 \sim -0.2$		?				

Table 7

F/D values of the t-channel Reggeon coupling for the s-channel helicity amplitudes

	$[F/D]_{++}$	$[F/D]_{+-}$
photon coupling ($J = 1, t = 0$)	∞	~ 0.31
σ_{tot} Regge-pole fit		
Michael [366] (using Berger–Fox fit [63])	≈ -5	
Barger, Phillips [55]	$-3 \sim -4$	
Barger [33] (FNAL data)	$\lvert F/D \rvert > 10$	
s-channel helicity conservation of f and ω		1/3
$\pi^- p \to \pi^0 n$ and $K^0_L p \to K^0_S p$		
Johnson et al. [306]	$-6.8 {}^{+1.3}_{-2.0}$	
Loos, Matthews [336]	-5.3	0.32
K^*–K^{**} exchange reactions		
Irving et al. [297]	-2.8	0.38
Martin et al. [357]	$-3.3 \sim -3.5$	$0.28 \sim 0.49$
Ward et al. [504]	-3.25	0.49
photoproduction		
Irving, Vanryckeghem [298] (π^0, η)	-3	0.38
Michael, Odorico [367] ($K\Lambda$, $K\Sigma$)	-2	0.27 ± 0.03
tensor-meson dominance (Renner [418])		1/3

values of $[F/D]_{+\pm}$ for the respective s-channel amplitudes. We can see from this table that $D/F \approx -0.2$ for the nonflip amplitude† ($\sim A'$) and $F/D \approx 1/3$ for the flip amplitude ($\sim A$). Using $[\nu B/A']_\rho \approx 10$, we get $F/D \approx 0.5$ for the t-channel helicity-flip amplitude ($\sim B$).‡ (See also [366, 367, 451] for reviews.)

Crossing invariance

The s-, t- and u-channels are identical in 0^-–0^- scattering, so that the spectrum of the t-channel Reggeons must go into the same spectrum in the s- and u-channels under (s,t) and (u,t) crossing. Actually, the SU (3) vector $\frac{16}{3}[1] + \frac{5}{3}[8_D] + 3[8_F]$ of the solution $(\underline{1} \oplus \underline{8}) \leftrightarrow \underline{8}$ (eq. (3.20)) is an even eigenvector of the SU (3) crossing matrix, thus ensuring the crossing invariance.

Similarly in 0^-–$1/2^+$ scattering, the s- and u-channels are identical. Therefore, the $s(u)$-channel baryon spectrum must go into the same spectrum in the $u(s)$-channel under the (s,u) crossing. Since we have both crossing-even and -odd amplitudes in this case, we must find even and odd eigenvectors of the (s,t) crossing matrix by suitable linear combinations of the natural- and unnatural-parity exchange-degenerate pairs. This requirement of crossing invariance would fix the relative strength of the couplings of the natural and unnatural baryon trajectories. Hence it determines the F/D ratios of the t-channel Reggeon.

In such an attempt, an (s,t) crossing even vector can be made by an appropriate combination of exchange-degenerate pairs of eq. (3.22); it can be given by the difference of the SU (3) vectors corresponding to (i) and (ii) [340, 23, 421]. However, no crossing-odd vectors can be constructed from any combination of eq. (3.22).

The task is to find a pair of SU (3) vectors (I, II) being interchanged with each other under the (s,u) crossing operation out of exchange-degenerate solutions. Then the combinations I $\pm$ II form even and odd or odd and even eigenvectors according to I $\rightleftarrows \pm$ II. Here the two solutions I and II correspond to those with natural and unnatural parities. To see the structure of scattering amplitudes, we begin by noting that the imaginary part of s-channel helicity amplitude $\bar{f}_{+\pm}$ is expressed as the sum and difference of the resonance sequences with unnatural and natural parities, i.e., $\mathrm{Im}\,\bar{f}_{++} \sim \mathrm{II} + \mathrm{I}$ and $\mathrm{Im}\,\bar{f}_{+-} \sim \mathrm{II} - \mathrm{I}$. These amplitudes are also described in terms of the bivariate dual terms as $\bar{f}_{++} \sim B(s,u)$ and $\bar{f}_{+-} \sim A'(s,u)$ for $s \to \infty$, u fixed (see Appendix A). Therefore, $\mathrm{Im}\,B(s,u) \sim \mathrm{II} + \mathrm{I}$ is odd and $\mathrm{Im}\,A'(s,u) \sim \mathrm{II} - \mathrm{I}$ is even under (s,u) crossing if I $\rightleftarrows -$ II.§ (The full amplitudes are obtained by multiplying the appropriate signature factors [167, 212].)

This problem can be solved by making use of a pair of four-trajectory solutions $(\underline{1} \oplus \underline{8}) \leftrightarrow (\underline{8} \oplus \underline{10})$. We find the baryon spectrum [167, 212].

$$\mathrm{I}: (\underline{1} \oplus \underline{8}_{f_1})_\gamma \overset{\mathrm{EXD}}{\leftrightarrow} (\underline{8}_{f_1'} \oplus \underline{10})_\alpha \overset{X_{su}}{\rightleftarrows} \mathrm{II}: (\underline{1} \oplus \underline{8}_{f_2})_\beta \overset{\mathrm{EXD}}{\leftrightarrow} (\underline{8}_{f_2'} \oplus \underline{10})_\delta \tag{3.24}$$

with $f_1 + 3f_1 f_2 + f_2 = 1$. Here f_1' and f_2' are given by f_1 and f_2 respectively, so that we have one free parameter in this solution. (If we choose this parameter so as to give $f_1' \equiv [F/D]_{8\alpha} = 2/3$ the $\underline{1}_\beta$ decouples from the external meson-baryon system.) The t-channel Reggeon F/D ratios in this

†The Johnson–Treiman relations, $\Delta\sigma(\mathrm{K}^\mp \mathrm{p}) = 2\Delta\sigma(\mathrm{K}^\mp \mathrm{n}) = 2\Delta\sigma(\pi^\pm \mathrm{p})$, implying $D/F = 0$, [305] are satisfied at FNAL energies [33], better than at lower energies.

‡With the aid of the vector-dominance model, the amplitudes $(A + \nu B, A)$ are related to the Dirac–Pauli form factors $(F_1, -F_2)$, while $((1 - t/4M^2)\cdot A', \nu B)$ correspond to the Sachs form factors (G_E, G_M). The SU (6) leads to $D/F = 0$ for A' and $F/D = 2/3$ for B. See Michael [366].

§The interchange I $\rightleftarrows -$ II under the (s,u) crossing implies that the natural-parity trajectory in the s-channel goes into the unnatural-parity trajectory in the u-channel and vice versa.

solution are $[F/D]_V = [F/D]_T = 1/3$ for the amplitude $A(s,t) \sim \bar{f}_{+-} \sim \mathrm{II} - \mathrm{I}$ and in addition the singlet tensor is decoupled from this amplitude, which leads to the decoupling of the f and ω from this amplitude. For the amplitude $A'(s,t) \sim \bar{f}_{++} \sim \mathrm{II} + 1$, the t-channel F/D ratios become $[F/D]_V = [F/D]_T \ll -1$ in agreement with experiments if we choose the above parameter so as to reproduce the actual baryon-resonance couplings. (For $[F/D]_{8\alpha} = 2/3$, we have $[F/D]_V = [F/D]_T = -7/3$.) We list typical F/D ratios in table 8, which should be compared with experimental values in tables 5 and 7. It should also be noted that the choice of $2/3 < [F/D]_{8\alpha} < 1$ correctly predicts the alternation of F/D ratios for the α–γ series around one.

3.6. Duality diagrams

As a consequence of the exchange degeneracy, the Reggeon vertices take the nonet couplings:

$$\Gamma_{M_1 VM_2} = \frac{1}{\sqrt{2}} \gamma_{VMM} \mathrm{Tr}(M_1[V,M_2]) \tag{3.25}$$

$$\Gamma_{M_1 TM_2} = \frac{1}{\sqrt{2}} \gamma_{TMM} \mathrm{Tr}(M_1\{T,M_2\}) \tag{3.26}$$

with $\gamma_{VMM} = \gamma_{TMM} (\equiv \gamma_M)$

$$\Gamma_{\bar{B}_1 RB_2} = \frac{1}{\sqrt{2}} \gamma_{RB\bar{B}} \{F_R \mathrm{Tr}(\bar{B}_1[R,B_2]) + D_R \mathrm{Tr}(\bar{B}_1\{R,B_1\}) + (F_R - D_R)\mathrm{Tr}(\bar{B}_1 B_2)\mathrm{Tr}R\}, \qquad R = T,V, \tag{3.27}$$

with $\gamma_{VB\bar{B}} = \gamma_{TB\bar{B}} (\equiv \gamma_B)$ and $[F/D]_V = [F/D]_T$.

Here M and B are the 3×3 matrices of 0^- and $1/2^+$ octets, and V and T denote the vector- and tensor-nonet matrices [480].† The absence of the term $\mathrm{Tr}(M_1 M_2)\mathrm{Tr}T$ in eq. (3.26) is required by $\gamma^2_{T_1} = \gamma^2_{T_8}$, and the last term in eq. (3.27) ensures f′ and ϕ to decouple from nucleons.

Equations (3.25) and (3.26) are represented by the diagram (a) in fig. 11 in terms of quarks. (Note that the indices of meson matrix are just that of quarks.) Using the representation $B^{ij,k}$ $(B^i_j \equiv (1/\sqrt{2})\epsilon^{ikl}B_{kl,j})$ in which the quark indices are explicit, eq. (3.27) leads to

$$\Gamma_{\bar{B}_1 RB_2} = \frac{\gamma_B}{\sqrt{2}} M^k_j [(\bar{B}_1)^{mn,j}(B_2)_{mn,k} + (F-D)\{(\bar{B}_1)^{mj,l}(B_2)_{mk,l} + (\bar{B}_1)^{jn,l}(B_2)_{kn,l}\}]. \tag{3.28}$$

Table 8
Predicted F/D ratios for the baryon octets and those for the t-channel Reggeons in the crossing-invariant solution of exchange degeneracy. The underlined value is the input of calculation. The values should be compared with those in table 5 and 7.

$\underline{8}_\alpha$	$\underline{8}_\beta$	$\underline{8}_\gamma$	$\underline{8}_\delta$	$\bar{f}_{++}$	$\bar{f}_{+-}$
$\underline{2/3}$	−1/3	∞	−1/3	−7/3	1/3
$\underline{0.82}$	−0.16	2.20	−1.45	−130	1/3

†See footnote on page 260. Note that $M = (1/\sqrt{2})\, \Sigma\lambda_\alpha\phi_\alpha$, $B = (1/\sqrt{2})\, \Sigma\lambda_\alpha\psi_\alpha$ etc., and $\mathrm{Tr}(\lambda_\alpha[\lambda_\beta,\lambda_\gamma]) = 4if_{\alpha\beta\gamma}$, $\mathrm{Tr}(\lambda_\alpha\{\lambda_\beta\lambda_\gamma\}) = 4d_{\alpha\beta\gamma}$.

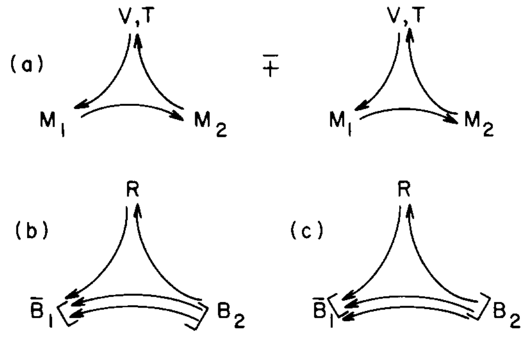

Fig. 11.

Here the first term corresponds to the diagram (b) and the second to (c) in fig. 11 (in this figure square brackets mean the antisymmetrization of quark wave functions). Thus, only connected diagrams appear for Reggeon vertices, and two ends of a single quark line cannot belong to the same external particle (the OZI rule) [390, 518, 285, 286].

Suppose we consider scattering $AB \to \bar{D}\bar{C}$ (we adopt here the convention that all external particles are incoming). The Regge amplitude for this process is

$$f(\nu,t) = \Gamma_{AVD}\Gamma_{CVB}\,\frac{1-e^{-i\pi\alpha}}{\sin\pi\alpha}\,\nu^{\alpha} + \Gamma_{ATD}\Gamma_{CTB}\,\frac{-1-e^{-i\pi\alpha}}{\sin\pi\alpha}\,\nu^{\alpha}. \tag{3.29}$$

Substituting eqs. (3.25)–(3.28) into eq. (3.29) and contracting the quarks of V and T, we obtain the following expression [425]: For $M_1M_2 \to \bar{M}_4\bar{M}_3$

$$f(\nu,t) = 2\gamma_M^2\Big\{[(M_1)_i^j(M_2)_j^l(M_3)_l^k(M_4)_k^i + (M_4)_i^j(M_3)_j^l(M_2)_l^k(M_1)_k^i]\,\frac{-\exp(-i\pi\alpha_{j\bar{k}})}{\sin\pi\alpha_{j\bar{k}}}$$
$$+\,[(M_1)_i^j(M_3)_j^l(M_2)_l^k(M_4)_k^i + (M_4)_i^j(M_2)_j^l(M_3)_l^k(M_1)_k^i]\,\frac{-1}{\sin\pi\alpha_{j\bar{k}}}\Big\}\,\nu^{\alpha_{j\bar{k}}(t)}. \tag{3.30}$$

For $M_1B_2 \to \bar{M}_4\bar{B}_3$

$$f(\nu,t) = 2\gamma_M\gamma_B\{(\bar{B}_3)^{mn,j}(B_2)_{mn,k} + (F-D)\,[(\bar{B}_3)^{mn,p}(B_2)_{mk,p} + (\bar{B}_3)^{jn,p}(B_2)_{kn,p}]\}$$
$$\times\left[(M_4)_j^l(M_1)_l^k\,\frac{-\exp(-i\pi\alpha_{k\bar{j}})}{\sin\pi\alpha_{k\bar{j}}} + (M_1)_j^l(M_4)_l^k\,\frac{-1}{\sin\pi\alpha_{k\bar{j}}}\right]\nu^{\alpha_{k\bar{j}}(t)}. \tag{3.31}$$

Here the factor like $\mathrm{Tr}(M_1M_2M_3M_4)$, $\mathrm{Tr}(M_1M_3M_2M_4)$ etc. is called the Paton–Chan factor [398].

The term with rotational phase and the term with real phase in eqs. (3.30) and (3.31) are expressed by diagrams (a) and (b) in figs. 12 and 13, respectively. In fig. 12 we omit another diagram with quark lines in an opposite direction.) The planar diagram (a) shows that there are resonances in the s-channel, Reggeons in the t-channel, exhibiting duality among both channels. Needless to say, there are no singularities in the u-channel as it is exotic. On the other hand, in the non-planar diagram (b) the s-channel is exotic and has no resonances. The t-channel Regge poles in this case are built by the u-channel resonances. The diagram (b) becomes planar when particles 2 and 3 are exchanged, exhibiting duality between the u- and t-channels.

Therefore, the following simple rule has been derived for the *duality diagram* [288, 245, 425].

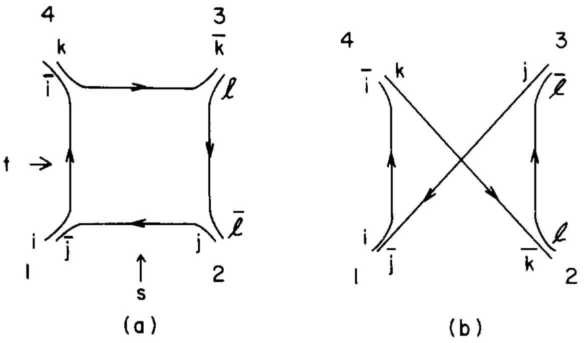

Fig. 12.

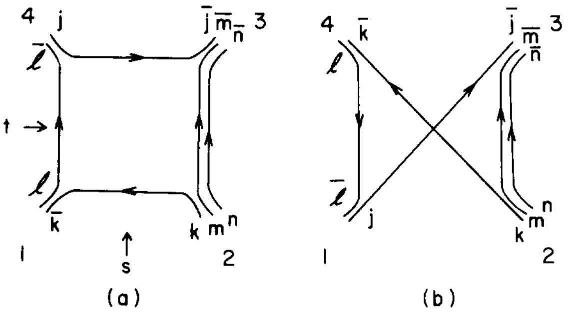

Fig. 13

(i) Represent mesons by $q\bar{q}$ and baryons by qqq.
(ii) Write all the connected graphs, connecting the same kind of quarks.† The two ends of a single quark line should not belong to the same external particle, the diagram as a whole must not be disconnected (the OZI rule).
(iii) A given graph will then exhibit duality among the channels in which it can be written in the planar form.

These kinds of graphs are generally called duality diagrams or quark diagrams. The duality diagram asserts that *any scattering amplitude can be written as a sum of bivariate dual amplitudes* in which singularities lack in one of the three channels (planar duality). There are only three types of duality diagrams, the (s,t), (u,t) and (s,u) dual diagrams‡ which are sometimes called the H-, X-, and Z-type diagrams, respectively. For instance, the reactions $\pi^+\pi^- \to \pi^+\pi^-$ and $\bar{K}N \to \bar{K}N$ are of (s,t) dual and $\bar{K}N \to K\Xi$ is of (s,u) dual.

The above rules are easily generalized to those for any hadronic process.

Exchange degeneracies in hypercharge-exchange reaction

As an interesting example, let us consider $K^-n \to \pi^-\Lambda$. We have no (s,t) dual term but only (s,u) and (u,t) terms, as shown in fig. 14, which indicates that the amplitude for $K^-n \to \pi^-\Lambda$ is purely real for large s with t fixed, even though no channel is exotic. This implies the s-channel resonances should cancel each other. This is also a kind of exchange degeneracy, and is often called "anti-exchange degeneracy". Correspondingly, the K^* and K^{**} trajectories are exchange degenerate in the t-channel giving a real phase, just as in the reaction with the exotic s-channel. Similar arguments also hold for $\bar{K}N \to \pi\Sigma$.

In fig. 15, we show the Y_1^* couplings in the reaction $\bar{K}N \to \pi\Lambda$ at $t = m_{K^*}^2$, [455]. The parent resonances on the Σ_α–Σ_γ($1/2^+$–$3/2^-$–$5/2^+$–...) and the Σ_δ–Σ_β($3/2^+$–$5/2^-$–$7/2^+$–...) tend to cancel each other independently in each amplitude, A' or B. Table 9 shows the signs of parent Y^* resonances in $\bar{K}N \to \pi\Lambda$ and $\bar{K}N \to \pi\Sigma$.

With the exchange degeneracy, the differential cross sections of $K^-n \to \pi^-\Lambda$ and $K^-p \to \pi^-\Sigma^+$ should be equal to that of the line-reversed reactions $\pi^+n \to K^+\Lambda$ (or $\pi^-p \to K^0\Lambda$) and $\pi^+p \to K^+\Sigma^+$ at $s \to \infty$, t fixed respectively. (Here the former reactions should have a real phase ~1 and the

†In order to satisfy the C-parity conservation automatically one has to keep two kinds of duality diagrams (clockwise and counter-clockwise) [454].

‡The (s,t) dual diagram has two sub-components as seen in eq. (3.31) for meson–baryon scattering. Similarly the (s,u) dual diagram is decomposed into three components. The SU (3) structure of these components has been studied [382, 223].

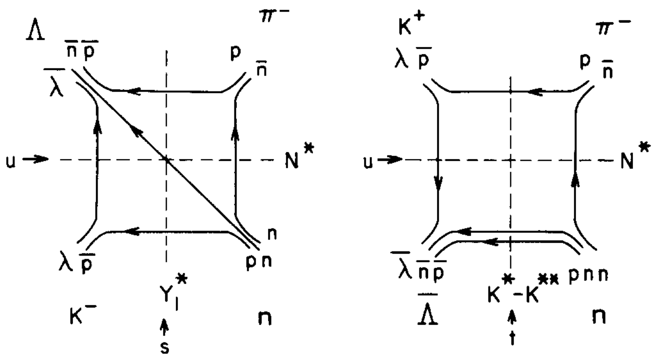

Fig. 14. The planar duality diagrams for $K^-n \to \pi^-\Lambda$.

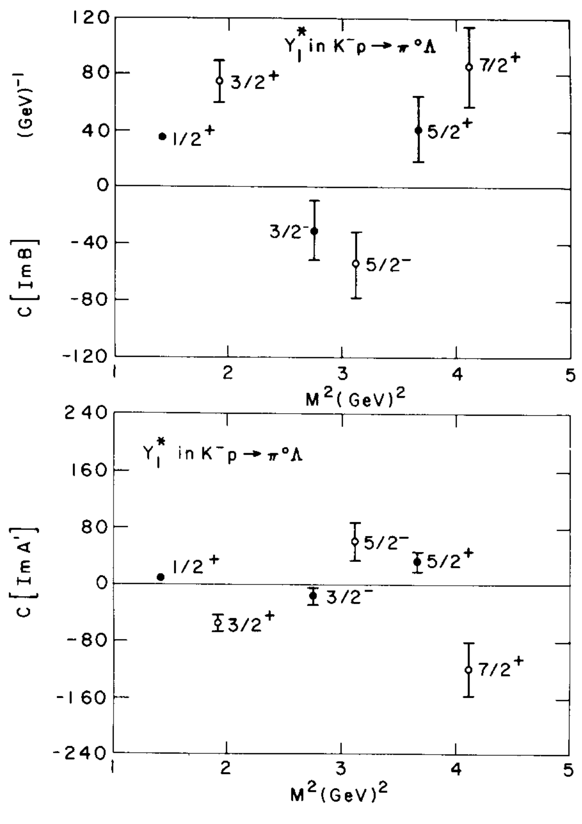

Fig. 15. Contributions of the Y_1^* in the reactions $K^-p \to \pi^0\Lambda$ at $t = m^2_{K^*}$. Here, solid circles imply the $\Sigma_\alpha - \Sigma_\gamma$ series while open circles denote the $\Sigma_\delta - \Sigma_\beta$ series (from Schmid and Storrow [455]).

latter a rotating phase $\sim e^{-i\pi\alpha}$.) These equations seem to hold well at $t = 0$, but the slopes of forward peaks are steeper in $\pi N \to K\Lambda(\Sigma)$ than in $\bar{K}N \to \pi\Lambda(\Sigma)$ [135, 323, 336]. This is, particularly, clear in the experiment in which relative normalization has been carefully done [66]. As a consequence, the integrated cross section of $\bar{K}N \to \pi\Lambda(\Sigma)$ becomes larger than that of $\pi N \to K\Lambda(\Sigma)$. This breaking of exchange degeneracy is seen by a factor of two in the cross sections even at

Table 9

Signs of the couplings of leading Y^* resonances (from Schmid [451]; see also PDG [397]). Here we adopt the meson-first convention. If the baryon-first convention is adopted, the signs of Y_0^* and Y_1^* in $\bar{K}N \to \pi\Sigma$ are reversed.

		$1/2^+$	$3/2^-$	$5/2^+$	$7/2^-$	$3/2^+$	$5/2^-$	$7/2^+$
$\bar{K}N \to \pi\Sigma$	Y_1^*	+	−	+	?	+	−	+
	Y_0^*	+	−	+	−		weak	
$\bar{K}N \to \pi\Lambda$	Y_1^*	−	+	−	?	+	−	+

$p_L \approx 15$ GeV/c, where K^-p charge-exchange cross sections are almost equal to those of K^+n charge-exchange. (We will mention this breaking in section 4.5.)

According to the FESR calculation ($\bar{K}N \to \pi\Lambda$, $\pi N \to K\Lambda$) [194; see also 300], the relation $\beta_{K^*} = \beta_{K^{**}}$ does not necessarily hold well (especially for the A' amplitude), i.e., the imaginary part of the $\bar{K}N \to \pi\Lambda$ amplitudes does not vanish. However, the features characteristic of the exchange degeneracy can still be observed:

(i) The phases of the amplitudes of $\pi N \to K\Lambda$ grow linearly as $\sim -\pi\alpha(t)$ as $-t$ increases, while those of the $\bar{K}N \to \pi\Lambda$ amplitudes are approximately fixed.

(ii) The imaginary parts of the $\pi N \to K\Lambda$ amplitudes have zeros characteristic of the Regge-pole exchange with non-vanishing imaginary part, whereas such zeros are missing in the $\bar{K}N \to \pi\Lambda$ amplitudes.

A substantial imaginary part has been found in $A'(\bar{K}N \to \pi\Lambda, \Sigma)$ also at higher energies in contrary to the prediction [47, 125, 504].† (This imaginary part is necessary to give the observed large polarizations.) A zero is missing again in Im $A'(KN \to \pi\Lambda, \Sigma)$. (But it exists in Im $A'(\pi N \to K\Lambda, \Sigma)$.) The partial-wave projection of Im $A'(\bar{K}N \to \pi\Lambda, \Sigma)$ suggests that the exchange degeneracy is broken in low-partial-wave components but it is held in peripheral components.

Remarks on the Okubo–Zweig–Iizuka (OZI) rule

The OZI rule forbids a disconnected diagram; e.g., $\phi \sim \bar{\lambda}\lambda$ cannot decay into non-strange hadrons. Actually, the partial width $\Gamma(\phi \to 3\pi) \simeq 0.66$ MeV is much suppressed compared with $\Gamma(\omega \to 3\pi) \simeq 9.0$ MeV. The suppression of disconnected diagram is also seen in production experiments (e.g., $\sigma(\pi^-p \to \phi n)/\sigma(\pi^-p \to \omega n) \simeq 0.0035 \pm 0.0010$ at $5 \sim 6$ GeV/c [25]) or in the Reggeon coupling at $t = 0$, [52]. The forbidden decay mode $\phi \to$ (non-strange hadrons) can exist only due to a deviation from the ideal mixing. The non-strange-quark component in the physical ϕ can be determined from the mass formula as well as from the production processes, and thus it is found to be about 10%, which is consistent mutually among various estimations (see table 10). There is a similar suppression in the 2^+ nonet: The upper bound of $f' \to \pi\pi$ is $\Gamma(f' \to \pi\pi)/\Gamma(f' \to \text{all}) \lesssim 1/100$ or $\Gamma(f' \to \pi\pi)/\Gamma(f \to \pi\pi) \lesssim 1/400$ [70]. The Regge residues are also consistent with the decoupling of f' from nucleons at $t = 0$, [52].

One may suppose that such a higher order vertex diagram as in fig. 16a, which violates the OZI rule, may contribute to the decay $\bar{\lambda}\lambda \to$ (non-strange hadrons). If this diagram is regarded as equivalent to that in fig. 16b, which represents an allowed vertex with particle mixing, violation of the OZI rule is given by the mass mixing.

†In these analyses the Regge phase is assumed for the K^* and K^{**} exchange in the s-channel helicity-flip amplitude.

Table 10
Deviations from the ideal mixing for 1^- and 2^+. Here ϵ is defined as $\omega(\mathrm{f}) = (\bar{\mathrm{p}}\mathrm{p} + \bar{\mathrm{n}}\mathrm{n})/\sqrt{2} + \epsilon\bar{\lambda}\lambda$.

1^-: mass formula	$\epsilon = -9.2 \pm 2.5\%$
$\Gamma(\phi \to \pi^0\gamma)^a/\Gamma(\omega \to \pi^0\gamma)$	$\lvert\epsilon\rvert \simeq 9.7\%$ or 5.3%
$\Gamma(\phi \to \rho^0\pi^0)^b/\Gamma(\omega \to \pi^0\gamma)$	$\lvert\epsilon\rvert \lesssim 12\%$
$\sigma(\pi^-\mathrm{p} \to \phi\mathrm{n})^c/\sigma(\pi^-\mathrm{p} \to \omega\mathrm{n})$	$\lvert\epsilon\rvert \simeq 6\%$
2^+: mass formula	$\epsilon = +10.5 \pm 5.0\%$
$\Gamma(\mathrm{f}' \to \pi\pi)^d/\Gamma(\mathrm{f} \to \pi\pi)$	$\lvert\epsilon\rvert \lesssim 3.5\%$
$\Gamma(\mathrm{f}' \to \pi\pi)^e/\Gamma(\mathrm{f} \to \pi\pi)$	$\epsilon = +5.1 \pm 2.0\%$
fit to the $2^+ \to 0^- + 0^-$ decay[f]	$\epsilon = +2 \pm 22\%$

[a]Benaksas et al. [62] or Cosme et al. [522].
[b]Assuming the $\phi \to \rho\pi$ dominance in the $\phi \to 3\pi$ decay.
[c]Ayres et al. [25].
[d]Beusch et al. [70].
[e]Pawlicki et al. [523]: The f–f′ interference is known in $\pi\mathrm{N} \to \mathrm{K}^-\mathrm{K}^+\mathrm{N}$.
[f]Samios et al. [440]. We take the decay widths from PDG [397] unless otherwise specified.

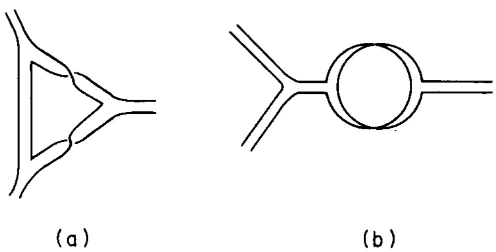

Fig. 16.

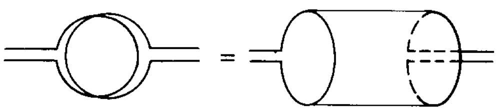

Fig. 17.

The Paton–Chan factor corresponding to the diagram in fig. 17[†], which is often called the cylinder diagram, suggests that the breaking of the OZI rule occurs in a unitary singlet since $\Sigma_{x,y}\mathrm{Tr}(\lambda_i\lambda_x\lambda_y) \cdot \mathrm{Tr}(\lambda_j\lambda_x\lambda_y) = 2\,\mathrm{Tr}(\lambda_i)\mathrm{Tr}(\lambda_j) = 12\delta_{i0}\delta_{j0}$. Indeed the masses of the neutral vector and tensor mesons are given by the eigenvalues of the mass-squared matrix

$$\begin{bmatrix} m_0^2 & \delta & \delta \\ \delta & m_0^2 & \delta \\ \delta & \delta & m_0^2 + \Delta m^2 \end{bmatrix},$$

where the breaking occurs in an SU (3) singlet [14]. (Here we take a vector ($\bar{\mathrm{p}}\mathrm{p}$, $\bar{\mathrm{n}}\mathrm{n}$, $\bar{\lambda}\lambda$) as a basis

[†]This diagram should contribute to $1^-(C = -)$ and 2^+ $(C = +)$ with equal strengths but in opposite signs. This can easily be seen if we keep two diagrams which differ as to the direction of their quark lines. (Note that $|C = \pm\rangle = |\bar{q}q\rangle \pm |q\bar{q}\rangle$.)

of the matrix.) This singlet contribution brings a renormalization of the f and f′ trajectories as well as a mixing between them.

The cylinder diagram is also considered to give the pomeron for the $C = +$ channel† [206, 237, 210, 341]. We consider the t-channel partial wave of $\pi\pi$ scattering amplitude in the $I_t = 0$ channel, then the J-plane structure is given by

$$F(J,t) = g\,\frac{1}{J-\alpha_{\rm f}}\,g + g\,\frac{1}{J-\alpha_{\rm f}}\,G\,\frac{1}{J-\alpha_{\rm P}}\,G\,\frac{1}{J-\alpha_{\rm f}}\,g, \tag{3.32}$$

where g and G denote the $\pi\pi$f residue and the pomeron-f (cylinder-f) coupling, respectively. The second term‡ (cylinder term) corresponds to the pomeron, which couples to the external particles through f (and/or f′) [341, 96] (see also section 5.6). This term gives a leading contribution as $s \to \infty$, with t fixed,

$$F(s,t) \simeq \pi\left(\frac{g}{\alpha_{\rm P}-\alpha_{\rm f}}\right)^2 G^2\,\frac{-1-\exp(-{\rm i}\pi\alpha_{\rm P})}{\sin\pi\alpha_{\rm P}}\,(\alpha' s)^{\alpha_{\rm P}}.$$

On the other hand, this cylinder term represents the particle-mixing interaction. Equation (3.32) reads

$$F(J,t) \simeq \frac{g^2}{J-(\alpha_{\rm f}+\Delta\alpha_{\rm f})}, \qquad \Delta\alpha_{\rm f} \approx G_{\rm f}^2/(J-\alpha_{\rm P}). \tag{3.33}$$

Hence, we have the f trajectory shifted by $G^2/(\alpha_{\rm f}-\alpha_{\rm P})$ due to the cylinder correction. (If we keep higher-order terms in eq. (3.32), the pomeron trajectory is also shifted.) Corresponding to $\sigma^{\rm tot}(\pi\pi) \simeq 12$ mb, we have $G^2 \simeq 0.07$, or $\alpha_\rho(0) - \alpha_{\rm f}(0) \approx 0.14$ (here $g^2_{{\rm f}\pi\pi}/4\pi = g^2_{\rho\pi\pi}/4\pi = 2$ is assumed). (This is consistent with $\alpha'(m^2_{\rm A_2} - m^2_{\rm f}) \approx 0.1$, if $\alpha'_{\rm P} = 0$.) This implies that a contribution of the pomeron at high energy is consistent with the f–f′ mixing which is fairly small [512].

Another approach has recently been developed by combining the duality diagram with the unitarity. A brief sketch will be found in the note added at the end of section 5.6.

3.7. The $B\bar{B}$ problem

In the preceding sections, we have confined our discussions to MM and MB scattering. It has been known that no non-trivial solution to the duality constraints, eq. (3.17), exists in $B\bar{B}$ scattering. This can easily be seen in $\Delta\bar{\Delta} \to \Delta\bar{\Delta}$ scattering, in which there are four isospin amplitudes ($I = 0 \sim 3$) in both s- and t-channels. The (s,t) crossing relation, eq. (3.17a), has no nontrivial solution with only $I = 0$ and 1 contributions in both channels.

The simplest way to keep duality is to introduce exotic mesons [424, 435]. This can be demonstrated in the duality diagrams.§ There are two types of planar diagrams appearing in $B\bar{B}$ scattering: One corresponds to ordinary resonances in the s-channel, which is dual to exotic exchanges $(\overline{qq\bar{q}\bar{q}})$ in the t-channel (fig. 18a), and the other to ordinary Regge exchanges being dual to exotic resonances in the s-channel (fig. 18b). In this picture, the exotic resonances should have a

†In the dual resonance model, the nonplanar-orientable loop has a peculiar singularity: a branch point at $\alpha_{\rm c}(t) = 1/3 + 1/2\cdot\alpha' t$, independent of the intercept of input trajectory [237, 210]. This singularity becomes a pole ($\alpha_{\rm P} = 2 + 1/2\cdot\alpha' t$) at the critical dimension $d = 26$ for the Reggeon trajectory $\alpha_{\rm R} = 1 + \alpha' t$, [341].

‡In this context we have assumed originally a singularity near $\alpha_{\rm P}(0) = 1$ for the cylinder, [512]. There is another attempt without assuming such singularity [423].

§An explicit dual model for $B\bar{B}$ scattering can be constructed by introducing these exotic mesons [202].

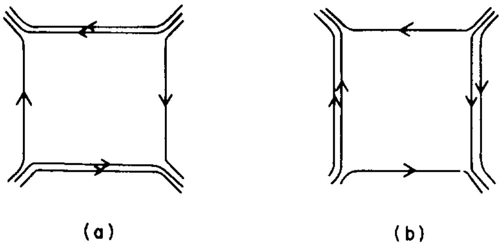

Fig. 18. The planar diagrams for $B\bar{B}$ scattering.

dominant role at low energies, since high energy amplitudes are dominated by Regge-pole exchanges. There are some indications in inclusive reactions that the s-channel resonances build Regge trajectories with low intercept such as $\alpha(0) \approx -0.5$. (It will be mentioned in section 3.9.)

These exotic mesons, introduced here, do not couple to MM channels. In the planar diagrams in fig. 18, they always appear in combinations as $qq\bar{q}\bar{q}$ in such a way that they can not be separated in two parts having triality zero. If we keep the rule that the two ends of a single quark line should not belong to the same external particle, the exotic meson $M_4 = qq\bar{q}\bar{q}$ is forbidden to decay into MM and can only decay to $B\bar{B}(+nM)$, so that it does not appear in the MM and MB scattering at least in lowest-order duality diagrams [207]. This property can be visualized in a string picture of hadrons [378, 379, 482] (see fig. 19).

3.8. Veneziano models (B_4 models)

A crossing-symmetric model which manifestly exhibits duality between two channels was firstly obtained by Veneziano [492], as a solution of the FESR bootstrap for $\pi\pi \to \pi\omega$ [2] within the narrow-width approximation.

Let us take $\pi\pi$ scattering as a simple example to elucidate the model. The Veneziano amplitude for $\pi^+\pi^-$ scattering [337, 469, 468] becomes

$$B_4(s,t) = -\lambda \frac{\Gamma(1-\alpha(s))\Gamma(1-\alpha(t))}{\Gamma(1-\alpha(s)-\alpha(t))} \tag{3.34}$$

with $\alpha(s) = \alpha' s + \alpha_0$.

The prominent features of the B_4 amplitude (3.34) are as follows:

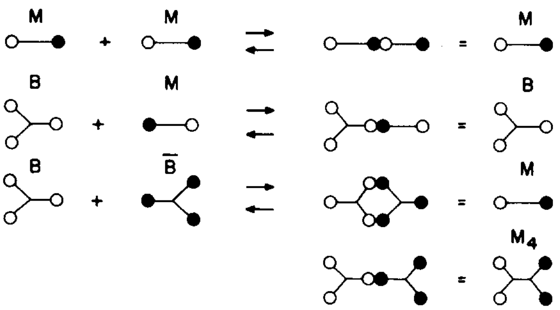

Fig. 19. String picture of hadronic reactions. Open and solid points represent quark and anti-quark, respectively.

(i) $B_4(s,t)$ has simple poles at $\alpha(s) = n$ (n is a positive integer), and can be expressed as a sum of them

$$B_4(s,t) = \lambda \sum_{n=1}^{\infty} \frac{R_n(t)}{n - \alpha(s)} \tag{3.35}$$

for $\alpha(t) < 0$. Here,

$$R_n(t) = \binom{\alpha(t) + n - 1}{n - 1} = \frac{\alpha(t)\,(\alpha(t) + 1) \ldots (\alpha(t) + n - 1)}{(n-1)!}\,. \tag{3.36}$$

Since $\alpha(t)$ is linear in t and hence in $\cos\theta_s$, this polynomial residue corresponds to resonances with $J = 0, 1, 2, \ldots, n$ in the s-channel. Similarly in the t-channel, we have

$$B_4(s,t) = \lambda \sum_{n=1}^{\infty} \frac{R_n(s)}{n - \alpha(t)} \tag{3.37}$$

which converges for $\alpha(s) < 0$.

Equations (3.35) and (3.37) are equivalent expressions. The t-channel poles (s-channel poles) are already contained in the infinite sum of the s-channel poles (t-channel poles). We have therefore a model with a manifest expression of duality. Then we can define a mathematical form of duality (Veneziano duality) by this model amplitude.

(ii) The asymptotic behaviour of $B_4(s,t)$ for large s with t fixed is given, using the Stirling formula, as

$$B_4(s,t) \to \lambda \frac{\pi}{\Gamma(\alpha(t))} \frac{-\mathrm{e}^{-i\pi\alpha(t)}}{\sin\pi\alpha(t)} (\alpha' s)^{\alpha(t)}. \tag{3.38}$$

It must be noticed, however, that the Stirling formula does not hold within an infinitesimal wedge around the positive real axis where the poles are. We therefore do not get the Regge asymptotic behaviour for the real s but obtain it off the real axis.

On the other hand, $B_4(u,t)$ has the asymptotic form

$$B_4(u,t) \to \lambda \frac{\pi}{\Gamma(\alpha(t))} \frac{-1}{\sin\pi\alpha(t)} (\alpha' s)^{\alpha(t)}. \tag{3.39}$$

Combining eq. (3.39) with eq. (3.38), we have the signatured Regge amplitude. We note that the scale parameter of the Regge amplitude is fixed as $s_0 = 1/\alpha'$. The amplitude $B_4(s,u)$ falls exponentially off the real axis as $s \to \infty$.

(iii) The B_4 amplitude explicitly exhibits the FESR duality. If we calculate $\int \mathrm{d}\nu \operatorname{Im} B_4(\nu,t)$ by substituting all resonances included in the B_4 amplitude up to $\nu = \nu_N$ (here ν is defined as $\nu = (s - u)/2$), we obtain

$$\int_0^{\nu_N} \mathrm{d}\nu \operatorname{Im} B_4(\nu,t) = \frac{\lambda}{\alpha'} \frac{\pi}{\Gamma(\alpha(t))} \frac{(\alpha' \nu_N)^{\alpha(t)+1}}{\alpha(t) + 1} \frac{1}{\Phi_N(\alpha(t))}\,, \tag{3.40}$$

where the value ν_N is taken to be half-way between the nth and $(n + 1)$th resonances, and Φ_N is a function indicating how well the resonance saturation is satisfied. The function Φ_N has the property $\Phi_N(\alpha(t)) \to 1$ for $N \to \infty$ with $\alpha(t)$ fixed, and further $\Phi_N(\alpha(t)) \simeq 1$ holds very well for $|\alpha(t)| < N$, which includes a physical region at $\nu = \nu_N$ (fig. 20).

For further details of properties of the B_4 amplitude, see [513, 514, 474].

The property (i) is in marked contrast to that in the conventional field theory where the

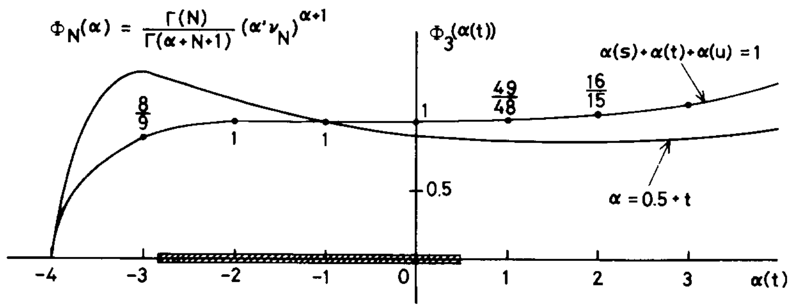

Fig. 20. An example of the Φ-function [2]. The region with hatching represents the physical region at the cut-off energy.

t-channel poles should be added to the s-channel poles. For an illustration of the relation between the dual amplitude and the conventional Feynman amplitude, we take a simple B_4 amplitude as $B_4(s,t) = \lambda\Gamma(-\alpha(s))\Gamma(-\alpha(t))/\Gamma(-\alpha(s)-\alpha(t))$. Suppose we take the limit $\alpha' \to 0$ and $\lambda \to 0$ in such a way that $g^2 = \lambda/\alpha'$ is finite and the mass of the ground state is kept fixed so that only one particle appears in each channel, then the B_4 amplitude reduces to a sum of the Born terms in the s- and t-channels [443, 377]

$$\lambda\frac{\Gamma(-\alpha(s))\Gamma(-\alpha(t))}{\Gamma(-\alpha(s)-\alpha(t))} \to \frac{\lambda}{\alpha'}\left(\frac{1}{m^2-s}+\frac{1}{m^2-t}\right).$$

Hence the dual model gives the $g\phi^3$ Lagrangian theory in the zero-slope limit. (This is also true for higher-order diagrams including loops [516].)

Equation (3.30) is immediately generalized in a crossing-symmetric form so as to construct the 0^-–0^- dual amplitudes [425, 398]. Represent mesons by $q\bar{q}$ and write all the connected diagrams. Then we obtain

$$f = \sum_{\text{perm.}} \mathrm{Tr}(M_1 M_\alpha M_\beta M_\gamma) B_4(\alpha_{i\bar{k}}(s_{1\alpha}), \alpha_{i\bar{j}}(s_{1\gamma})) \tag{3.41}$$

with $s_{1\alpha} = (p_1 + p_\alpha)^2$, $s_{1\gamma} = (p_1 + p_\gamma)^2$. Here, Σ means to take a sum over all permutations of $\alpha, \beta, \gamma = 2, 3, 4$ which give planar diagrams (see fig. 21). For instance, eq. (3.41) gives

$$f = \tfrac{1}{2}\{B_4(s,t) + B_4(u,t) - B_4(s,u)\} \qquad \text{for } \pi^+\pi^0 \to \pi^+\pi^0,$$

$$f = \tfrac{1}{2}\{B_4(s,t) + B_4(u,t) + B_4(s,u)\} \qquad \text{for } \pi^0\pi^0 \to \pi^0\pi^0. \tag{3.42}$$

The nonet scheme with ideal mixing can easily be incorporated in the B_4 amplitude, by taking the three classes of meson trajectories (eq. (3.15)) into eq. (3.41) [309].

Mathematical structures of the Veneziano model have been investigated in great detail through the operator formalism, and many interesting results have been obtained. They are, however, highly

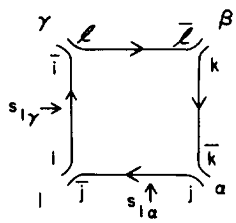

Fig. 21.

technical and too formal for our review and are not within the scope of this article. We refer the reader to review articles [6, 465, 496, 416, 201, 392, 351].

The Veneziano model itself involves some idealized assumptions (e.g., the narrow-width approximation). Therefore, it should be considered only as a mathematical model embodying duality rather than as a realistic model. This model, however, contains qualitative essence of hadronic interactions. Thus many properties abstracted from this model seem to hold in the real world.

We add some remarks for the B_4 amplitude.

Semi-local duality

The FESR such as eq. (3.40) is satisfied for any arbitrary moment if we take the B_4 amplitude. It is sufficient to take $[0,N]$ as an integration interval instead of $[N,N]$. (The FESR of this type has already been derived assuming the absence of wrong-signature fixed pole.)

Equation (3.40) with $\Phi_N \simeq 1$ suggests that only several resonances (even one resonance as an extreme case) in the interval $[0,\nu_N]$ are sufficient to give Regge behaviours at high energy, and ν_N is not necessarily to be in the asymptotic region. Further we have

$$\frac{1}{\Delta\nu}\int_{\nu_1-\Delta\nu/2}^{\nu_1+\Delta\nu/2} \mathrm{d}\nu \operatorname{Im} B_4(\nu,t) = \lambda \frac{\pi}{\Gamma(\alpha(t))} (\alpha'\nu_1)^{\alpha(t)} \frac{1}{\Phi'(\alpha(t))}. \tag{3.43}$$

Here, Φ' is very similar to Φ_N, and $\Delta\nu$ is an interval between two adjacent resonances $\Delta\nu \simeq 1/\alpha'$ ($\Delta\nu \simeq 2/\alpha'$ when trajectories are not exchange degenerate). Equation (3.43) implies that each resonance tower averaged over $1/\alpha'$ (or $2/\alpha'$) immediately gives a high-energy Regge amplitude, and conversely it ensures that the smooth Regge amplitude at high energies, if extrapolated to low energies, gives an average description of the behaviour in the resonant region in a semi-local sense. This semi-local duality gives a basis of s-channel models as will be seen in the following section.

On the other hand, if the t-channel is exotic, the FESR is of a superconvergent type and we meet with a seious cut-off problem [164, 445, 453]. Take the process $\pi^+\pi^- \to \pi^-\pi^+$ as an example. The residue of direct-channel-resonance pole grows as $\sim s^{\alpha_\rho}$ in the B_4 model, so that the relative contributions from $n = 1, 2, 3, 4, \ldots$ poles are $1{:}\,(-4.5){:}(10.4){:}(-15.7){:}\,\ldots$ at $t = 0$ in the first-moment FESR. Hence it is dangerous to cut off after a few resonances.† This is why the superconvergence relations have not been successful in practical applications. A fast drop off of the exotic amplitude in s at fixed t arises from cancellation of the neighbouring resonance towers with alternating signs when one integrates them over a sufficiently large energy interval.

Regge-residue functions

The Veneziano model gives a Regge-residue function of the form $\beta(t) = 1/\Gamma(\alpha(t))$ which is occasionally referred to. The empirical $\pi\pi$ amplitude seems to have such a Regge residue (see fig. 22).

Supplementary conditions and absence of odd-daughter resonances

Veneziano [492] has imposed a supplementary condition $\alpha(s) + \alpha(t) + \alpha(u) = 1$ on the trajectory,

†Although the cancellation is not so good, the FESR (CMSR) for $I_t = 2$, in practice, gives a low intercept of effective trajectory such as $\alpha(0) < -1$. Further the integrated amplitude does not show any characteristics of Regge-pole exchange [489].

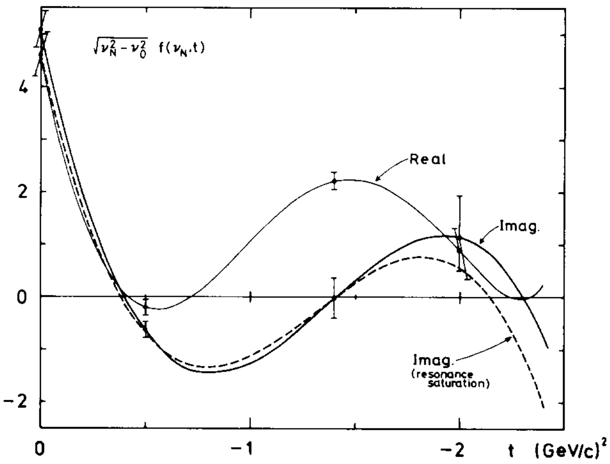

Fig. 22. The $I_t = 1$ amplitude of $\pi\pi$ scattering as a function of t from the CMSR ($\gamma = 0$ and $\gamma = 1$ in eq. (2.13)) using phase-shift data. (The cut-off is taken midway between f and g.) Note that both the imaginary and real parts show the characteristics of the ρ Regge-pole exchange (from Ukawa et al. [489]).

which is equivalent to $3\alpha(0) + 4\alpha'\mu^2 = 1$ in the case of $\pi\pi$ scattering.†‡ This condition leads to $R_n(t) = (-1)^n R_n(u)$ for the residue function, which eliminates odd daughters, leaving only daughters spaced by two units of angular momentum. Correspondingly if we make the Regge asymptotic expansion of $B_4(s,t)$ using $\mathscr{P}_\alpha(z) \equiv -Q_{-\alpha-1}(z)\tan\pi\alpha/\pi$ as

$$B_4(s,t) \sim \sum \beta_i(t)\,\mathscr{P}_{\alpha_i(t)}\,(-\nu/\nu_0),$$

the above condition also leads to $\beta_{i=\mathrm{odd}}(t) = 0$, i.e., it eliminates all odd-daughter Regge residues.

This kind of supplementary condition is automatically satisfied in the ghost-free dual resonance models owing to the Virasoro condition§ [499], so that odd-daughter resonances are absent in these models. There are some other theoretical indications suggestive of the absence of odd daughters: (i) In the quark model the odd daughters have unnatural parity, hence do not couple to 0^-–0^- systems. (ii) The same is also true for the daughters in a Lorentz pole. (iii) Partial waves of the Regge-pole amplitude contain only even daughters (see section 3.3).

We have no conclusive evidences for daughter resonances at present. However, the $\rho''(1600)$ observed in $\gamma p \to 2\pi p$, $4\pi p$ and $e^+e^- \to 4\pi$, [9, 71, 146, 31] can be assigned as the second daughter of the g(1680). On the other hand there are no firm evidences for the $\rho'(1250)$ which could be assigned as the first daughter of f(1270).

In spite of persistent efforts, partial-wave analyses of $\pi\pi$ scattering so far cannot provide any definitive evidences for daughter resonances [271, 182]: No $\rho'(1250)$ is seen in the solutions. No D-wave resonance is found at the position of the first daughter of g(1680). In the S-wave a broad enhancement can be seen at $\sqrt{s} = 0.9 \sim 1.3$ GeV after the substraction¶ of the S*, but its resonance

†If we take this condition seriously, it reduces to $\alpha_\rho(0) \approx 1/3$, which is somewhat unrealistic for the physical pion mass. However, our main purpose here is to investigate the essence implied by this condition.

‡Several attempts have also been proposed to construct dual models without any odd daughter independent of the intercept of trajectory [348, 200].

§In the scalar model, $B_4 = \Gamma(-\alpha(s))\Gamma(-\alpha(t))/\Gamma(-\alpha(s)-\alpha(t))$ with $\alpha(s) = 1 + \alpha' s$, the supplementary condition $3\alpha(0) + 4\alpha'\mu^2 = -1$ being equivalent to $\alpha(s) + \alpha(t) + \alpha(u) = -1$ is satisfied as $3 \times 1 + 4 \times (-1) = -1$. In the Neveu–Schwarz model [380], $\pi\pi$ scattering is described by eq. (3.34) with $\alpha_\rho(s) = 1 + \alpha' s$ and $\alpha_\pi(s) = 1/2 + \alpha' s$, then we have $3 \times 1 + 4 \times (-1/2) = 1$.

¶See Fujii and Fukugita [211], and Morgan [374].

interpretation is questionable. For the rest of the daughters, the situation is quite uncertain. In particular these analyses fail to confirm the $\rho''(1600)$. Therefore the elasticity of the $\rho''(1600)$ should be considerably small.

In partial-wave analyses of $K\pi$ scattering, a possibility of the S-wave resonance (κ) under K^* (890) is now excluded [358], but the S-wave phase shift passes through 90° slowly at $M_{K\pi} = 1.1 \sim 1.4$ GeV. This is claimed as a candidate for a scalar meson [196, 517, 326] which may be an SU (3) partner of the possible $\epsilon'(0.9 \sim 1.3)$.

The B_4 phenomenology

The Veneziano amplitude for $\pi^+\pi^- \to \pi^+\pi^-$ is not necessarily unique as eq. (3.34) but there are infinite degrees of freedom in adding satellite terms, which give great flexibility, i.e.,

$$f(s,t) = \sum_{n=1}^{\infty} \sum_{k=n}^{2n} C_{nk} \frac{\Gamma(n-\alpha(s))\Gamma(n-\alpha(t))}{\Gamma(k-\alpha(s)-\alpha(t))} \quad . \tag{3.44}$$

In order to give a predictive power to the model, a simplicity ansatz that there is only a minimum number of B_4 terms is usually assumed.

Semi-quantitative predictions can be made for several quantities which are not much affected by the structure of daughters and are insensitive to the necessitated unitarity corrections. For instance, the relative strength of parent resonances can correctly be predicted by the B_4 model (see table 11, for an example). Further the model gives correct phase shifts for exotic partial waves such as δ_0^2, δ_2^2 etc. in $\pi\pi$ scattering. The B_4 model is expected to be predictive also for the partial wave with $l > l$ (parent) $= \alpha(s)$, mainly because of its correct threshold behaviour (see [451]).

The B_4 model diminishes its predictive power where the narrow-width approximation does not hold and thus unitarity corrections† become important. The empirical structure of daughter resonances (or of daughter partial waves) do not seem so simple as in the B_4 model.

An application of the Veneziano model for meson–baryon scattering is very interesting as a realistic problem.‡ There have been many attempts [277, 291, 284, 412, 338, 63, 460, 292] along these lines. We mention here a model for kaon-nucleon scattering with the B_4 terms of the (s,t) type alone. The simplest model was constructed for the invariant amplitudes A and B [291]. This model gives (i) Regge asymptotic behaviour in all channels; (ii) poles for mesons at $\alpha(t) = 1,2, \ldots$, as well as for Λ's and Σ's with appropriate spins and parities. This model provides

Table 11

Elastic partial widths of parent resonances in the Veneziano model for $\pi\pi$ scattering with the ρ trajectory $\alpha_\rho(t) = 0.48 + 0.90t$. The widths are normalized to $\Gamma_\rho = 150$ MeV ($g^2_{\rho\pi\pi}/4\pi = 2.9$).

J^P	$1^-(\rho)$	$2^+(f)$	$3^-(g)$	4^+	5^-	6^+
calc.	150	129	51	46	19	17
expt. [397]	150 ± 10	141 ± 26	47 ± 12	?	?	?

†For practical applications, the unitarization is done as an expediency by introducing an imaginary part to trajectory functions [337] or by making use of a K-matrix [339, 502].

‡As for the B_5 phenomenology we refer the reader to articles by Peterson and Törnqvist [403] and by Chan et al. [110]. See also Jacob [302] for a review.

not only a strong connection between forward and backward amplitudes at high energies, but a parametrization of the variation of resonance widths as a function of their masses. Good agreement is found between the prediction and the experiment for the cross sections of KN backward scattering at small u as well as of $\bar{\mathrm{K}}$N charge exchange at small t, when the normalization of the model is given at $t = 0$. The elastic widths of Λ- and Σ-resonances, however, are predicted to be small by a factor 2 or 3† [291].

Although Veneziano model was partially successful in explaining qualitative features of high energy amplitudes, the models are confronted with well-known difficulties associated with the spin of baryons (e.g., the problem of spin crossing relation [452, 278], the parity-doubling problem). The ghost problem also becomes serious, since we deal with the trajectory with low intercept. These problems must be resolved to construct a satisfactory model for meson–baryon scattering.

3.9. Duality for Reggeon–particle scattering

In multi-particle theory of the dual model duality should hold for Reggeon–particle or for Reggeon–Reggeon scattering as well as for particle–particle scattering. Duality for Reggeon–particle (Reggeon–Reggeon) scattering can be studied through the triple-Regge (di-triple-Regge) limit of inclusive reactions.

The single-particle distribution of the inclusive reaction a + b → c + X is given by a discontinuity in $M_X^2 = (p_a + p_b - p_c)^2$ of the forward a + b + $\bar{\mathrm{c}}$ → a + b + $\bar{\mathrm{c}}$ scattering amplitude (fig. 23) [376, 477]. For $s = (p_a + p_b)^2 \gg M_X^2$, $t = (p_c - p_a)^2$, the Regge analysis for the 3-body to 3-body amplitude [155] shows

$$E_c \frac{d^3\sigma}{dp_c^3} \sim \sum s^{\alpha_i(t) + \alpha_j(t) - 1} \operatorname{disc}_{M^2} f_{ij}(\nu, t) \tag{3.45}$$

where $f_{ij}(\nu,t)$ is the forward Reggeon–particle amplitude for $\alpha_i(t) + b \to \alpha_j(t) + b$ with maximum-helicity flip in the $\mathrm{b}\bar{\mathrm{b}} \to \bar{\alpha}_i\alpha_j$ channel, and $\nu = p_b(p_a - p_c) = \frac{1}{2}(M_X^2 - t - m_a^2)$ denotes the sub-energy ($\cos\theta_{\bar{\alpha}_i \mathrm{b}}$) for this reaction (see fig. 23c). The Reggeon–particle amplitude $f_{ij}(\nu,t)$ satisfies a dispersion relation in ν like the ordinary two-body amplitude, as f_{ij} is analytic in ν and has crossing properties,

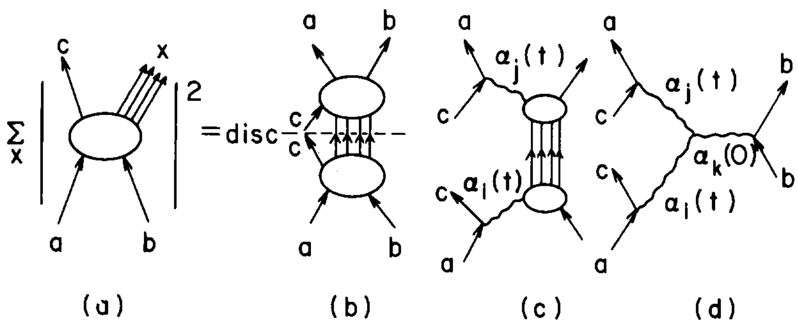

Fig. 23.

†This mismatch may be attributed to the daughters too strong near $l \approx 0$ in the B_4 amplitude. This problem of strong daughters is always encountered in Regge-pole descriptions. This will be discussed in the following section.

which can be shown in the perturbation theory [324], in dual model [341, 391, 156] and in Reggeon field theory [235]. On the other hand, for $M^2 \to \infty$, but $s/M^2 \to \infty$, f_{ij} is described in terms of Reggeons in the $\mathrm{b\bar{b}}$ channel by the triple-Regge formula [155, 371] as

$$f_{ij}(\nu,t) \sim (M_X^2)^{\alpha_k(0)-\alpha_i(t)-\alpha_j(t)}\gamma(t) \tag{3.46}$$

(see fig. 23d). Then we have the FESR for $\alpha_i + \mathrm{b} \to \alpha_j + \mathrm{b}$,

$$\int_0^N \mathrm{d}\nu\, \nu^n \left[E_\mathrm{c} \frac{\mathrm{d}^3\sigma}{\mathrm{d}p_\mathrm{c}^3}(\mathrm{a+b\to c+X}) - (-1)^n E_\mathrm{a} \frac{\mathrm{d}^3\sigma}{\mathrm{d}p_\mathrm{a}^3}(\mathrm{c+b\to a+X})\right]$$

$$= \sum_{i,j,k} \gamma_{ijk}(t) s^{\alpha_i(t)+\alpha_j(t)-1} \frac{N^{\alpha_k(0)-\alpha_i(t)-\alpha_j(t)+n+1}}{\alpha_k(0)-\alpha_i(t)-\alpha_j(t)+n+1}\,. \tag{3.47}$$

This is called the finite-mass sum rule (FMSR) [391, 174, 304, 175, 441, 321].

With the exception of the diffractive production the 3-body to 3-body amplitude is represented by the sum of seven duality components [493, 176, 177, 488], as an extension of the two-component duality in the 2-body amplitude. Among the seven components, only three survive for $s \to \infty$ with t fixed: Two of them are the components in which resonances in the αb channel are dual to the ordinary Reggeon in the $\mathrm{b\bar{b}}$ channel, and the other represents non-resonating background in the αb channel being dual to the pomeron exchange in the $\mathrm{b\bar{b}}$ channel. Then, Reggeon–particle scattering reduces to the two-component picture [105] which implies that the $\mathrm{a\bar{c}}$ system can be regarded as quasi-particle in the limit of $s \to \infty$ with t fixed so far as the $\mathrm{a\bar{c}}$ system has neither exotic nor vacuum quantum number.

Under the assumption of two-component picture, eq. (3.47) can be written in a semi-local form as

$$\left\langle \frac{\mathrm{d}\sigma}{\mathrm{d}t\mathrm{d}M^2}(\mathrm{a+b\to c+Res.})\right\rangle \sim (M_X^2)^{\alpha_k(0)-2\alpha_i(t)} \tag{3.48}$$

for X = resonances (when $i = j$). In fact this relation is verified in various reactions [268, 193, 395]. A similar relation with $\alpha_k(0) = 1$ is expected to hold for the non-resonance production.

If one makes full use of inclusive reactions, one can test cases which are not easy in the ordinary two-body reactions. One of the interesting examples is $\mathrm{K}^- +$ "K^+" forward scattering extracted from an inclusive reaction $\mathrm{K}^- + \mathrm{p} \to \Lambda + \mathrm{X}$ in the target-fragmentation region. (Here "K^+" means the K^+ Reggeon.) If we select only non-strange mesons (pions) in the product X, we obtain $\alpha_k(0) \approx 0$ in consistency with the ϕ–f′ exchange [295]. This shows that the ρ–f series are dual to the ϕ–f′ Regge exchanges (and not dual to the ρ–f) as seen in the duality diagram (fig. 24).

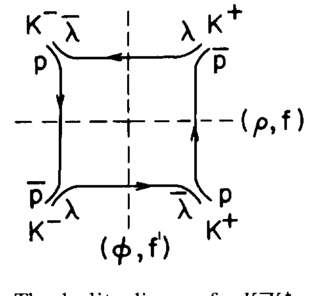

Fig. 24. The duality diagram for $\mathrm{K^-K^+ \to K^-K^+}$.

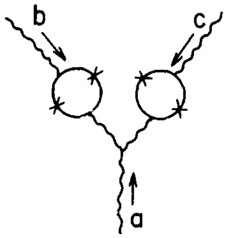

Fig. 25.

Another interesting example is a test of duality in the $B\bar{B}$ annihilation processes. Investigating the reaction $\pi^- + p \to p + X$ in the projectile-fragmentation region, we can obtain the information on $p + "\Delta^{++}" \to p + "\Delta^{++}"$ scattering. If we select only meson resonances as X, we have $\alpha_k(0) \approx -1/2$ which is much lower than ordinary meson trajectories [269]. This supports the idea that the meson resonances are dual to the exotic exchange (or Regge–Regge cuts) in $B\bar{B}$ scattering as suggested by the duality diagram (see section 3.7).

On the other hand, the validity of the two-component duality is controversial in pomeron–particle scattering extracted from the diffractive production (a = c). A naive argument in the unitarity summation leads to the two-component duality; diffractive resonance production builds the PPR component ($\alpha_i = \alpha_j = P$, $\alpha_k = R$) and the diffractive production of non-resonating background builds the PPP component. An alternative argument, however, is that the diffractive production always builds the PPP component (hence the PPR does not exist at all). In other words, the diffractively-produced resonance is also dual to the pomeron exchange [176, 177]. This is the case in the dual resonance model; in the "PPR"-type coupling in fig. 25 the pomeron singularity appears also in the channel a as well as in the b and c channels [511]. Phenomenological analyses so far does not seem to discriminate either view point, mainly due to ambiguities of the separation of various Regge terms [256, 257 (the former form is favoured); 106, 92, 433, 193 (the latter form is favoured); see also 267 for discussion].

There are some interesting constraints on the pomeron coupling. We refer to a review article [88].

4. Direct-channel view point of hadronic reactions

4.1. Success and failure of simple Regge-pole description

One of the most important evidences for the Regge-pole exchange is that charge-exchange scattering described by one Regge pole or an exchange-degenerate pair of Regge poles in the Regge pole theory continues to shrink with energy corresponding to the universal slope $\alpha' \simeq 1\,(\mathrm{GeV}/c)^{-2}$. The Regge trajectory was well determined by making use of experimental data at the Serpukhov and FNAL energies which still exhibit clear shrinkage together with those at intermediate energies. (For a review, see [33].) It should also be noted that this strong shrinkage still persists up to $t \simeq -5(\mathrm{GeV}/c)^2$ at intermediate energies (fig. 26). Elastic scattering of $\pi^\pm p$ also shows shrinkage with $\alpha' \simeq 1\,(\mathrm{GeV}/c)^2$ at large t where diffraction is not important [82]. Regge shrinkage is observed also for baryon exchange processes [e.g., 471, 45] and for π-exchange processes [181, 524]. Elastic

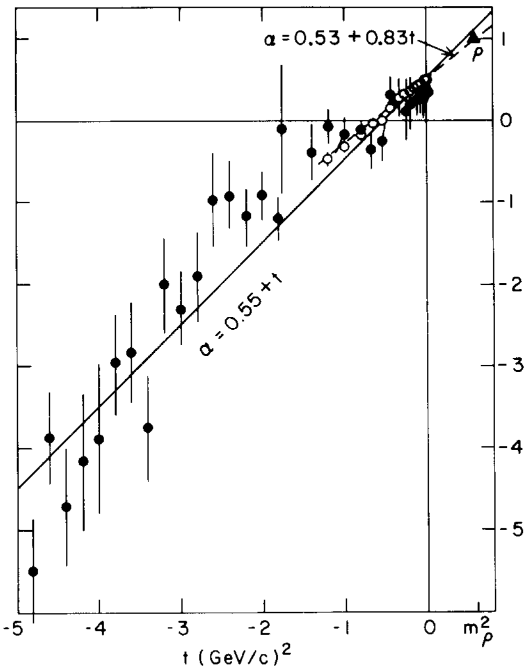

Fig. 26. The ρ trajectory deduced from $\pi^-p \to \pi^0 n$ data [85] in the lab. momentum range $2 < p_L < 5$GeV/c (from Barger and Phillips [56]). The same trajectory determined using the data at the FNAL energies [33] is also shown (open circles).

scattering where more than two Regge poles with different intercepts are exchanged, appear to show no or weak shrinkage. However, if one separates each Regge-pole contribution by an appropriate method, ordinary Regge-pole contribution seems to exhibit strong shrinkage with $\alpha' \simeq 1(\mathrm{GeV}/c)^{-2}$ (e.g., the ω–ρ exchange (mostly ω) in $K^\pm p$ [450]; the f exchange in $\pi^\pm p$ [145] and in $\gamma p \to \rho^0 p$ [104]).

Another important feature of the Regge-pole exchange is the energy-phase relation. This relation is confirmed at $t = 0$ by making use of the optical theorem (see, e.g., Bolotov et al. [77] for the πN charge exchange; Phillips [406] for the $K_L^0 p \to K_S^0 p$ regeneration), or by dispersion-relation calculations [264, 265, 98].

The simple Regge-pole model incorporating exchange degeneracy also gives a satisfactory description of the t dependence as well as s dependence for differential cross sections of charge-exchange scattering (e.g., $\pi^-p \to \pi^0 n$, $\pi^-p \to \eta n$, $K^-p \to \bar{K}^0 n$, $K^+n \to K^0 p$, $\pi N \to \pi\Delta$, $\pi N \to \eta\Delta$, $\bar{K}N \to \bar{K}\Delta$, $KN \to K\Delta$), and for polarizations of $\pi^\pm p$ and $K^\pm p$ elastic scattering.

On the contrary, there are several experimental data for $t < 0$ which the simple Regge pole model fails to explain, i.e.;

(1) the non-vanishing polarization for $\pi^-p \to \pi^0 n$ [78, 259],

(2) the crossover phenomena at $t \simeq -0.2(\mathrm{GeV}/c)^2$ in elastic scattering (non-factorization problem [41]),

(3) the absence of dip at $\alpha_\rho = 0$ in $\pi^-p \to \omega n$ and $\gamma p \to \eta p$ in contrast to $\pi^-p \to \pi^0 n$ and $\pi N \to \pi\Delta$. This suggests the necessity of introducing additional J-plane singularities such as Regge cuts, secondary poles and so on. We remember here that the important consequences of a simple Regge-pole exchange or an exchange of an exchange-degenerate pair are the followings:

(i) *Each helicity amplitude* has the same energy dependence and the same phase controlled by the *single* $\alpha(t)$ of one Regge pole or an exchange-degenerate pair of Regge poles.

(ii) The position of zeros of the amplitude depends only on the value of $\alpha(t)$ and not on the helicity structure of the amplitude.

In this section we consider hadronic reactions from the view point of an s-channel picture as an alternative to the Regge-pole description in the t-channel. The s-channel picture often gives us a complementary simple view in case where the t-channel description is complicated. In general, the t-channel picture has been successful in describing the s-dependence of hadronic amplitudes while the s-channel picture offers a simple description for the structure of amplitudes as a function of t.

Hereafter we mainly use the s-channel helicity amplitude, since it is suitable for description in the s-channel picture. The s-channel helicity amplitude behaves for $s \to \infty$ with t fixed as

$$f_{++}(\Delta\lambda = 0) \sim A'$$

$$f_{+-}(\Delta\lambda = 1) \sim \frac{\sqrt{-t}}{2M} A \qquad (A \approx -\nu B \text{ if } |f_{+-}| \gg |f_{++}|).$$

(Here $\Delta\lambda$ is a net s-channel helicity flip.) See Appendix A.

4.2. The impact-parameter representation

It is often very convenient to represent the high energy amplitude as a function of l, or equivalently to use the impact-parameter ($b = l/q$) representation, when we discuss hadron reactions from the s-channel point of view. Generally it is difficult to obtain the partial-wave representation of the amplitude directly from experimental data at high energy, without relying upon precise amplitude analyses. However, as a special case, the partial waves of the high energy amplitude can be obtained [147] in the following approximation. Let us consider the $K^{\pm}p$ elastic scattering, where both pomeron (P) and ordinary Regge poles (R) are exchanged. We neglect the R^2 term compared with P^2, but keep the interference term $P \cdot R$. We also assume the P to be purely imaginary and to conserve the s-channel helicity. Further we assume R to be purely real in K^+p as there are no resonances in this channel. Since R interferes with P with the same phase and same helicity structure, we obtain

$$\frac{d\sigma}{dt}(K^+p) \sim |P|^2$$

$$\frac{d\sigma}{dt}(K^-p) \sim |P|^2 + 2|P| \operatorname{Im} R_{\Delta\lambda=0}, \tag{4.1}$$

where $\Delta\lambda$ denotes the net s-channel helicity flip. Then we have

$$\operatorname{Im} R_{\Delta\lambda=0} = \left\{\frac{d\sigma}{dt}(K^-p) - \frac{d\sigma}{dt}(K^+p)\right\} / 2\sqrt{\frac{d\sigma}{dt}(K^+p)}. \tag{4.2}$$

As is shown in fig. 27, $\operatorname{Im} R_{\Delta\lambda=0}$ (at p_L = 5GeV/c) possesses qualitative features of the function $J_0(R\sqrt{-t})$ with $R \simeq 1$ fm, which is easily understood by having one dominant band of partial waves centred around $l + 1/2 \sim qR$. In order to have strong Regge shrinkage, however, $J_0(R\sqrt{-t})$ must be multiplied by a shrinkage factor $\exp\{B(s)t\}$ with $B(s) \sim \alpha' \ln s/s_0$. In the impact parameter language† this means that the width of the band expands as $\Delta b(s) \sim (\ln s)^{1/2}$ with energy.

†The Hankel transform of $\exp(Bt) J_0(R\sqrt{-t})$ is $(1/2B)\exp\{-(R^2 + b^2)/4B\} I_0(Rb/2B) \simeq (1/2\sqrt{\pi BRb}) \exp\{-(R - b)^2/4B\}$.

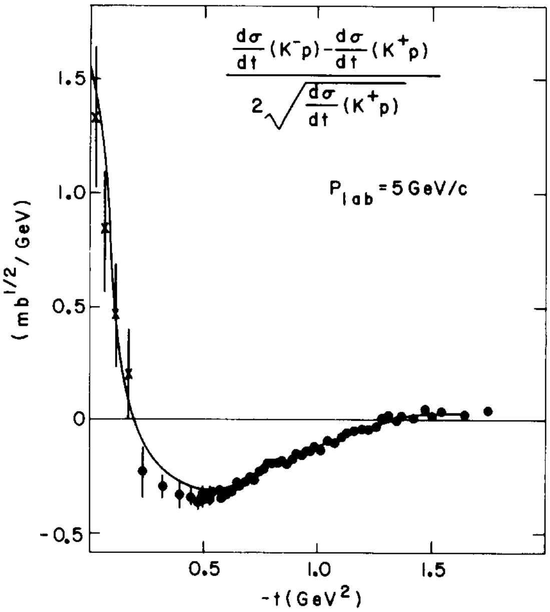

Fig. 27. The experimental result for Im $R_{\Delta\lambda=0}(t)$ calculated from eq. (4.2) at p_L = 5GeV/c. The curve shows 1.6 exp $(1.3t)J_0(4.8\sqrt{-t})$ (from Davier and Harari [147]).

Actually, as is expected, the partial-wave decomposition of the above amplitude exhibits the peripheral band centred at $l \approx qR \approx 7$ ($b \approx R$ = 1 fm) and extends up to $l \approx 10$, which is almost the parent trajectory Y_0^* at $p_L \simeq$ 5GeV/c (fig. 28).

Let us now mention the helicity-flip amplitude. The partial-wave expansion of the imaginary part of the Regge-pole amplitude with the residue function of the form $\beta(t) \sim \alpha(\alpha + 1)$ ... (this form has been verified for the helicity-flip amplitude), also has a peripheral band centred around $b \approx R$ = 1 fm.† (Note that this type of amplitude has a strong $l < qR$ component for the helicity-nonflip kinematics.†) Indeed, the partial waves of the imaginary part of π^-p charge-exchange

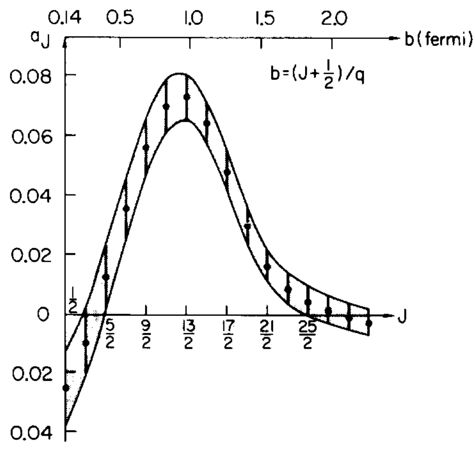

Fig. 28. Partial waves of the amplitude Im $R_{\Delta\lambda=0}$ shown in fig. 27. The corresponding impact parameter is also shown (from Davier and Harari [147]).

†This argument depends on the intercept of the t-channel trajectory. We consider here the ρ trajectory with $\alpha(t)$ = 0.5 + t.

amplitude (the model amplitude of Barger and Phillips [541]) show the same characteristics both in the helicity nonflip and in the flip amplitudes [261].

When contributing partial waves dominate around l_0, the position of the first zero (and possibly the second zero) of the s-channel helicity nonflip amplitude is given by those of $P_{l_0}(z) \approx J_0(l_0\theta)$.† The position of zeros is assured to be independent of energy if $l_0 \sim qR \sim \sqrt{s}$, [164, 290, 247]. (With this relation, the amplitude at $t = 0$ also grows as $\sim\sqrt{s}$, implying $\alpha(0) \approx 0.5$, unless the dominant partial waves decrease their magnitude.) Similarly, the zeros of the helicity flip amplitude are given as the zeros of $P_{l_0}'(z)$ or of $J_1(l_0\theta)$. (Note that the position of these first zeros just coincides to that of $\alpha_\rho(t) = \alpha_\omega(t) = \alpha_f(t) = \alpha_{A_2}(t) = 0$.) Therefore, the first zero in the nonflip amplitude is closer to the forward direction than that in the flip amplitude. Thus, the t-dependence depends on the s-channel helicity.

The zero of Im A' found at $t \simeq -0.15(\mathrm{GeV}/c)^2$ and that of Im νB at $t \simeq -0.5(\mathrm{GeV}/c)^2$ in the FESR analysis of π^-p charge-exchange scattering just correspond to the above situation. In the resonance region ($p_L \lesssim 2\mathrm{GeV}/c$) the parent resonance dominates the daughter resonance and the parent trajectory is in accord with the line of $b \simeq 1$ fm. Actually the impact-parameter representation of the resonant amplitude in its energy region exhibits the dominance of peripheral partial waves [216], producing zeros at $t \simeq -0.15$ and $-0.5(\mathrm{GeV}/c)^2$ in the helicity nonflip and flip amplitudes respectively [164, 217] (see figs. 29 and 30).

On the other hand, in the t-channel Regge pole model the imaginary part of each t-channel helicity amplitude has zeros at $\alpha(t) = 0, -1, -2, \ldots$ by exchange degeneracy and their positions depend only on $\alpha(t)$ and not on any helicity structure. The Veneziano model eliminates the difference between the flip and nonflip angular distributions by having strong daughters (fig. 31). Both the low and the high energy analyses suggest that the t-channel pole model with exchange degeneracy must be modified by additional J-plane singularities and the substantial suppression of daughters is needed.

We now briefly touch on the real part. In general, if Im $f(\nu,t) \to \nu^{c(t)}$ for $\nu \to \infty$ with t fixed, Re $f(\nu,t) \to \nu^{c(t)}\{\mp 1 - \cos\pi c(t)\}/\sin\pi c(t)$ according as $f(\nu,t)$ is crossing even or odd. (Even if a logarithmic factor is present, this relation is true in the limit $\log \nu \to \infty$ [311].) Provided that Im $A(\nu,t)$ is dominated by the $l \sim qR$ partial waves, and the above relation between the phase and energy dependence is obeyed, it is usually impossible to have the $l \sim qR$ partial waves that dominate the real part. This is really the case both for the helicity nonflip and flip amplitudes [e.g., 422, 261].

Absorption models

The absorptive correction due to the Regge-pole-pomeron cut is one of the prescriptions to suppress the low partial waves in the Regge pole model [18, 19, 313, 254, 431; see 299 and 405 for reviews]. According to the absorption model, the strong competition among many open channels suppresses the contribution of low partial waves through unitarity: Namely in the absorbed amplitude $f_\ell = R_\ell + \mathrm{i}\lambda P_\ell \cdot R_\ell$ (R = Regge pole amplitude, λ = strength of the absorption), the pomeron amplitude P_ℓ is almost purely imaginary and contains strong low partial-wave components, then the

†Further out in t the zeros are not found at the positions of zeros of $J_0(R\sqrt{-t})$ nor at those of $P_{l_0}(z)$ owing to the strong cancellations within the band of important partial waves. In reality, zeros of Im $R_{\Delta\lambda=1}$ are found at $t \simeq -0.5, -1.5, -2.5(\mathrm{GeV}/c)^2$ in $\pi^-\mathrm{p} \to \pi^0\mathrm{n}$ (see section 2.3). Zeros of helicity nonflip amplitude in the same reaction also appear to be spaced by $\Delta t \simeq 1(\mathrm{GeV}/c)^2$ [178]. The $\pi\pi$ FESR (ρ exchange) also supports the equal spacing of zeros; $t \simeq 0.4, -1.4, -2.4(\mathrm{GeV}/c)^2$ [489].

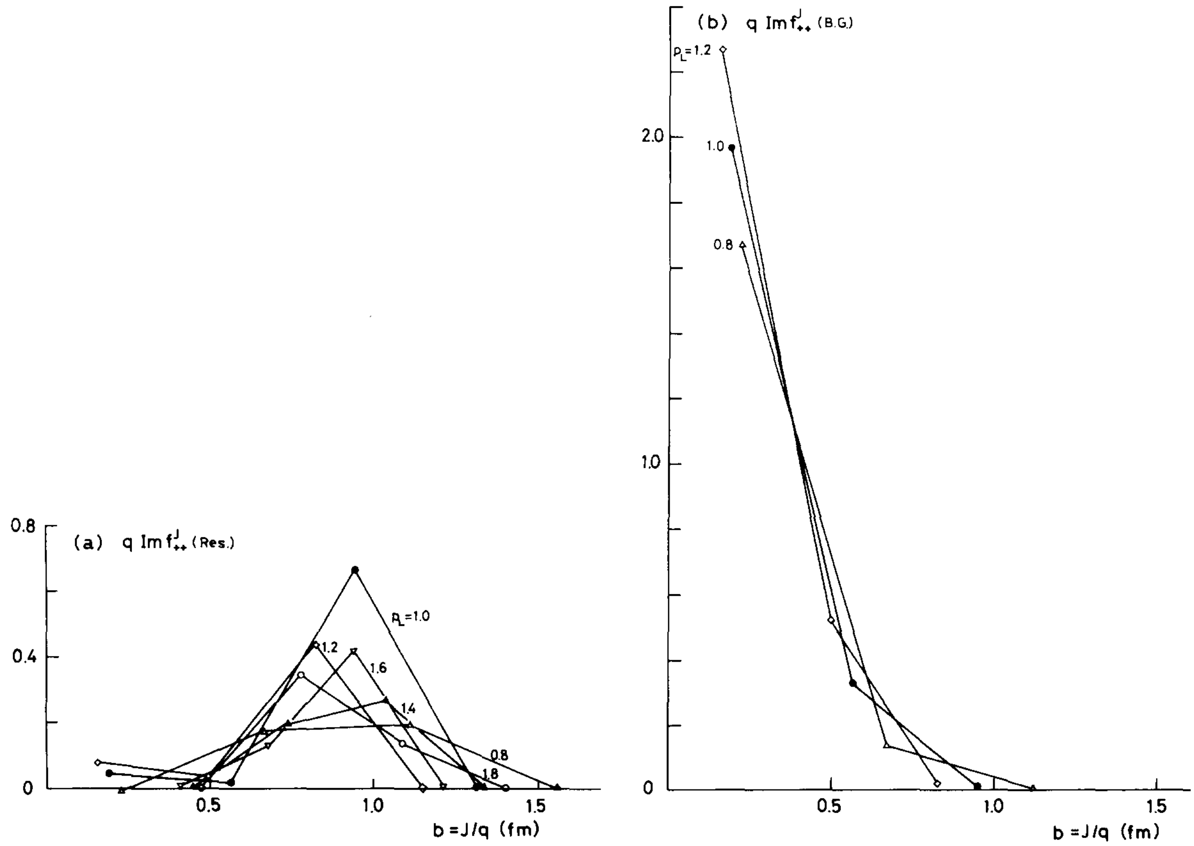

Fig. 29. (a) Imaginary part of the resonant amplitude of $\bar{K}N$ scattering ($I_t = 0$, $\Delta\lambda = 0$) as a function of impact parameter b in the resonance region ($0.8 \leqslant p_L \leqslant 1.8$GeV/$c$). (b) The similar figure for the non-resonating background amplitude (from Fukugita and Inami [216]).

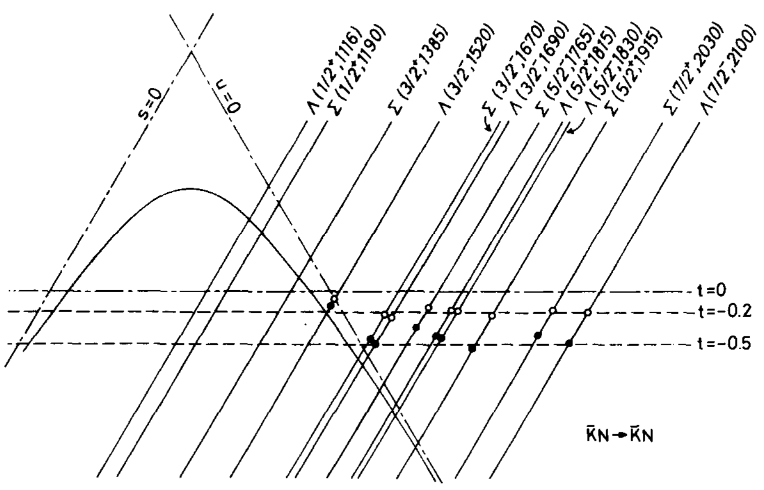

Fig. 30. First zeros of the prominent Y* resonances on the Mandelstam plane as contributed to the helicity nonflip (open circles) and to the helicity flip (solid circles) amplitudes.

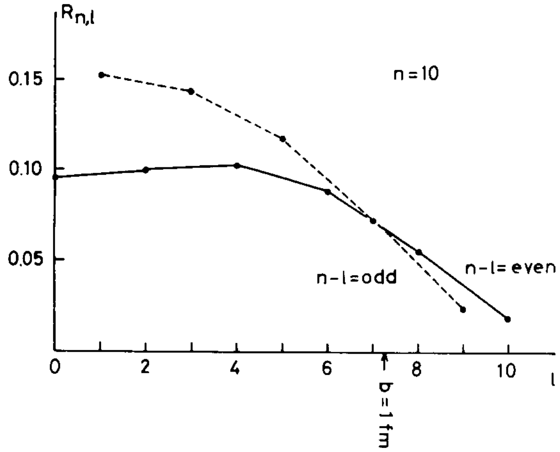

Fig. 31. Partial-wave components of the Veneziano-residue function $R_{n,l}$ with $\alpha(t) = 0.5 + t$; $R_n(t) = \sum_{l=0}^{\infty} (2l + 1)R_{n,l}P_l(z)$.

low partial-wave components of f_l are largely reduced from the original Regge-pole amplitude. Thus, the Regge cut acts so as to make the amplitude to be peripheral.

There are two schools of absorption models: the so-called Argonne model (the weak-cut model) and Michigan model (the strong-cut model). There was a long controversy between these opposing schools, but it appears phenomenologically that neither is right in its original form (for reviews, see [405, 198]). A common difficulty in all existing Regge-cut models is that they cannot reproduce the strong shrinkage especially for large t. Another trouble is that the absorptive cut makes not only the imaginary part peripheral but also has a tendency to make the real part more peripheral. This raises severe difficulty in reproducing the polarization of $\pi^- p \to \pi^0 n$ [515]. No successful Regge-cut model is known yet. It is a very important task to find a cut model which incoporates:

(i) duality (including exchange degeneracies),

(ii) "absorption" effects which are sometimes strong enough to make the imaginary part peripheral,

(iii) correct energy-phase relation for the amplitude in which the Regge-pole amplitude is already peripheral,

(iv) Regge shrinkage consistent with $\alpha' \simeq 1\,(\mathrm{GeV}/c)^{-2}$, especially at large t (at least in the intermediate energy region).

4.3. Dual absorptive models

Assuming that the imaginary part of the ordinary Regge component is dominated by resonances locally at any energy s, and that the prominent resonances obey a relation of the form $l \propto m_R = \sqrt{s}$, Harari proposed the following phenomenological picture summarizing the empirical regularities of two-body hadronic reactions [247, 248];

(i) The imaginary part of the R-component is dominated by the peripheral partial waves with $R \approx 1$ fm and therefore is given by a function of the form "$J_{\Delta\lambda}(R\sqrt{-t})$" in the small t region. (Here "$J_{\Delta\lambda}$" is meant to be a function which has the same characteristics as $J_{\Delta\lambda}\, e^{Bt}$.) In the language of the t-channel exchange picture, it is assumed that one will have a Regge cut which makes the amplitude to be peripheral when a single Regge-pole exchange is not yet peripheral.

(ii) The P-component has substantial contribution from all l ($\leqslant qR$) partial waves and is given by a smooth function of t such as e^{ct}. Furthermore, as the first approximation, the P-component is assumed to conserve the s-channel helicity and to be purely imaginary in the small t region.

(iii) When the imaginary part of Regge-pole amplitude is already peripheral and thus the Regge-cut contribution can be neglected, the phase of the amplitude approaches to an asymptotic value at lower energies and has the Regge phase. On the contrary when the Regge-pole amplitude is not peripheral, one should have a large contribution from Regge cuts and the phase approaches to an asymptotic value very slowly. In this case, the real part is not predictable.

In this picture, the scattering amplitude with the ρ–A_2–f–ω-exchange has the form such as

$$\mathrm{Im}\, R_{\Delta\lambda=0} \sim \text{“}J_0(R\sqrt{-t})\text{”}, \qquad \mathrm{Re} R_{\Delta\lambda=0} \sim \text{unpredictable},$$

$$\mathrm{Im}\, R_{\Delta\lambda=1} \sim \text{“}J_1(R\sqrt{-t})\text{”}, \qquad \mathrm{Re} F_{\Delta\lambda=1} \sim \mathrm{Im}\, R_{\Delta\lambda=1} \times \text{(appropriate signature factor)}, \tag{4.4}$$

namely $R_{\Delta\lambda=0}$ is substantially modified while $R_{\Delta\lambda=1}$ agrees with the predictions of the simple Regge pole model. We now summarize how the characteristics of various reactions for small t region can be understood [246, 247, 248].

(1) Elastic reactions: (i) The differential cross section is given by $\mathrm{d}\sigma/\mathrm{d}t \simeq |P|^2 + 2|P| \cdot \mathrm{Im}\, R_{\Delta\lambda=0}$. Since $\mathrm{Im}\, R_{\Delta\lambda=0} \approx$ “J_0” (a sum of s-channel resonance) should be positive in an elastic amplitude at $t = 0$, we have $\mathrm{d}\sigma/\mathrm{d}t(\bar{\mathrm{A}}\mathrm{B}) > \mathrm{d}\sigma/\mathrm{d}t(\mathrm{AB})$ ($\mathrm{A} = \pi$, K; B = N) at $t = 0$. There are cross-over phenomena at $t \simeq = -0.2$ and $-1.2(\mathrm{GeV}/c)^2$, since “J_0” changes sign at those points. The dip or break at $t = -0.6 \sim -0.8(\mathrm{GeV}/c)^2$ which dies away with the increasing energy is interpreted as the minimum of “J_0”. So far, this has been interpreted as a double-zero arising from the no-compensation mechanism $\beta(t) \sim \alpha^2(t)$ in the Regge pole model [121]. (ii) The polarization is given by $P\,\mathrm{d}\sigma/\mathrm{d}t \simeq 2|P| \cdot \mathrm{Re}\, R_{\Delta\lambda=1}$, which takes the form $J_1 \times$ (appropriate signature factor) as†

$$\begin{array}{ll} \pi^{\pm}\mathrm{p} \to \pi^{\pm}\mathrm{p} & P \sim \pm J_1 \tan \dfrac{\pi\alpha}{2} \\ \mathrm{K}^-\mathrm{p} \to \mathrm{K}^-\mathrm{p} & \quad \sim J_1 \cot\pi\alpha \sim \sqrt{-t}\cos\pi\alpha \\ \mathrm{K}^+\mathrm{p} \to \mathrm{K}^+\mathrm{p} & \quad \sim J_1 \dfrac{1}{\sin\pi\alpha} \sim \sqrt{-t}. \end{array}$$

These are just the same as in the Regge pole model.

(2) The prominent features observed in inelastic cross sections are the presence or the absence of dip at $t = -0.5 \sim -0.6(\mathrm{GeV}/c)^2$. This dip occurs when only the vector trajectory is exchanged and further $\Delta\lambda = 1$ amplitude is dominant. As was seen in sections 2.3 and 3.5, the $\omega\mathrm{N}\bar{\mathrm{N}}$ and the $\mathrm{fN}\bar{\mathrm{N}}$ vertex conserve the s-channel helicity, and the $\rho\mathrm{N}\bar{\mathrm{N}}$ and the $\mathrm{A_2N}\bar{\mathrm{N}}$ vertex are dominated by the helicity flip. For the boson vertex, the helicity structure of the Reggeon–0^-–1^- coupling is not unique, but it is usually assumed to be the same as that of the Reggeon–0^-–γ coupling (the helicity-flip dominance). Thus we are led to the dip systematics in table 12.

Finally we add a remark that the simple Regge pole model for the ρ–ω–f–A_2-exchange correctly predicts the $\Delta\lambda = 1$ amplitude. For example, the angular distributions of charge exchange scattering and of polarizations of elastic scattering, which are dominated by the $\Delta\lambda = 1$ amplitude, are correctly given. On the other hand it fails in the case of the $\Delta\lambda = 0$ amplitude.‡ For example,

†The f and ω conserve the s-channel helicity, so that their contribution to polarization is negligible.

‡There are many indications, however, that at $t = 0$ the $\Delta\lambda = 0$ amplitude seems to be well described by a pole alone; (i) the energy-phase relation, (ii) the line-reversal equality for an exchange-degenerate pair of reactions, (iii) results from FESR or CMSR for $\pi^-\mathrm{p}$ charge exchange at $t = 0$, (iv) the effective-pole analysis of Barger and Phillips, in which contributions of the ρ' vanishes at $t = 0$ in $\pi^-\mathrm{p} \to \pi^0\mathrm{n}$. Off the forward direction this is not the case.

Table 12

Systematics of dips at $t \simeq -0.5 \sim -0.6\,(\mathrm{GeV}/c)^2$

processes	Regge poles	vertex meson	helicity nucleon	flip net	dip?
$\pi^- p \to \pi^0 n$ $\pi^+ p \to \pi^0 \Delta^{++}$	ρ	0	1	1	Yes
$\pi^- p \to \eta n$ $\pi^+ p \to \eta \Delta^{++}$	A_2	0	1	1	No
$K^- p \to \bar{K}^0 n$, $\bar{K}\Delta$ $K^+ n \to K^0 p$, $K\Delta$	$\pm\rho + A_2$	0	1	1	No
$\pi N \to \omega N$, $\omega\Delta$	ρ	1	1	0 or 2	No
$\pi N \to \rho N$ (separating $I_t = 0$)	ω	1	0	1	Yes
$\gamma p \to \eta p$	ρ	1	1	0 or 2	No
$\gamma p \to \pi^0 p$	ω	1	0	1	Yes

the cross-over phenomena, cross sections of $\pi N \to \omega N$ and $\gamma p \to \eta p$, and polarizations of charge-exchange scattering, which are controlled by the $\Delta\lambda = 0$ amplitude, are not given correctly.

Some remarks on the peripherality

The simple picture based on the peripherality of the imaginary part leads to the qualitative understanding of the characteristics of hadronic reactions. We have clear evidences for the peripherality of the ρ and ω exchanges as seen in the cross-over phenomena in $\pi^\pm p$, $K^\pm p$ and $\bar{p}p$ (pp) elastic scattering [e.g., 11, 83]. There is, however, some controversy as to whether the peripherality holds for any Regge exchange, especially for the tensor exchange, because of the difficulties in separating the contribution of each exchange (see [199] for a review).

As regards the f exchange, for example, the dip at $t \simeq -0.6 \sim -0.8(\mathrm{GeV}/c)^2$ in the $d\sigma/dt(\pi^- p) + d\sigma/dt(\pi^+ p)$ which is observed to disappear as the energy increases allows two different interpretations; (i) peripheral (as a minimum of J_0) [230, 145], (ii) non-peripheral (no-compensation mechanism) [42]. The separation of the f exchange from the pomeron using their energy dependences shows that the f exchange is peripheral if $\alpha'_P \gtrsim 0.7(\mathrm{GeV}/c)^{-2}$, while it is not peripheral if $\alpha'_P \lesssim 0.4(\mathrm{GeV}/c)^{-2}$ [63, 42]. The effective slope of pomeron trajectory seems to decrease with increasing energy as has been found in K^+p and pp scattering. If we take a value $\alpha'_P \simeq 0.77(\mathrm{GeV}/c)^{-2}$ corresponding to K^+p scattering in the relevant energy region [42], the f exchange should be peripheral. (This value of α'_P brings an appreciable real part to the pomeron component for $t \neq 0$.) Another way to separate the f exchange is that by the resonance approximation. The dominance of peripheral resonances in the FESR calculations, which has led to the ρ exchange to be peripheral, may also make the f exchange peripheral. Actually, the FESR calculation with resonance saturation gives a zero at $t \simeq -0.25(\mathrm{GeV}/c)^2$ in the A' amplitude [224].

In $K^\pm N$ scattering, the assumption of resonance saturation leads to the vector–tensor exchange degeneracy, which implies that the f and the A_2 exchange should show same shapes in the impact-parameter representation as that of the ω and the ρ, respectively. The imaginary part of the amplitude corresponding to the $\rho + A_2$ or the $f + \omega$ combination in $\bar{K}N$ scattering is shown to be peripheral at the intermediate energy† [216]. If the tensor exchange turns out to be non-peripheral,

†The evaluation of FESR using partial-wave data often suggests the non-peripherality of the A_2 exchange [143, 179]. The results, however, heavily depend on the input phase-shift data of K^+n and K^+p (see section 2.3) and those results seem to be unreliable.

the K^+N channel should have substantial imaginary part apart from the diffraction.

The K^{**} exchange is often reported to be non-peripheral [47, 125]. This is a reflection of the breaking of exchange-degeneracy among Y^*'s in lower-daughter level, which gives central imaginary components to the reaction $\bar{K}N \to \pi\Sigma(\Lambda)$. The reaction $\bar{K}N \to \pi\Sigma(\Lambda)$ still keeps a peripherality in the imaginary part.

The amplitude having a rotating phase, i.e., the amplitude corresponding to a planar duality diagram, always seems to keep its peripherality, even if a separation of tensor exchange would lose its peripherality.

The peripherality for baryon-exchange processes will be discussed in section 4.7.

4.4. Resonance models

Duality asserts that the imaginary part is represented either by resonances or by Regge exchanges, but it does not say directly much about the real part.

In order to discuss the real part, we start off with the dispersion relation

$$\begin{aligned} f(\nu,t) &= \frac{1}{\pi}\int_{-\infty}^{0} d\nu' \frac{\operatorname{Im} f(\nu',t)}{\nu'-\nu} + \frac{1}{\pi}\int_{0}^{\infty} d\nu' \frac{\operatorname{Im} f(\nu',t)}{\nu'-\nu} \\ &= \frac{1}{\pi}\int_{0}^{\infty} d\nu' \left[\pm\frac{1}{\nu'+\nu} + \frac{1}{\nu'-\nu}\right] \operatorname{Im} f(\nu',t). \end{aligned} \tag{4.5}$$

Here the first and the second terms receive contributions from the u-channel and the s-channel resonances respectively, so that we have

$$f(\nu,t) = \pm\sum(u\text{-channel resonances}) + \sum(s\text{-channel resonances}) \tag{4.6}$$

in the resonance approximation. Correspondingly in terms of the Regge expression,

$$f(\nu,t) \sim [\mp 1 - e^{-i\pi\alpha}]s^\alpha = \mp s^\alpha - (-s)^\alpha. \tag{4.7}$$

Here the second (or first) term represents the s-channel (u-channel) discontinuity, i.e., the full Regge behaviour originates from two parts: s^α that comes from u-channel resonances and $(-s)^\alpha$ from s-channel resonances.

Coulter, Ma and Shaw [132] noticed that the first term of eq. (4.5) or (4.6) is purely real and smooth, and thus can be well approximated by the first term of eq. (4.7), while the second term of eq. (4.5) or (4.6) varies rapidly with energy and only its average is given by the second term of eq. (4.7). They proposed that the sum of the first term of eq. (4.7) and the second term of eq. (4.6), i.e.,

$$\mp s^\alpha + \sum(s\text{-channel resonances}) \tag{4.8}$$

gives a good approximation to the non-diffractive part of $f(\nu,t)$ in the energy region with fluctuation due to resonances.

This prescription becomes most explicit in terms of the Veneziano model. Namely, when the amplitude is expressed as

$$(s,t) + (s,u) + (u,t), \tag{4.9}$$

the sum $(s,t) + (s,u)$ which has s-channel discontinuities and thus corresponds to the second term of eqs. (4.5)–(4.7) should be replaced by the sum of s-channel resonances. (The (u,t) term shows precocious Regge behaviours, since it is in the opposite side of wedge where the asymptotic expansion is impossible. This can be seen experimentally in K^+N scattering.) In general, when one considers the resonance model, it is more convenient to separate the amplitude into bivariate terms as in eq. (4.9), rather than to separate it into signatured terms.

This interference model is different from the old one [34] in which the amplitude is given by the sum of a full term of eq. (4.7) and the second term of eq. (4.6), thus leading to the double-counting problem (see section 3.2). The opposite approach has been used by several authors [160, 137] who used only the s-channel resonances (the second term of eq. (4.6) alone and no Regge terms) for the full amplitude. It is obvious from our consideration that neither of these two models is in agreement with duality.

When the above prescription is put into practice, there still remain some problems in the treatment of the (s,t) term, since one can take into account only a finite number of s-channel resonances in some energy domain. Specifically:

(i) Contributions from the tails of far-away resonances (especially those from the high-energy tails of lower-energy resonances) are hard to take in. This problem is crucial for the real part, since the real part is not saturated locally by resonances.

(ii) It is difficult to evaluate the contributions from daughter resonances which are not identified as individual resonances because of their large widths and their small elasticities.

These problems become serious in the forward region where all resonances contribute constructively. This prescription is, however, successful in the description of backward scattering where many resonances cancel against each other and the fluctuation of the amplitude is still prominent. It is often used for the determination of resonance parameters [132, 344, 345, 420].

Peripheral-resonance models

Let us argue the amplitude which is constructed collectively by the resonances with strong coupling along the line $l \approx qR$. We consider here the amplitude corresponding to the (s,t) term. (For the (s,u) term one has only to replace z by $-z$ in the subsequent discussions.) The imaginary part of the amplitude is dominated by the peripheral partial waves with $l \approx qR$, since it is dominated locally by the resonances. The resonances, however, do not dominate locally the real part. Instead, the low-energy tails of high-mass resonances contribute to the real part for $l > qR$, while the contribution from the high-energy tails of low-mass resonances dominates for $l < qR$. Therefore, the real part of the amplitude changes its sign at $l \approx qR$, or $b \approx R$ (fig. 32) [289, 216, 461]. (This sign change is also seen in the partial waves of the Regge-pole amplitude.) As a consequence of the collective distribution of resonances along a line $l \approx qR$, one has an amplitude of the form $f(b) \sim 1/(b - R - \mathrm{i}\Delta b/2)$.

The model based on the peripheral band of resonances differs from the optical or geometrical

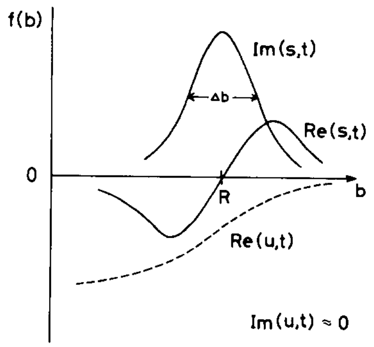

Fig. 32. Schematic view of the amplitude with the peripheral-resonance dominance as a function of impact parameter b.

model [139, 231, 476, 140] or the strong-cut model [313, 254, 431], in that the real part is never dominated by peripheral partial waves in the resonance model while the real as well as the imaginary parts are peripheral in the latter models.

We now consider the angular distributions. Suggested by the above arguments, we assume that

$$f_l(s) \simeq \frac{\gamma(s)}{l - \tilde{\alpha}(s)}, \tag{4.10}$$

where $\tilde{\alpha}(s)$ is an effective "trajectory". The real part of $\tilde{\alpha}(s)$ is taken as Re $\tilde{\alpha}(s) \simeq qR$, and the imaginary part corresponds to the width of peripheral band, i.e., Im $\tilde{\alpha}(s) \simeq q\Delta b/2$.†‡ It is convenient to follow the Sommerfeld's treatment [475] to get a sum of partial waves [318, 462]. By ignoring the background integral, we obtain

$$f(s,t) \simeq -a(s)\,\frac{P_{\tilde{\alpha}(s)}(-\cos\theta_s)}{\sin\pi\tilde{\alpha}(s)}\ . \tag{4.11}$$

In the small t region, this amplitude can be approximated by the Hankel function of the first kind, $H_n^1(z) \equiv J_n(z) + \mathrm{i}N_n(z)$ [287, 222, 461, 462] as

$$f(s,t) \simeq \mathrm{i}a(s)H_0^1\left(\frac{\tilde{\alpha}(s)}{q}\sqrt{-t}\right). \tag{4.12}$$

(One has only to replace P_l by P_l' and H_0^1 by H_1^1 for the helicity-flip amplitude.) A divergence at $t = 0$ in the real parts of eqs. (4.11) and (4.12) can be removed by taking into account the correct behaviour of f_l for $l \to \infty$ ($f_l \sim \exp\{-2\mu_\pi l/q\}$) in eq. (4.10) [243]. For $t \lesssim -0.2(\mathrm{GeV}/c)^2$, where the large l behaviour of f_l is not so relevant, eq. (4.12) has a phase factor $\sim \exp(\mathrm{i}R\sqrt{-t})$. The comparison with the Regge phase immediately gives us the effective t-channel trajectory, $\alpha^{\mathrm{eff}}(t) = -(R/\pi)\sqrt{-t}$ + constant.§ Here the constant is the phase of the residue function $a(s)$. (The $a(s)$ could also include a log s term accompanied with its phase.) This trajectory is almost linear in the small t region of our interest except for $|t| < 0.2(\mathrm{GeV}/c)^2$, and is in good agreement with $\alpha_\rho = 0.5 + t$ [463].

The amplitude for $\Delta\lambda = 1$ constructed in this way has a t-dependence similar to that of the Regge-pole amplitude in the small t region except for $t \approx 0$. The model also accommodates the peripherality of the imaginary part for both $\Delta\lambda = 0$ and $\Delta\lambda = 1$ amplitudes. The peripheral-resonance model is successful in describing the t-dependence of each helicity amplitude, while it needs additional assumptions to explain the s-dependence of the amplitude [318, 222, 463, 243].

The amplitude $f(b)$ corresponding to the (u,t) term is given by a sum of the tails of u-channel

†The width of the peripheral band should not be confused with that of the individual resonance. In the low-energy region such as $p_L \lesssim 2\mathrm{GeV}/c$, Im $\tilde{\alpha}$ is controlled by the width of individual resonance [318, 243]. Therefore, the meaning of the model is somewhat different from that at higher energies.

‡An example of the analytic expression of such a "trajectory" is [461]

$$\tilde{\alpha}(s) = -\frac{R}{\pi}\frac{\sqrt{-s}}{2}\log\frac{-s}{s_0} = \begin{cases} R\dfrac{\sqrt{s}}{2} + \mathrm{i}\dfrac{R}{\pi}\dfrac{\sqrt{s}}{2}\log\dfrac{s}{s_0} & \text{for } s > 0 \\ -\dfrac{R}{\pi}\dfrac{\sqrt{-s}}{2}\log\dfrac{|s|}{s_0} & \text{for } s < 0. \end{cases}$$

§Equation (4.12) also includes a factor $\exp\{-\mathrm{Im}\,\tilde{\alpha}(s)\sqrt{-t}/q\}$, which gives a shrinkage. If we put Im $\tilde{\alpha}(s) = R\sqrt{s}\log(s/s_0)/2\pi$ (see preceding footnote), we have $\exp\{-\mathrm{Im}\,\tilde{\alpha}(s)\sqrt{-t}/q\} = (s/s_0)^{-R\sqrt{-t}/\pi} = (s/s_0)^{\alpha^{\mathrm{eff}}(t)}$.

resonances. It is expected to be predominantly real and negative definite and has behaviour smooth in b (see fig. 32). It is interesting to observe that impact-parameter distributions corresponding to the combination $-(u,t) + (s,t)$ are in qualitative agreement with empirical ones (fig. 33) obtained in πN charge-exchange scattering [422, 261] for both real and imaginary parts as well as for both $\Delta\lambda = 0$ and $\Delta\lambda = 1$ amplitudes. There have been several attempts at explicit construction of the (u,t) term; by making use of the line-reversal equality $f(u,t) \simeq |f(s,t)|$, [222] or by continuing analytically the (s,t) term to $s < 0$, [463, 242].

4.5. s-channel picture of t-channel couplings

We have already seen that if we assume the towers of direct-channel resonances with spin l_R and momentum q_R satisfying the relation $l_R \approx q_R R$, the fixed-t structure of the amplitude is assured and a sum of direct-channel resonances produces the Regge exchange (with possible Regge-cut corrections). In this section, we elucidate how the same s-channel resonances build the t-channel Regge exchange with different coupling patterns.

We take the $\bar{K}$N scattering as an example. It has been known by many partial-wave analyses that the two series of parent resonances $\Lambda_\alpha - \Lambda_\gamma$ and $\Sigma_\delta - \Sigma_\beta$ with the impact parameter ~1 fm dominate the imaginary part of non-diffractive amplitudes. Let us first consider the $I_t = 0$ amplitude (in which the f and ω are exchanged) at $t = 0$. The $\Lambda_\alpha - \Lambda_\gamma$ and the $\Sigma_\delta - \Sigma_\beta$ contribute additively to the $\Delta\lambda = 0$ amplitude (f_{++}) such as $\frac{1}{2}(\Lambda_\alpha + \Lambda_\gamma) + \frac{3}{2}(\Sigma_\beta + \Sigma_\delta)$, while they contribute destructively as $-\frac{1}{2}(\Lambda_\alpha + \Lambda_\gamma) + \frac{3}{2}(\Sigma_\beta + \Sigma_\delta)$ to the $\Delta\lambda = 1$ amplitude (f_{+-}) (see Appendix). Hence we have $\mathrm{Im}\, f_{++} \gg |\mathrm{Im}\, f_{+-}|$ for the f$-\omega$ exchange at $t = 0$, so that we have $|f_{++}| \gg |f_{+-}|$ if the appropriate signature factor is taken into account. As for the $I_t = 1$ ($\rho - A_2$) exchange, the $\Lambda_\alpha - \Lambda_\gamma$ and the $\Sigma_\delta - \Sigma_\beta$ contribute to the helicity amplitudes as,

$$\mathrm{Im}\, f_{++}\colon \tfrac{1}{2}(\Lambda_\alpha + \Lambda_\gamma) - \tfrac{1}{2}(\Sigma_\beta + \Sigma_\delta), \qquad \mathrm{Im}\, f_{+-}\colon -\tfrac{1}{2}(\Lambda_\alpha + \Lambda_\gamma) - \tfrac{1}{2}(\Sigma_\beta + \Sigma_\delta).$$

We obtain $|\mathrm{Im}\, f_{+-}| \gg |\mathrm{Im}\, f_{++}|$, and hence $|f_{+-}| \gg |f_{++}|$ for the ρ and A_2 exchanges at $t = 0$. When

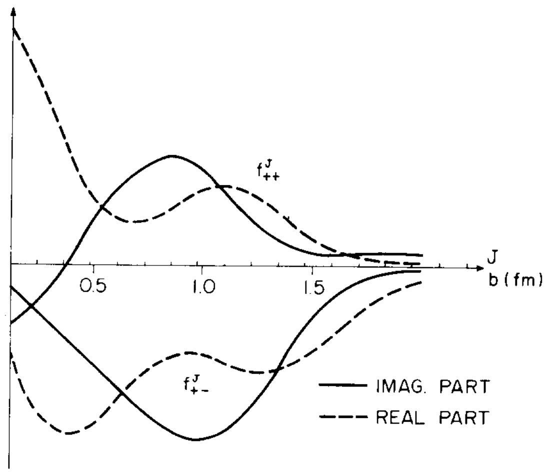

Fig. 33. Partial waves of the s-channel helicity amplitudes for πN charge-exchange scattering at 6(GeV/c). (We show them as a function of impact parameter.) The elaborate Regge fit of Barger and Phillips' is used as the input amplitude [261].

particular resonance series dominate, the kinematical difference of the s-channel helicity amplitudes thus leads to the difference in Reggeon couplings.†

The factorization of t-channel exchanges also requires the helicity-nonflip dominance of the f exchange and the helicity-flip dominance of the ρ exchange in πN scattering. This is indeed ensured by the dominance of the Δ_δ and the N_α (and the N_γ) in the s-channel.

An example of the whole correlation between the t-channel Reggeon coupling and the s-channel resonance coupling can be seen in the crossing-invariant solution of the exchange degeneracy (see section 3.5).

The factorization property in the t-channel seems to be well satisfied at $t = 0$. In the broken SU (3) world, however, the breaking of the factorization in the t-channel is apparent in the t-dependence of the amplitude, as it reflects a difference in the structure of s-channel resonances. For instance, since the forward slope of the amplitude is related to the average radius of interaction as $B/2 = (\partial \ln f/\partial t)_{t=0} \sim \langle b^2 \rangle /4$ ($f = \exp\{Bt/2\}$), a difference in the s-channel trajectories, say $\alpha_{N^*,\Delta} > \alpha_{Y_0^*,Y_1^*}$, leads to a difference in the forward slope of the amplitude; $B_i(\pi N) > B_i(KN)$ for each Regge exchange i. Such difference in the average radius of interactions would cause a breaking of the line-reversal equality of cross sections in hypercharge-exchange reactions: The slopes of π induced reactions ($\pi N \to K\Lambda(\Sigma)$) are steeper than those of $\bar{K}$ induced reactions ($\bar{K}N \to \pi\Lambda(\Sigma)$). The position of the amplitude zero also reflects the impact-parameter of s-channel resonances; e.g., for the ρ exchange, we can see the first zero at $t = -0.4 \sim -0.5(\mathrm{GeV}/c)^2$ in $\pi\pi$ scattering corresponding to the small impact parameter of the ρ and f resonances ($b = 0.7 \sim 0.8$ fm), while we can see that at $t \simeq -0.2(\mathrm{GeV}/c)^2$ in πN or KN scattering.

4.6. Duality in exotic peaks

The reaction with the exotic crossed channel such as $K^-p \to \bar{K}^0 n$ in the backward direction provides us an instructive example for the duality and the resonance picture. At low energies, the $K^-p \to \bar{K}^0 n$ reaction contains Y^* resonances in the s-channel, and we can see a strong backward peak in this reaction for $p_L \lesssim 1.5\,\mathrm{GeV}/c$ (fig. 34). The FESR duality, however, implies that these resonances should average out to zero at fixed u. Then one may suspect that the observed peak is consistent with the duality.

Figure 35 shows the amplitude in the backward direction. Here we can see the alternation of the amplitude around zero with the phase which is 90° ahead (or equivalently $\Delta s \simeq 1/2\alpha'$ behind) in the real part compared with the imaginary part. Since the neighbouring resonance towers have alternating signs, an averaging to zero occurs when integrated over a sufficiently large interval ($\Delta s \simeq 2/\alpha'$). The individual resonance tower, however, makes the backward peak. Namely, we have $\langle f(180°)\rangle_{\mathrm{Ave.}} = 0$ but $(d\sigma/dt)_{180°} = \langle |f(180°)|^2\rangle_{\mathrm{Ave.}} \neq 0$. As total widths of resonances increase with energy ($m_R\Gamma_R \gtrsim 1/\alpha'$), the adjacent resonance towers tend to overlap, and thus the backward peak falls off rapidly [84].

Experimentally, the 180° (or 0°) cross section of the exotic reaction is known to fall off as $s^{-9.5} \sim s^{-10}$ (Chabaud et al. [101, 102, 103] and Eide et al. [173] for $K^-p \to pK^-$, $\bar{p}p \to K^+K^-$ and $\bar{p}p \to \bar{p}p$; Akerlof et al. [3] for $\pi^-p \to K^+\Sigma^-$, $K^-p \to \pi^+\Sigma^-$ and $K^-p \to K^+\Xi^-$).‡ The backward peak is

†We can see the fixed-t zero characteristic of the Regge exchange persisting down to $p_L \simeq 1\,\mathrm{GeV}/c$ in the helicity amplitude in which resonances add constructively, such as $\mathrm{Im}\, f_{++}(I_t = 0)$ or $\mathrm{Im}\, f_{+-}(I_t = 1)$. On the other hand, a large cancellation makes the amplitude such as $\mathrm{Im}\, f_{+-}(I_t = 0)$ or $\mathrm{Im}\, f_{++}(I_t = 1)$ quite small and there can be seen a large fluctuation with energy. Such amplitude does not exhibit regularities until the energy becomes sufficiently high and widths of resonances becomes broad enough [217, 215].

‡We exclude here a data point of $\pi^-p \to K^+\Sigma^-$ at the highest energy, where the s-dependence seems to become flat as $\sim s^{-2}$. This may be regarded as an evidence of the onset of Regge–Regge cuts.

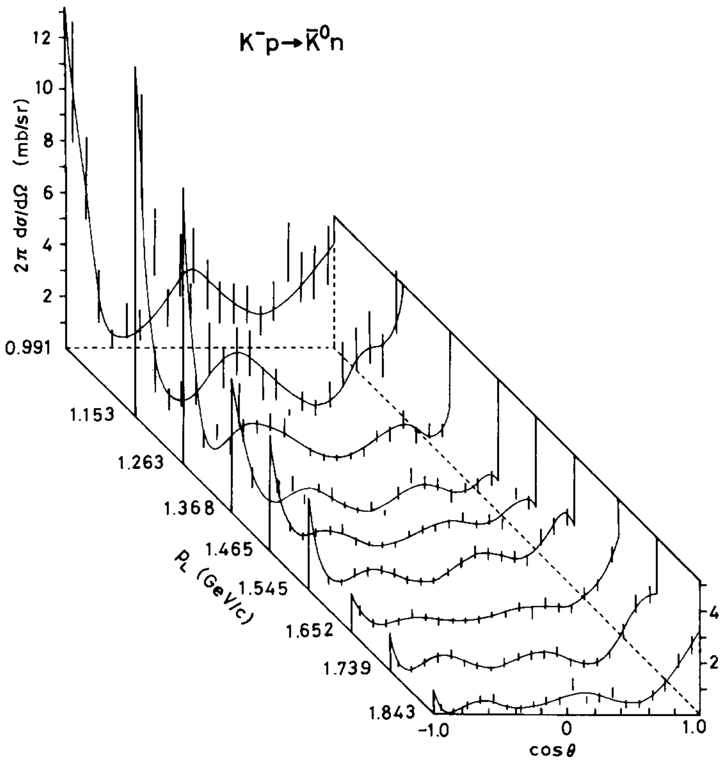

Fig. 34. Differential cross section for $K^-p \to \bar{K}^0 n$ (data from Armenteros et al. [16], Litchfield et al. [331]). Strong backward peaks in a low-energy region should be noted.

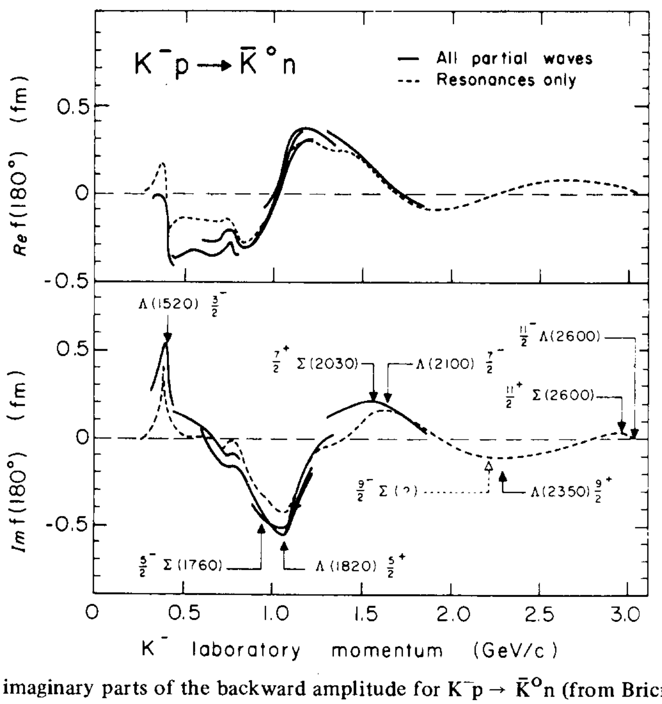

Fig. 35. Real and imaginary parts of the backward amplitude for $K^-p \to \bar{K}^0 n$ (from Bricman et al. [84]).

often observed even at considerably high energy such as $p_L \simeq 5\,\mathrm{GeV}/c$†, though the cross section is quite small compared with a non-exotic one: $\sigma_{K^-p}(180°)/\sigma_{K^+p}(180°) \approx 1/100$, [101]; $\sigma_{\bar{p}p\to K^+K^-}(0°)/\sigma_{\bar{p}p\to K^-K^+}(0°) \approx 1/200$, [103].

This pattern of semi-local cancellation is also realized in the Veneziano model with the Regge trajectories spaced by two units of angular momentum [279, 172]. Let us consider $\pi^+\pi^- \to \pi^+\pi^-$ scattering, for simplicity. Since odd-daughter trajectories are absent in this model, only even (or odd) angular momentum states are present in each resonance tower, which give a forward–backward symmetric contribution to the amplitude. The crucial difference between the forward (non-exotic) and the backward (exotic) peaks is the alternating signs of subsequent resonance towers in the backward peak. The behaviour embodying exotic characteristics arises only through the introduction of total widths, namely the introduction of an overlap between subsequent resonance towers.

The B_4 amplitude is expressed as a sum of narrow-width resonances,

$$B_4(s,t) = \sum_{n,l} \frac{\Gamma_{n,l}}{n - \alpha(s)} P_l(z). \tag{4.13}$$

To introduce total width, let us replace expediently $\alpha(s)$ in eq. (4.13) by $\alpha(s) + \mathrm{i}\,\mathrm{Im}\,\alpha(s)$. Then we have

$$B'_4(s,t) = \sum_{n,l} \frac{\Gamma_{n,l}}{n - \alpha(s) - \mathrm{i}\,\mathrm{Im}\,\alpha(s)} P_l(z). \tag{4.14}$$

This corresponds to the prescription "keeping z fixed, replace $\alpha(s)$ by $\alpha(s) + \mathrm{i}\,\mathrm{Im}\,\alpha(s)$ in the B_4 amplitude (4.13)" [450, 279, 172]. This amplitude leads to

$$B'_4(s,t) \sim -\Gamma(1-\alpha(t))\,\mathrm{e}^{-\mathrm{i}\pi\alpha(t)}(\alpha' s)^{\alpha(t)} \tag{4.15a}$$

in the forward direction, and

$$\sim 2\pi\mathrm{i}\,\mathrm{e}^{-\pi \mathrm{Im}\,\alpha(s)}\mathrm{e}^{\mathrm{i}\pi\alpha(s)} \left\{ 1/\Gamma\left[\alpha(u) + \mathrm{i}\frac{\mathrm{Im}\,\alpha(s)}{4q^2}\,u\right]\right\} (\alpha' s)^{\alpha(u)} \tag{4.15b}$$

in the backward direction. Therefore, the amplitude $B'_4(s,t)$ exhibits the Regge behaviours at small t and starts to deviate from it as $|t|$ increases and then it changes smoothly into exotic behaviours at small u with the following characteristics:

(i) The amplitude exhibits the oscillation with a damping factor $\sim\exp\{-\pi\mathrm{Im}\,\alpha(s)\} = \exp\{-\pi\alpha' m_s\Gamma_s\}$ with a phase which is 90° ahead in the real part, caused by the cancellation of neighbouring resonance towers with the alternating signs.

(ii) There appear distinct backward peaks with slopes and *relative* heights similar to the non-exotic ones, even though no Regge exchange is allowed in the u-channel.

Thus eq. (4.15b) concisely embodies our empirical knowledge of the exotic amplitude. The s-channel resonance models such as stated in section 4.4 [318, 243] also have similar behaviours; i.e., $|f(s,\theta=\pi)/f(s,\theta=0)| \simeq \exp\{-\pi\mathrm{Im}\,\tilde{\alpha}(s)\}$.

Several authors [39, 314, 95] have postulated a local cancellation between the even- and the odd-daughter resonances without semi-local averaging over two towers of resonance. Indeed the conventional B_4 model of $\pi^+\pi^-$ scattering ($\alpha(s) = 1/2 + s$, $\mu_\pi^2 \approx 0$) shows complete local

†These peaks had usually been attributed to the Regge–Regge-cut exchange [365, 414]. Such exotic cut, however, cannot explain the s-dependence of the rapid fall-off.

cancellation at $u = 0$; but this cancellation does not happen at almost all other u-values. Thus the semi-local cancellation turns out to be essential also in this case [84].

In the meson–baryon system the situation becomes slightly more complicated because of the presence of the two independent amplitudes. Take $\bar{K}N$ scattering as an example. As was discussed in section 4.5, we have $|f_{+-}| \gg |f_{++}|$ at $t = 0$ in $K^-p \to \bar{K}^0 n$, which gives a turnover in the forward direction. Since the d-function has symmetry in z, the inequality continues to hold also in the backward direction, when the overlap between resonance towers with opposite signatures is still small. Hence a sharp backward peak would arise in such a case (see fig. 34). On the other hand, we have $|f_{++}| \gg |f_{+-}|$ in $K^-p \to K^-p$ even apart from the pomeron contribution, so that the shape of backward cross section tends to be more or less flat. The backward peak is thus less prominent than in $K^-p \to \bar{K}^0 n$ [214].

An interesting example can be seen in $A^{(+)}(\pi N)$, which possesses characteristics of the exotic peak, i.e.,

(i) $|A^{(+)}|^2$ has a forward peak decreasing rapidly with energy.

(ii) Both Re $A^{(+)}(0)$ and Im $A^{(+)}(0)$ alternate around zero with the phase which is 90° ahead in the real part (fig. 36). This suggests that $A^{(+)}$ is described by only the (s,u) term, owing to the decoupling of f from $A^{(+)}$ amplitude though the t-channel is not exotic (cf. eqs. (5.5) and (5.6)).

4.7. Duality for baryon exchanges

At the end of this section, we argue the baryon-exchange process. This process is interesting, because the baryon-Regge-pole amplitude, when extrapolated to its resonance pole, is connected to the knowledge of the direct channel. Here we shall be confronted with the problem characteristic of baryon system such as parity doubling.

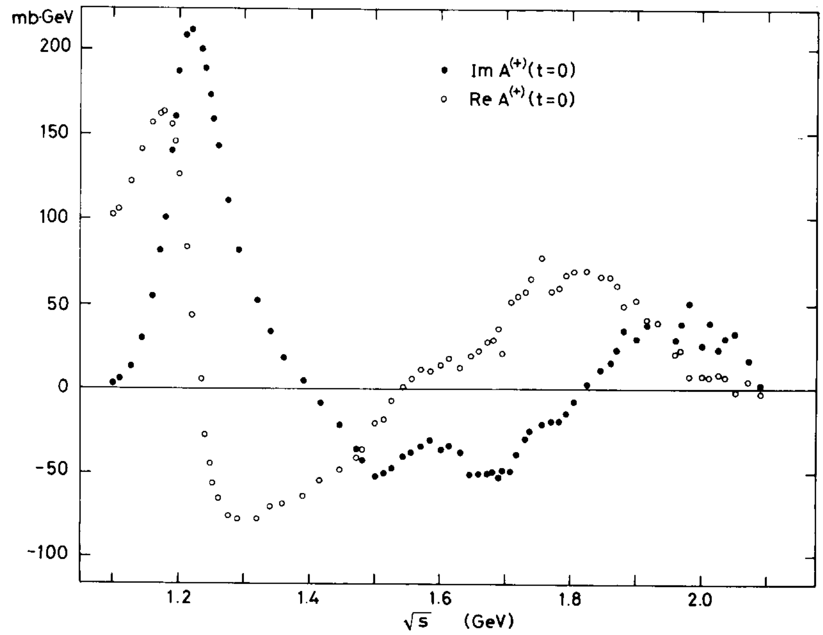

Fig. 36. $A^{(+)}(\pi N) = A(\pi^0 p \to \pi^0 p)$ at the forward direction from the phase-shift data by Almehed and Lovelace [7].

Baryon Regge poles

We begin with some kinematical considerations. The baryon exchange is reggeized with respect to the parity-conserving kinematical-singularity-free helicity amplitudes [220, 124, 35],

$$\tilde{F}^{\pm}(\sqrt{u},s) = \mp(A + M_{\mathrm{N}}B) - \sqrt{u}B, \tag{4.16}$$

such as

$$\tilde{F}^{\pm}(\sqrt{u},s) = \gamma^{\pm}(\sqrt{u})R(\bar{\alpha}^{\pm})\,\frac{1+\tau\exp(-i\pi\bar{\alpha}^{\pm})}{\sin\pi\bar{\alpha}^{\pm}}\left(\frac{s-t}{2s_0}\right)^{\bar{\alpha}^{\pm}}, \tag{4.17}$$

where $R(\bar{\alpha}^{\pm}) = 1/\Gamma(\bar{\alpha}^{\pm}+1)$ for instance $(\bar{\alpha}^{\pm} \equiv \alpha^{\pm} - 1/2)$. The MacDowell symmetry (A.20) leads us to the relation

$$\alpha^{+}(\sqrt{u}) = \alpha^{-}(-\sqrt{u}), \qquad \gamma^{+}(\sqrt{u}) = -\gamma^{-}(-\sqrt{u}) \tag{4.18}$$

between the Regge poles [234]. Here $\pm$ indicates the naturality τP of Regge poles. In this section, we assume the trajectory to be linear,† i.e., $\alpha^{+}(\sqrt{u}) = \alpha^{-}(\sqrt{u}) \equiv \alpha(u) = \alpha' u + \alpha_0$.

At a resonance pole, $u = M_{\mathrm{R}}^2$, the A' and the B amplitudes behave as $s^{J_{\mathrm{R}}-1/2}$ for $s \to \infty$ $(A' = A + M_{\mathrm{N}}B$ in this limit). One can easily deduce the constraints from eq. (4.16) [456],

$$[A'/B]_{u=M_{\mathrm{R}}^2} = \pm M_{\mathrm{R}} \quad \text{for } \tau\mathrm{P} = \pm. \tag{4.19}$$

The Gribov relation, eq. (4.18), implies that if a trajectory is linear (even in $\sqrt{u}$), another trajectory with the opposite parity should be degenerate. However, no known resonance seems to exist in parity doublets.‡ Equation (4.19) just corresponds to the condition for no parity doublets.

One way out of this difficulty is to assume that the residue of one of the twin trajectories vanishes when $\bar{\alpha}$ passes through a physical integer, i.e., to require eq. (4.19) at each resonance pole. This implies that $\gamma^{+}(\sqrt{u})$ contains a factor $\sim(1 \pm \sqrt{u}/M_{\mathrm{R}})$ for each $\tau\mathrm{P} = \pm$ resonance. Phenomenological baryon-Regge residues contain this factor or its product eliminating one or several parity doublets [e.g., 124, 35, 456, 277, 291, 338, 63]. One can also eliminate an infinite number of parity doublets, if necessary, by introducing a transcendental function§ [370, 478].

Another way is to introduce a fixed cut in the angular momentum plane at $u = 0$ [97]. This prescription requires eq. (4.19) to hold not only at resonance poles but for any $u > 0$, i.e.,

$$[A'/B]_{s\to\pm\infty} = \pm\sqrt{u} \qquad \text{for any } u > 0. \tag{4.20}$$

Thus, in order for A' and B to be analytic, one has to introduce a cut with a branch point at $u = 0$, which would move parity doublets into an unphysical sheet. In the Carlitz–Kislinger model [97], A' contains only poles while B has very strong cut contributions. In this model, the simple relation is lost between scattering regions and resonance regions. Further, this prescription is not satisfactory in phenomenological analyses [65].

† Arguments for non-linear-trajectory will be given in section 5.5.

‡ Once pairs of the N's and of Λ's at $J = 5/2$, i.e., the pair $\mathrm{N}_\alpha(1688)$ and $\mathrm{N}_\beta(1670)$ $(\Delta m^2 \sim 0.06\,\mathrm{GeV}^2)$ and the pair $\Lambda_\alpha(1815)$ and $\Lambda_\beta(1830)$ $(\Delta m^2 \sim 0.05\,\mathrm{GeV}^2)$, were considered to be evidences of such parity doublets [37, 38]. However the Σ members of these multiplets, $\Sigma_\alpha(1915)$ and $\Sigma_\beta(1765)$, are obviously non-degenerate $(\Delta m^2 \cong 1/2\,\mathrm{GeV}^2)$. Further since we have $\alpha_{\Sigma\delta\beta}(0) - \alpha_{\Sigma_\alpha\gamma}(0) \approx 1/2$, these two trajectories do not satisfy the Gribov conspiracy at $u = 0$. In addition, these octets have very different F/D ratios: $[F/D]_{5/2^+} \approx 0.8$ and $[F/D]_{5/2^-} \approx -0.1$. It follows from the requirement of duality that F/D ratios are nearly constant along the respective trajectories, so that these two trajectories do not seem to be parity partners. Thus we may conclude that there is no such evidence of parity doublets.

§ For example, $\gamma^{+}(\sqrt{u}) \sim \exp\{P(\sqrt{u})\}\prod_{n=1}^{\infty}(1 + \sqrt{u}/M_n)\exp[-\sqrt{u}/M_n + u/2M_n^2]$ with $P(\sqrt{u})$ a polynomial of $\sqrt{u}$.

Now the spin nonflip to flip ratio A'/B is kinematically fixed at the pole position, but not fixed in the physical regions within the Regge-pole framework.† When a single pole or an exchange degenerate pair of poles is exchanged, the differential cross section is given by

$$d\sigma/du \propto [|A'|^2 + |B\sqrt{-u}|^2] = |\tilde{F}^+(\sqrt{u},s)|^2 \tag{4.21}$$

for $s \to \infty$. Here $\tilde{F}^+$ has two phases; ϕ = Regge phase, $\theta = \mathrm{arctg}\,(B\sqrt{-u}/A')$. The phase ϕ is fixed by the Regge trajectory, but the phase θ, and hence $A'/B \equiv f(u)$ is left free [479]. In order to determine a value of θ, one needs spin-correlation measurements:

$$A'/\sqrt{-u}B \simeq -(\tilde{R} + iP)/(1 - \tilde{A}). \tag{4.22}$$

Here $P = 0$ in the present case, see eq. (A.10).

The Regge-pole amplitude, when extrapolated to $u = M_R^2$, does not give a unique coupling strength Γ_R (the partial width of the resonance R) unless this ambiguity of Regge parameters is resolved. Namely, though $d\sigma/du$ is invariant under any change in the form of $f(u)$, the extrapolated value Γ_R varies for a wide range. It is a well-known problem that the extrapolation of Δ_δ Regge pole in $\pi^-p \to p\pi^-$ gives too small a value for $\Gamma_{\Delta(3/2^+)}$ [36, 282, 65]. These analyses assume a factor $\gamma^+(\sqrt{u}) = 1 - \sqrt{u}/M_\Delta$ in the residue functions which eliminates the lowest parity partner, so that they keep $f(u) = A'/B = -M_\Delta$ in the extrapolation procedure. We present in fig. 37 the A'/B ratio in the following cases:

(i) γ^+ contains a factor eliminating the n lowest parity partners (n = 1, 2, 3).

(ii) γ^+ is chosen so as to give the correct width $\Gamma_{\Delta(3/2^+)}$ as well as angular distributions of $\pi^-p \to p\pi^-$ (here the first parity partner is eliminated) [434]. We denote this case as RRPM in fig. 37.

As is seen in the case (ii), A'/B at $u \simeq 0$ is only 1/4 of the value at the pole position ($u = M_\Delta^2$), while conventional Regge analyses assumed it to be constant with respect to u.

On the other hand, the successful extrapolation of the N_α Regge pole in $\pi^+p \to p\pi^+$ and $K^-N \to \Lambda\pi$ to its pole position [36, 65, 355, 209, 58] are ascribed to the fact that A'/B does not vary so much between at the N_α pole and at $u \simeq 0$. (A'/B at $u \simeq 0$ is only 25% smaller than that of $u = M_N^2$, [434].)

Another interesting example is given by $\pi^-p \to K^0\Lambda$, in which two exchange-degenerate pairs of Regge poles, $(\Sigma_\alpha, \Sigma_\gamma)$ and $(\Sigma_\delta, \Sigma_\beta)$ would be equally important. The assumption of equal con-

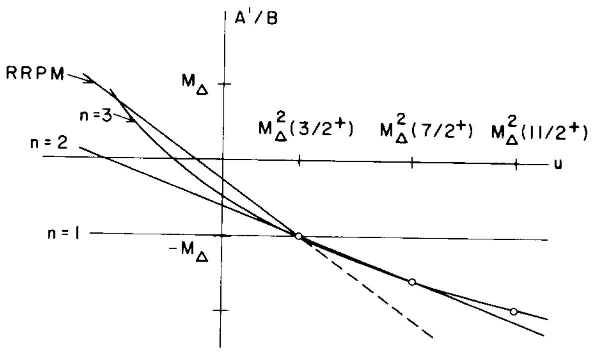

Fig. 37. Spin nonflip to flip ratio A'/B of Δ_δ Regge-pole amplitudes as a function of u for the cases described in the text.

†This arbitrariness is not characteristic of baryon exchanges but it generally occurs in the Regge-pole analysis without the FESR or the spin-correlation data as an input [144]. In the analysis of forward scattering, however, Regge residues are assumed to have a simple form. This enables us to determine $\nu B/A'$ at $t = 0$.

tributions of two-exchange-degenerate pairs with opposite naturalities, together with $\alpha_{\Sigma_{\delta\beta}} - \alpha_{\Sigma_{\alpha\gamma}} \simeq 1/2$, makes A'/B purely imaginary and gives maximal polarization† at $u' \approx -0.2 \sim -0.4(\mathrm{GeV}/c)^2$. The purely imaginary A'/B is verified by the recent spin-correlation measurement [21] (see fig. 38).

Duality for baryon exchange

The spin-nonflip to flip ratio A'/B is also interesting from the duality view point. We can express this ratio in terms of s-channel resonance contributions as

$$\left[\frac{A'}{M_R B}\right]_{\substack{u \text{ fixed} \\ s\to\infty}} = \sqrt{s}\,\frac{\bar{f}_{+-}}{\bar{f}_{++}} \simeq \frac{\sqrt{s}}{q\langle r\rangle}\,\frac{[\beta]-[\alpha]-[\delta]+[\gamma]}{[\beta]+[\alpha]-[\delta]-[\gamma]}\,. \tag{4.23}$$

Here $[\alpha], \dots, [\delta]$ implies the semi-local average of the contributions from the $\alpha, \dots, \delta$ resonances and $\langle r\rangle$ is an effective radius of interactions satisfying $q\langle r\rangle \propto \sqrt{s}$. If the $\tau P = -(+)$ resonance dominates in the s-channel, $A'/M_R B$ approaches to a positive (negative) constant, which implies that the $\tau P = +(-)$ Regge pole dominates in the u-channel. This means that the s-channel resonances build most dominantly the u-channel baryon Regge poles with the opposite naturality [213]. This is also required by the (s,u) crossing symmetry of $A'(s,u)$ and $B(s,u)$ and fixes the relative importance of the natural to unnatural baryon resonances as was seen in section 3.5.

So far the dual structure of the baryon-exchange processes is hardly known because of the lack of reliable FESR analyses owing to the difficulties in estimations of the contributions from $B\bar{B} \to MM$ channel (especially those from unphysical regions).

Qualitative features of the baryon exchange, however, can be studied by assuming the semi-local form of duality, i.e., by averaging the resonance contributions over $\Delta s = 2/\alpha'$ ($\times n$) [213]. In a region where parent resonances dominate, this averaging implies that one (or n) from each of the $\alpha, \beta, \gamma, \delta$ multiplets should be included in the integral. The integral of the N^* and the Δ with

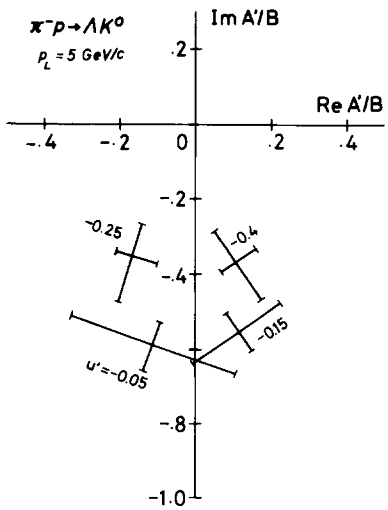

Fig. 38. Spin nonflip to flip ratio A'/B for $\pi^- p \to K^0\Lambda$ from the measurement of spin-correlation parameters [21]. The value $|A'/B|$ is consistent with the Regge residue which eliminates 2 or 3 parity partners.

†Note that $P = 1$ implies $A'/B \sim -i$ (remember that $P^2 + R^2 + A^2 = 1$ and eq. (4.22)).

$J = 3/2 \sim 9/2$ gives $g^2_{\pi NN}/4\pi \approx 13$ and $\Gamma_\Delta \approx 0.12$GeV at $u = M_N^2$ and M_Δ^2, respectively. In this estimation A'/B is specified by the resonance, so that the ambiguity mentioned before does not appear. We show in table 13 the ratios A'/B at $u = 1$ (GeV/c)$^2 \approx M_N^2 \approx M_\Delta^2$ for several reactions. Although these values fluctuate depending upon how resonances are summed up, but they indicate the $\tau P = -$ exchange dominance in the Δ exchange processes and the $\tau P = +$ dominance in the processes in which the N can be exchanged except for $K^- p \to \Sigma^- \pi^+$. The N_α does not dominate in $K^- p \to \Sigma^- \pi^+$, since $g^2_{KN\Sigma}$ is very small due to $F/D \approx 1$.

We can also study the qualitative structure of the scattering amplitude in a similar manner. Shown in fig. 39 is the u-dependence of the imaginary part of the amplitude obtained by a semi-local integration of the resonances [213]. (Here the integral is made at fixed u' since the regularity is seen better at fixed u' rather than at fixed u in the low-energy region [46].)

Table 13

The A'/B ratio at $u = 1$ (GeV/c)^2 in terms of semi-local averaging of s-channel resonances (A' in mb · GeV: B in mb)

	u-channel Regge poles	s-channel resonances		sign
		$J = 5/2$ and $7/2$	$J = 3/2 \sim 9/2$	
$\pi^+ p \to p\pi^+$	N, Δ	−269/−196	−365/−694	+
$\pi^- p \to p\pi^-$	Δ	−56/+186	−264/+245	−
$K^- p \to \Sigma^- \pi^+$	N, Δ	+11/−196		?(≈0)
$K^- p \to \Sigma^+ \pi^-$	Δ	+75/−147		−
$K^- p \to \Lambda \pi^0$	N	−104/−295		+

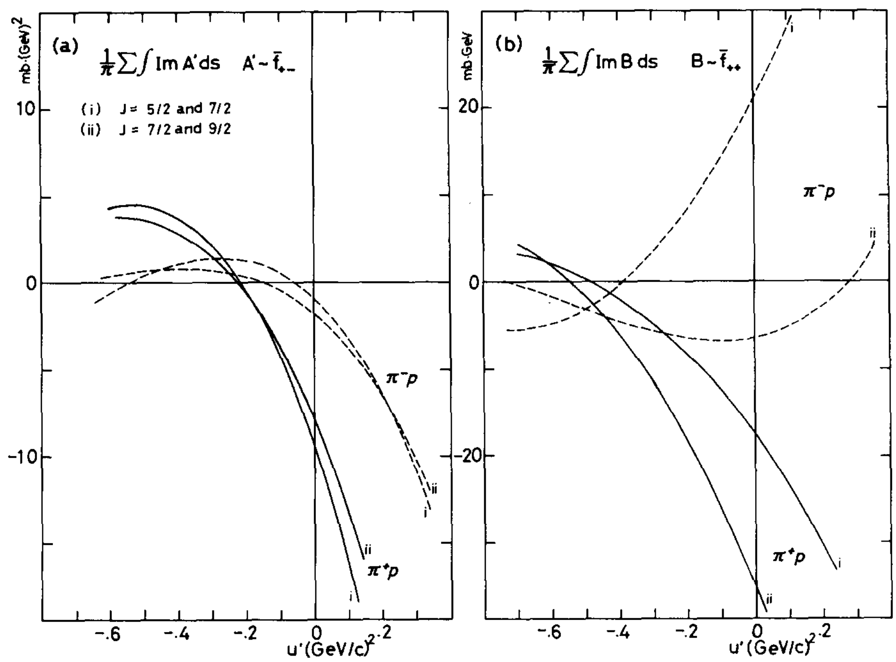

Fig. 39. Imaginary parts of the elastic $\pi^\pm p$ amplitudes in a backward region given by the semi-local averaging of s-channel resonances. The resonances with spin 5/2 and 7/2 or 7/2 and 9/2 are summed up (from Fukugita [213]).

The following features can be seen:

(i) At $u \approx 1$ (GeV/c)^2, the π^+p amplitudes have the sign of the N_α exchange and the π^-p amplitudes have that of the Δ_δ exchange.

(ii) The π^+p amplitudes have a simple structure as a consequence of the Δ_δ dominance in the s-channel: Im A' ($\sim$Im $\bar{f}_{+-}$) has the well-known zero at $u' = -0.2$(GeV/c)^2, which is attributed to the wrong-signature-nonsense zero of the N_α exchange as well as to the zero of "J_0". Im B ($\sim$Im $\bar{f}_{++}$) has a zero at $u' \simeq -0.5$(GeV/c)^2 in agreement with that of "J_1". High-energy analyses do not discriminate yet whether such a zero exists at $u' \simeq -0.5$ [e.g., 189] or -0.2(GeV/c)^2 in Im B [e.g., 50].

(iii) The π^-p amplitudes are rather complicated due to the cancellation among many prominent resonances in the s-channel: Im A' has a zero at $u' \simeq -0.1$(GeV/c)^2 which is also found by several high-energy analyses [189, 50]. It is difficult to say anything about Im B for $u' \lesssim 0$ due to ambiguities caused by the large cancellation among s-channel resonances.

It is interesting to ask whether the Δ_δ Regge pole has the wrong-signature-sense zero at $\alpha_\Delta = 1/2$ ($u \simeq 0.35$(GeV/c)^2) required by the exchange degeneracy with the N_β. (See example 3 in section 3.4.) The relative Regge phase between N_α and Δ_δ takes a value $\approx\pi - \pi/4$ or $\approx\pi/4$ at $u = 0$ (since $\alpha_\Delta - \alpha_N \approx 1/2$), according as the Δ_δ residue has a zero or not between $u = 0$ and M_Δ^2. (Here the N_α and Δ_δ dominance is assumed.) On the other hand, the cross sections of $\pi^\pm p \to p\pi^\pm$ and $\pi^- p \to n\pi^0$ at 180° give the relative phase of f(180°) which is consistent with $\pi/4$ [e.g., 316, 50]. Hence no such zero is indicated in f_{+-} between $u = 0$ and M_Δ^2. The same result can be seen in fig. 39a. One may suppose, however, that the zero at $u' \simeq -0.1$(GeV/c)^2 in A' is a trace of a wrong-signature-sense zero which has been shifted to that point by possible cut contributions. (We remind the reader of the cross-over phenomenon in that the wrong-signature zero at $\alpha_\rho = 0$ is shifted to $t \simeq -0.2$(GeV/c)^2 in the A' amplitude.) As for the spin-flip amplitude, several high-energy analyses [e.g., 189, 253, 483] give f_{++}(180°) with the sign suggesting a zero between $u = 0$ and M_Δ^2.

5. Further aspects of duality

5.1. Odorico zeros

Odorico has focused his attention on the zeros of the Veneziano amplitude [383, 384]. For brevity of explanation, let us consider the B_4 amplitude of the type

$$\frac{\Gamma(1-\alpha(s))\Gamma(1-\alpha(t))}{\Gamma(1-\alpha(s)-\alpha(t))} \,. \tag{5.1}$$

This amplitude has poles at $\alpha(s)$, $\alpha(t) = 1, 2, 3, \ldots$, and has zeros at $\alpha(s) + \alpha(t) = 1, 2, 3, \ldots$, which suppress double poles at the intersections of poles. These zeros appear at fixed u. This structure is not special to the B_4 amplitude, but quite general in the case where s- and t-channel poles coexist, i.e.,

$$\frac{\gamma_1}{m^2-s} + \frac{\gamma_2}{m^2-t} + c \approx \frac{\gamma - \gamma_2 s - \gamma_1 t}{(m^2-s)(m^2-t)} \,. \tag{5.2}$$

The B_4 amplitude specifies the residue as $\gamma_1 = \gamma_2$ and propagates the zeros to be linear. When resonance poles have finite widths, these zeros imply $d\sigma/d\Omega$ to have dips at these points.†

Such dips are most clearly observed when one of the crossed channels is exotic and the pomeron exchange is absent. In the angular distribution of $K^-p \to \bar{K}^0 n$, we can see clear dips at fixed values of u; $u \simeq -0.1$, -0.7 and $-1.7(\mathrm{GeV}/c)^2$. Crossing points of (ρ, A_2) in the t-channel and (Λ_α, Λ_γ) in the s-channel are $u \simeq 0.4$, -0.6, $-1.6(\mathrm{GeV}/c)^2$. This agrees well with our observation (Odorico [383, 384]; see also fig. 40), although the existence of (Σ_β, Σ_δ) may slightly modify the above values of u.

When the exotic channel is absent, the pattern of zero trajectories becomes slightly complicated. Let us take meson–meson scattering which is free from spin complications. Veneziano-type amplitudes for $\pi\pi$, πK, KK and $K\bar{K}$ are given by

$$\begin{aligned} \mathrm{I} &= B_4(s,t) \\ \mathrm{II}^\pm &= B_4(s,t) \pm B_4(u,t) \\ \mathrm{III}^\pm &= B_4(s,t) + B_4(u,t) \pm B_4(s,u) \end{aligned} \tag{5.3}$$

in the limit of the universal intercept of Regge trajectories.‡ If the supplementary condition

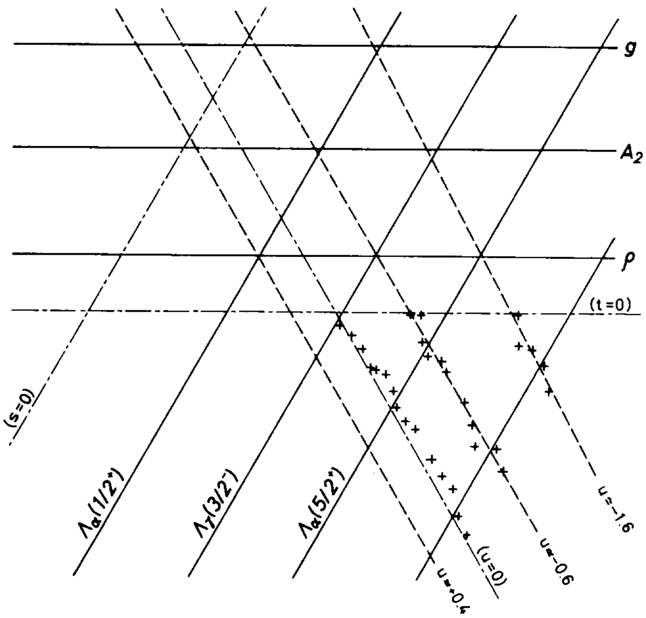

Fig. 40. Resonance poles (s channel: Λ_α–Λ_γ, t channel: ρ–A_2) and the amplitude zeros for $K^-p \to \bar{K}^0 n$ on the Mandelstam plane predicted by a simple B_4 amplitude. The position of dips observed in $K^-p \to \bar{K}^0 n$ angular distributions is also shown (crosses) (after Odorico [383, 384]).

†Suppose we can approximate an amplitude in terms of partial waves up to L, then the amplitude $f(z)$ is expressed by the product like $f(z) \simeq \prod_{k=1}^{L} (z - z_k)$. Here z_k becomes complex when widths are finite. Since the differential cross section can be written as $d\sigma/d\Omega = |f(z)|^2 \simeq \prod_{k=1}^{L} (z - z_k)(z - z_k^*)$, $d\sigma/d\Omega$ has a dip with half-width $|\mathrm{Im}\, z_k|$ at $z = \mathrm{Re}\, z_k$. (Thus $d\sigma/d\Omega$ is invariant under $z_k \to z_k^*$, i.e., under the change of sign of $\mathrm{Im}\, z_k$. This causes 2^L fold ambiguity in phase-shift analyses [221, 61].)

‡ I : $\pi^+\pi^- \to \pi^+\pi^-$, $K^+\pi^- \to K^+\pi^-$, $K\bar{K} \to K\bar{K}$;

II$^+$: $K^0\pi^0 \to K^0\pi^0$; II$^-$: $K^+\pi^- \to K^0\pi^0$;

III$^+$: $\pi^0\pi^0 \to \pi^0\pi^0$; III$^-$: $\pi^\pm\pi^0 \to \pi^\pm\pi^0$.

$\alpha(s)+\alpha(t)+\alpha(u)=1$ is imposed, the double-pole-killing zeros are required to lie along the following straight lines on the Mandelstam plane†‡

$$
\begin{aligned}
&\mathrm{I} &&: \alpha(u) = 0, -1, -2, \ldots \\
&\mathrm{II}^{+} &&: \alpha(t) = -1, -3, \ldots; \qquad \alpha(s)-\alpha(u) = \pm 1, \pm 3, \ldots \\
&\mathrm{II}^{-} &&: \alpha(t) = 0, -2, \ldots; \qquad \alpha(s)-\alpha(u) = 0, \pm 2, \ldots \\
&\mathrm{III}^{+} &&: \alpha(s), \alpha(t), \alpha(u) = -1, -3, \ldots \\
&\mathrm{III}^{-} &&: \alpha(t) = -1, -3, \ldots; \qquad \alpha(s), \alpha(u) = 0, -2, -4, \ldots\,.
\end{aligned}
\tag{5.4}
$$

Among the Veneziano type models, only the combinations I, $\mathrm{II}^{\pm}$, $\mathrm{III}^{\pm}$ of B_4 terms with the supplementary condition give us linear lines of zeros [385], but otherwise they give more complicated patterns of zeros [388, 170].

Though the observed zeros of $\pi\pi$ scattering may deviate from straight lines by about $0.3\,\mathrm{GeV}^2$ on the Mandelstam plane, the patterns of zeros, i.e., number of the zeros, the direction of their propagation and their approximate positions, are in good agreement with theoretical expectations. For example, figs. 41a and b correspond to the case I and II^{-}, respectively [170]. We add the following comments:

(i) The zero which propagates along $\alpha(u)\simeq 0$ is not the double-pole-killing zero but arises from a factor $1-\alpha(s)-\alpha(t)$ included in the $\pi\pi$ amplitude. This zero appears to bend towards the Adler zero as it approaches the Mandelstam triangle [401].

(ii) The entrance of the 2nd, 3rd, ... lth zeros into the physical region is observed as a decrease of the normalized harmonic moments, $\langle Y_3^0\rangle$, $\langle Y_5^0\rangle$, ... $\langle Y_{2l-1}^0\rangle$, [169]. A rapid decrease of $\langle Y_1^0\rangle$ at $\sqrt{s}\simeq 1\,\mathrm{GeV}$ in $\pi^+\pi^-$ scattering [8, 270] is related to the opening of $\mathrm{K\bar{K}}$ threshold, and is hardly related to the linear propagation of zero [386] whose effect appears as a decrease of $\langle Y_3^0\rangle$, [169].

The linear propagation of zeros is also observed in $\pi\mathrm{K}$ and $\pi\pi\to\mathrm{K\bar{K}}$ reactions [470].

Resonance couplings [385]

The amplitudes of type I and $\mathrm{III}^{\pm}$ give $\gamma_2/\gamma_1 = 1$ at the pole–pole intersection, and those of type $\mathrm{II}^{\pm}$ include $\gamma_2/\gamma_1 = \pm 1, 2$. These simple ratios of residues are just the manifestation of the nonet couplings of the 1^- and 2^+ mesons to 0^-0^-.

Further if we assume the reactions including η and $\eta'(958)$ as external particles to have amplitudes of the type I, $\mathrm{II}^{\pm}$, $\mathrm{III}^{\pm}$, we have two alternative coupling patterns: (i) The 0^- multiplet

†With this condition the wrong-signature zeros of Regge amplitude coincide with the Odorico zeros.

‡With this condition, $\mathrm{II}^{\pm}$ and $\mathrm{III}^{\pm}$ are written as

$$
\mathrm{II}^{\pm} = \frac{2^{1-\alpha(t)}}{\sqrt{\pi}}\,\Gamma(1-\alpha(s))\Gamma(1-\alpha(u))\left\{\begin{matrix} \Gamma\left(1-\frac{\alpha(t)}{2}\right)\Gamma^{-1}\left(\frac{1+\alpha(t)}{2}\right)\cos\frac{\pi}{2}(\alpha(u)-\alpha(s)) \\[2ex] \Gamma\left(\frac{1-\alpha(t)}{2}\right)\Gamma^{-1}\left(\frac{\alpha(t)}{2}\right)\sin\frac{\pi}{2}(\alpha(u)-\alpha(s)) \end{matrix}\right\}.
$$

$$
\mathrm{III}^{+} = 2\sqrt{\pi}\,\Gamma\left(1-\frac{\alpha(s)}{2}\right)\Gamma\left(1-\frac{\alpha(t)}{2}\right)\Gamma\left(1-\frac{\alpha(u)}{2}\right)\Big/\Gamma\left(-\frac{\alpha(t)+\alpha(u)}{2}\right)\Gamma\left(-\frac{\alpha(u)+\alpha(s)}{2}\right)\Gamma\left(-\frac{\alpha(s)+\alpha(t)}{2}\right) \quad \text{[Virasoro amplitude 498]}
$$

$$
\mathrm{III}^{-} = 2\sqrt{\pi}\,\Gamma\left(\frac{1-\alpha(s)}{2}\right)\Gamma\left(\frac{1-\alpha(u)}{2}\right)\Gamma\left(1-\frac{\alpha(t)}{2}\right)\Big/\Gamma\left(\frac{\alpha(s)}{2}\right)\Gamma\left(\frac{\alpha(u)}{2}\right)\Gamma\left(\frac{1+\alpha(t)}{2}\right).
$$

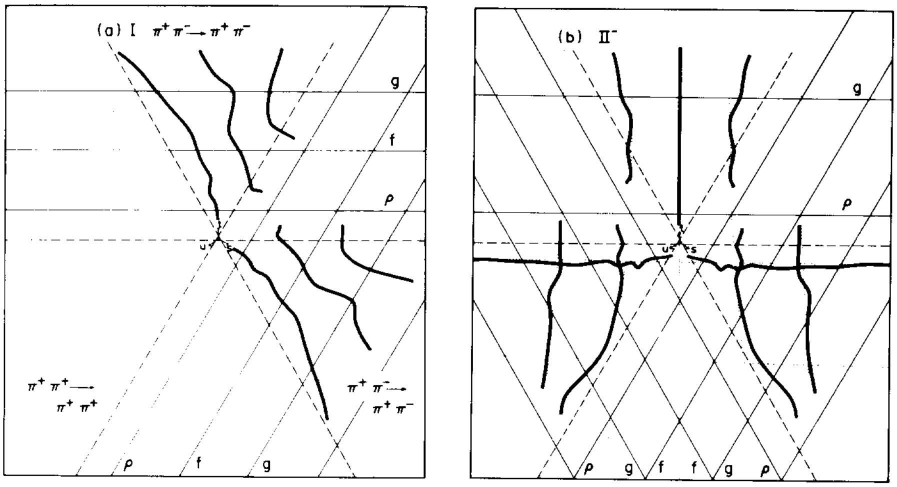

Fig. 41. Mandelstam plot of resonance poles and zero contours of the $\pi\pi$ scattering amplitude for the charge configurations corresponding to (a) I and (b) II$^-$(from Eguchi, Shimada and Fukugita [170]). For the case of type I, see also Pennington and Protopopescu [400] and Hyams et al. [270].

as well as 1^- and 2^+ forms an ideal-mixing nonet and all of the 0^-–0^-–$2^+(1^-)$ couplings obey the quark-model prediction [94]. (ii) The mixing angle of the 0^- multiplet has just an opposite sign to the ideal ones ($\tan\theta = -\sqrt{1/2}$) and the couplings including the singlet pseudoscalar ($\gamma_{P_8P_1T_8}$, $\gamma_{P_1P_1T_1}$) are one half of that in the quark model, while 1^- and 2^+ obey an ideal-mixing nonet scheme [385]. (In this solution the couplings of $A_2\pi\eta'$, $K^{**}K\eta$ and of $f\eta'\eta'$ vanish.)

We present the mixing angle of 0^- and $\gamma_{P_8P_1T_8}/\gamma_{P_8P_8T_8}$ in table 14.† This η–η' mixing causes a destructive interference of η_1 and η_8 in the $K^{**}K\eta$ and $A_2\pi\eta'$ couplings.

Table 14

The mixing angle of the 0^- multiplet and the coupling ratio $\gamma_{P_8P_1T_8}/\gamma_{P_8P_8T_8}$. The mixing angle is defined by $|\eta\rangle = -|\eta_1\rangle \sin\theta + |\eta_8\rangle \cos\theta$, $|\eta'\rangle = |\eta_1\rangle \cos\theta + |\eta_8\rangle \sin\theta$. Underlined values are the input of the analysis.

	θ	$\gamma_{P_8P_1T_8}/\gamma_{P_8P_8T_8}$
quark model	$+35.3°$ or $-54.7°$	1
quadratic mass formula	$\pm 10 \pm 1°$	
linear mass formula	$\pm 24 \pm 1°$	
$\Gamma(\eta \to 2\gamma)^a/\Gamma(\pi^0 \to 2\gamma)$	$-7.6 \pm 2.6°$	
Kotlewski et al. [319] [b]	$-15.5 \pm 1.7°$	
Martin and Michael [356] [c]	$-11°$	0.50
Moscoso et al. [375] [d]	$\underline{-10 \sim -11°}$	0.71 or -0.64
Bolotov et al. [76] [e]	$-20.6 \pm 2.2°$	$\underline{1}$
Apel et al. [13] [e]	$-19.1 \pm 1.8°$	$\underline{1}$

[a]The Cornell value [89]. We assume the quark-model value for $\langle\gamma\gamma|\eta_1\rangle/\langle\gamma\gamma|\eta_8\rangle$.
[b]From radiative decays of 0^- and 1^-.
[c]From various production experiments.
[d]From $K^-p \to \eta\Lambda$, $\eta'\Lambda$ at 3.95 GeV/c.
[e]From $\pi^-p \to \eta n$, $\eta' n$ at 40 GeV/c.

†There is an argument that the mixing angle of 0^- varies as the value of m^2 considerably such as $\theta(m_\eta^2) \simeq 6°$ and $\theta(m_{\eta'}^2) \simeq 20°$, [294].

5.2. Duality for baryons

Simple arguments do not hold for meson–baryon scattering because of the spin complexity and of the complication of the baryon spectrum. Experimentally, however, the angular distribution of various meson-baryon processes shows the simple dip systematics implied from eq. (5.3) [384].

Let us consider $\pi^\pm p \to \pi^\pm p$ scattering. We have the following dip systematics in the angular distributions. (Here we denote $\pi^+ p \to \pi^+ p$ as the s-channel.)

(ia) $t \simeq -0.6(\mathrm{GeV}/c)^2$ in $\pi^\pm$p: the wrong-signature zero of ρ (not in $d\sigma/d\Omega$, but in $|A|^2$, which is free from the diffraction).
(ib) $t \simeq -2.8(\mathrm{GeV}/c)^2$ in $\pi^\pm$p [e.g., 79, 437, 82].
(ic) $t \simeq -4.8(\mathrm{GeV}/c)^2$ in $\pi^\pm$p, [100].
(iia) $u \simeq -0.2(\mathrm{GeV}/c)^2$ in π^+p: wrong-signature zero of N_α.
(iib) $u \simeq -2.8(\mathrm{GeV}/c)^2$ in π^+p, [459, 368].
(iii) $s \simeq +0.3(\mathrm{GeV}/c)^2$ in π^-p: the wrong-signature sense zero of Δ_δ (expected from the exchange degeneracy, but not yet confirmed, see section 4.7).

The dip at $t \simeq -2.8(\mathrm{GeV}/c)^2$ has been known to travel down until it reaches the backward direction, where it produces a marked dip in the energy distribution of the 180° cross section of π^+p scattering at $s \simeq 4.85\,\mathrm{GeV}^2$ (this dip is also observed in π^-p, though the position is slightly shifted) [79]. Similarly in the π^+p channel, the dip expected in $|A|^2$ at $t \simeq -0.6(\mathrm{GeV}/c)^2$ produces a dip in the energy dependence of the 180° cross section (expected at $s \simeq 2.1\,\mathrm{GeV}^2$, but observed at $s \simeq 2.3\,\mathrm{GeV}^2$). Further the zero at $u \simeq -0.2(\mathrm{GeV}/c)^2$ is observed as a dip of the energy dependence of $|A|^2$ at $\theta = 0°$ (expected at $s \simeq 2.0\,\mathrm{GeV}^2$, observed at $s \simeq 2.3\,\mathrm{GeV}^2$), see fig. 42.

The systematics of dips is understood by a pattern of the double-pole-killing zero in fig. 43, indicating that $\pi^\pm$p scattering has the characteristics of the pattern III$^-$ in eq. (5.3). The expected dips in π^-p scattering are also observed, but their positions are slightly shifted due to the existence

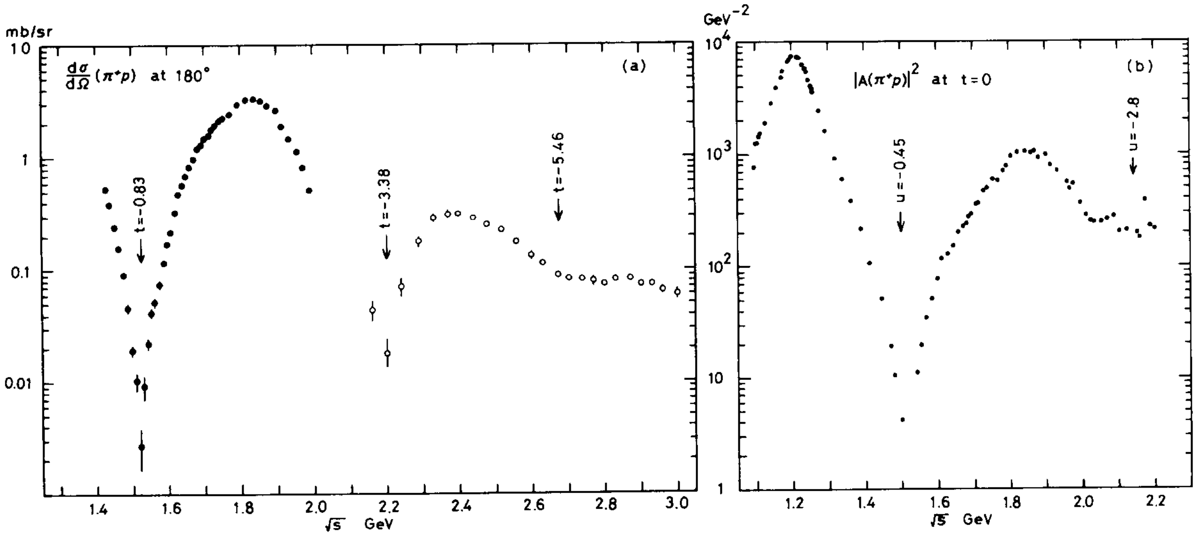

Fig. 42. (a) Differential cross section for π^+p elastic scattering at 180° as a function of energy (data from Rothschild et al. [432], Baker et al. [28]). (b) Energy dependence of $|A(\pi^+p \to \pi^+p)|^2$ at $t = 0$ calculated from the phase-shift data by Almehed and Lovelace [7].

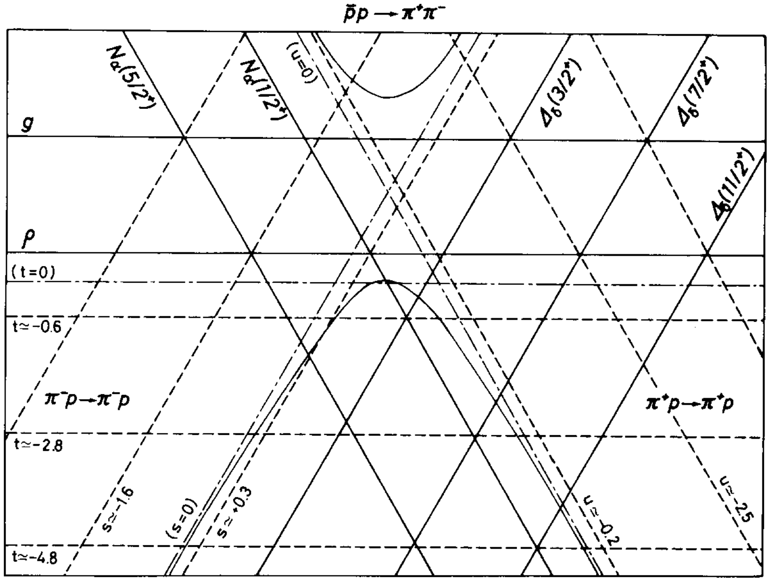

Fig. 43. Resonance poles (s-channel: Δ_δ; u-channel: N_α; t-channel: ρ–g) and amplitude zeros expected from the simple B_4 combinations III^- on the Mandelstam plane (Odorico [384]).

of N_γ and Δ_δ (Δs, $\Delta t \approx 0.4(\mathrm{GeV}/c)^2$). It should be noted that we omitted in fig. 43 by the reason explained later the resonance poles N_γ and Δ_δ in the u-channel and f(1270) in the t-channel which would also contribute.

Odorico proposed that the A amplitude has a simple structure and further he assumed that $A(\pi^+p)$ is described by $(s,u) - (s,t) + (u,t)$. Then we have [387]

$$A(\pi^+p \to \pi^+p) = (s,u) - (s,t) + (u,t)$$

$$A(\pi^-p \to \pi^-p) = (s,u) + (s,t) - (u,t)$$

$$A^{(+)}(\pi^0p \to \pi^0p) = (s,u)$$

$$\frac{1}{\sqrt{2}} A^{(-)}(\pi^-p \to \pi^0n) = (s,t) - (u,t). \tag{5.5}$$

These equations have several outstanding features.

(i) π^+p scattering should be dominated by the odd-signature resonances ($J = 3/2, 7/2, \ldots$) in the s-channel. This is realized by the Δ_δ dominance. The t-channel should be dominated by the odd-signature (ρ) exchange (the f should be decoupled).

(ii) In the π^-p channel, the resonances with $J = 1/2, 5/2, \ldots$ should dominate, while those with $J = 3/2, 7/2, \ldots$ should be suppressed. This means that the N_α should dominate in the π^-p channel and the N_γ and Δ_δ should cancel out each other, i.e., we have,

$$\sum_{J_i = 3/2} \int \mathrm{Im}\, F_i \mathrm{d}s = 0, \qquad \sum_{J_i = 7/2} \int \mathrm{Im}\, F_i \mathrm{d}s = 0, \ldots .$$

The ρ exchange also dominates in the t-channel.

(iii) The π^0p amplitude $F^{(+)}$ is superconvergent in the forward direction, i.e., f should be decoupled from this amplitude.

(iv) The imaginary part of the charge-exchange amplitude is superconvergent in the backward direction.

Figure 44a shows the resonance contribution to Im A at each J (at $t = m_\rho^2$). One can easily recognize the above feature (i) ~ (iii) in the figure. In particular, one can observe almost complete cancellation between $\Delta_\delta(3/2^+)$ and $N_\gamma(3/2^-)$ at $J = 3/2$, [387]. A significant cancellation is also seen between $\Delta_\delta(7/2^+)$ and $N_\gamma(7/2^-)$ at $J = 7/2$. (This is the reason why we omitted the poles N_γ and Δ_δ in fig. 43.)

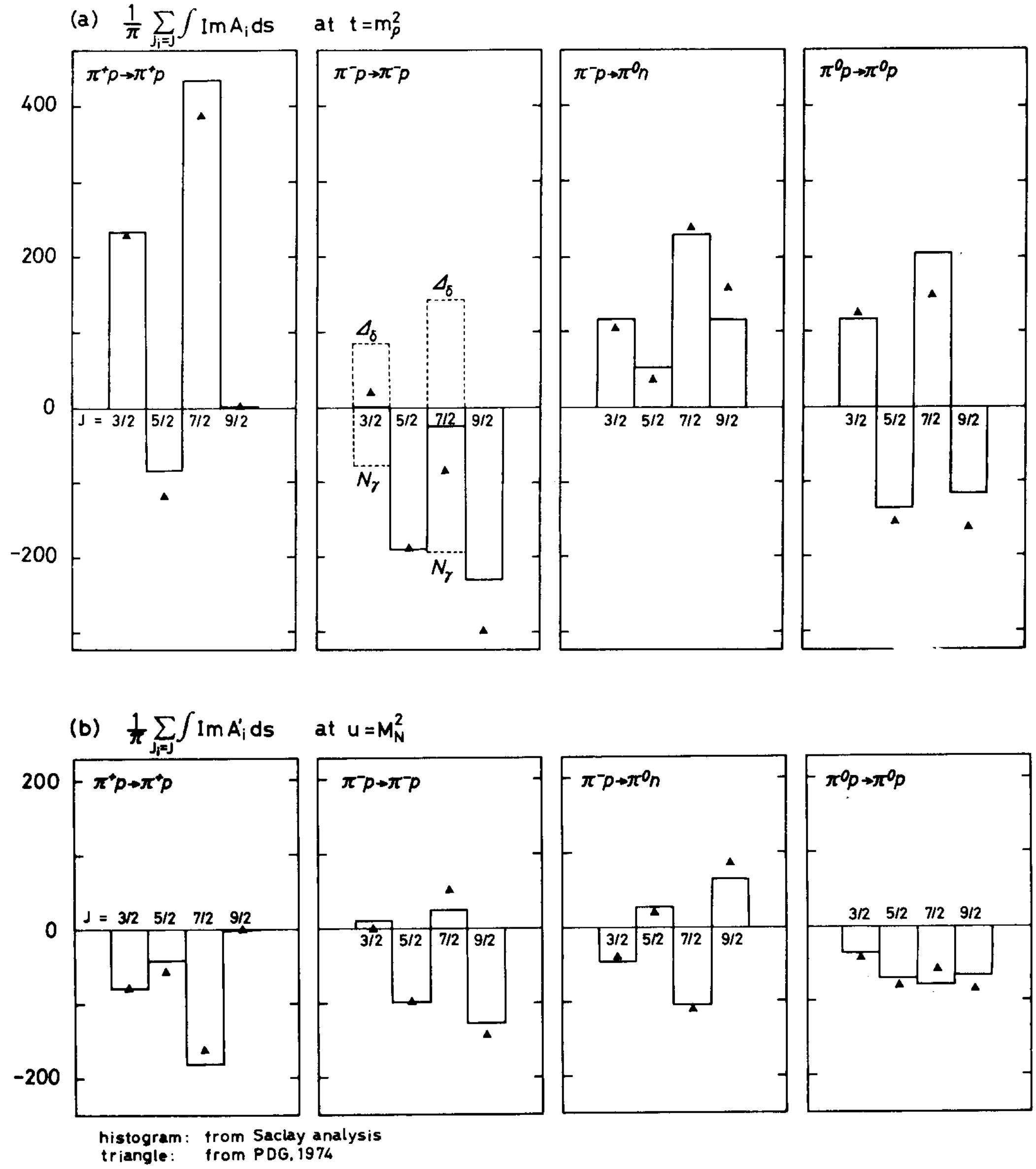

Fig. 44 (a) Contribution of the N* and the Δ resonances with spin J to Im A at $t = m_\rho^2$. (b) The similar figure for Im A' at $u = M_N^2$ (from Fukugita [213]).

On the other hand, the A amplitude does not show the expected structure in the backward direction, but the A' amplitude exhibits the structure expected from eq. (5.5) approximately (fig. 44b). The amplitude exhibiting the structure in eq. (5.5) should show behaviour like A and A' in the regions for $t \gtrsim 0$ and $u \gtrsim 0$, respectively. (Note that $\bar{f}_{+-}$ has such behaviour as $s \to \infty$.) Further it should have simple symmetry property in z. Since such an amplitude is not constructed yet, we work only at $t = m_\rho^2$ and $u = m_N^2$.

The crossing-invariant spectrum [167, 212] gives us a guide to understand the structure in eq. (5.5). The amplitude corresponding to the combination II–I, which behaves like $\sim A$ in the forward region and $\sim A'$ in the backward region, has the following structure:

$$\begin{aligned}
&\pi^+ p \sim -(s,t) + (u,t) + \zeta_1 \cdot (s,u) \\
&\pi^- p \sim +(s,t) - (u,t) + \zeta_1 \cdot (s,u) \\
&\pi^0 p \sim +\zeta_1 \cdot (s,u) \\
&\frac{1}{\sqrt{2}}(\pi^- p \to \pi^0 n) \sim +(s,t) - (u,t)
\end{aligned} \tag{5.6}$$

where $\zeta_1 = -(f^2 - 2f + 13/9)/(f^2 - 2f + 5/9)$, $(f \equiv [F/D]_{8\alpha})$. With $f = 1$, it follows that $\zeta_1 = 1$ and thus eq. (5.6) reduces to eq. (5.5). In this case the resonance spectrum with $\tau P = +$ reduces to $(1 \oplus 8_1)_\gamma \leftrightarrow (8_1)_\alpha$. If we put $f = 2/3$ and 0.82 corresponding to the values in table 8, we have $\zeta_1 = 5/3$ and 1.16 respectively. Figure 44 really suggests $\zeta_1 > 1$.

Similarly, corresponding to the combination II + I, we have the amplitude which exhibits the behaviour like $\sim A'$ in the forward region and the behaviour like $\sim$MB in the backward region. This amplitude has the structure of the form

$$\begin{aligned}
&\pi^+ p \sim -\zeta_1 \cdot (s,t) - \zeta_2 \cdot (u,t) + (s,u) \\
&\pi^- p \sim -\zeta_2 \cdot (s,t) - \zeta_1 \cdot (u,t) - (s,u) \\
&\pi^0 p \sim -\frac{\zeta_1 + \zeta_2}{2}\,[(s,t) + (u,t)] \\
&\frac{1}{\sqrt{2}}(\pi^- p \to \pi^0 n) \sim -\frac{\zeta_2 - \zeta_1}{2}\,[(s,t) - (u,t)] - V(s,u)
\end{aligned} \tag{5.7}$$

with $\zeta_2 = -3(9f^2 - 10f + 5)/(9f^2 - 18f + 5)$. If we put $f = 1$, 0.82 and 2/3, ζ_2 takes 3, 2.3 and 7/3, respectively. With such values of the parameter eq. (5.7) leads us to qualitative understanding of the observed structure of the A' amplitude at $t = m_\rho^2$ and of the B amplitude at $u = m_N^2$ as a function of J, [213].

5.3. Local superconvergence relation and symmetry [453]

The superconvergence relation (SCR) is valid if the crossed channel is exotic, but it does not lead to useful results if cut-off is taken after a few resonances. There is, however, the case where the convergence of SCR is sufficiently rapid and another class of SCR holds. Such SCR leads to the symmetry of resonance couplings [453].

If we assume parent-parent-pole duality and the degeneracy of all the trajectories, the B_4 amplitude with exotic t-channel is symmetric under the interchange of s and u; this implies symmetry in $z_t = \cos\theta_t$. Consider the amplitude for $K\bar{K} \to K\bar{K}$ with $I_t = 0$, then the Bose statistics requires that the amplitude must be antisymmetric in z_t. Therefore, the amplitude should vanish identically.†

The identical vanishing of the amplitude requires the pole residues to cancel locally. In our example, the combined residue of the s-channel 1^- pole (ρ, ω, ϕ) and 2^+ pole (A_2, f, f') must vanish at all t values. For 1^- pole, one has

$$\sum_{i=\rho,\omega,\phi} \int \mathrm{d}s \, \mathrm{Im}\, f_i(s,t) = 0, \tag{5.8}$$

which leads to

$$\tfrac{3}{2} g^2_{\rho K\bar{K}} - \tfrac{1}{2}(g^2_{\omega K\bar{K}} + g^2_{\phi K\bar{K}}) = 0. \tag{5.9}$$

This relation (local SCR) leads to the coupling ratio in agreement with the SU (3) coupling.

This differs from the usual exchange degeneracy in the following points:

(i) If the exotic t-channel is not antisymmetric, we merely have $\mathrm{Im}_t f = 0$ and this leads to the exchange degeneracy between the s-channel Regge poles with opposite signatures, so that we have a relation between the residues of 1^- and 2^+; $\gamma(1^-)^2 = \gamma(2^+)^2$.

(ii) If the exotic t-channel is antisymmetric, we have $f = 0$ and this gives the local SCR among 1^- poles and among 2^+ poles; $\Sigma_i \gamma_i(1^-)^2 = \Sigma_i \gamma_i(2^+)^2 = 0$.

Application to meson–baryon scattering

We consider the amplitudes which are exotic and anti-symmetric in the t-channel, i.e., $B^{[27]}$ and $A'^{[10,10^*]}$. If we saturate the local SCR with the $1/2^+$ and $3/2^+$ baryons which form a multiplet $\underline{56}$ of SU (6), we get

$$\sum_{i=1/2^+,\ 3/2^+} \int [\mathrm{Im}\, B_i^{[27]}]_{t=0} \mathrm{d}s = 0, \qquad [26] \tag{5.10a}$$

$$\sum_{i=1/2^+,\ 3/2^+} \int \left[\frac{\mathrm{d}}{\mathrm{d}t} \mathrm{Im}\, A_i'^{[10,10^*]}\right]_{t=0} \mathrm{d}s = 0. \tag{5.10b}$$

We confine our discussion in the limit $[\mu(0^-)/M(1/2^+)]^2 \approx 0$. Since the local SCR for A' is trivially satisfied in this limit, we work with the first derivative in t in eq. (5.10b). Then the spin kinematics is summed up by the following relation

$$\begin{bmatrix} B \\ 4M \dfrac{\mathrm{d}}{\mathrm{d}t} A' \end{bmatrix} \sim \begin{bmatrix} +1 & -1 \\ +1 & +2 \end{bmatrix} \cdot \begin{bmatrix} g^2(1/2^+) \\ g^2(3/2^+) \end{bmatrix} .$$

We have two equations for two free coupling ratios, and the solution is

$$[F/D]_{1/2^+} = 2/3$$

$$g^2_{10}(3/2^+)/g^2_8(1/2^+) = 4/25 \qquad \text{(experimental value} \sim 1/3.84)$$

in agreement with the SU $(6)_W$ predictions.

†The B_4 amplitude for $K\bar{K} \to K\bar{K}$ with $I_t = 0$ is given by

$$f = -\lambda\, [\Gamma(1-\alpha_\rho(s))\Gamma(1-\alpha_\phi(u))/\Gamma(1-\alpha_\rho(s)-\alpha_\phi(u)) - \Gamma(1-\alpha_\rho(u))\Gamma(1-\alpha_\phi(s))/\Gamma(1-\alpha_\rho(u)-\alpha_\phi(s))] .$$

If we assume the trajectories to be degenerate, then the amplitude vanish identically, i.e., $f = 0$.

Next, let us consider the reaction such as $\bar{K}N \to \bar{K}N$ where u-channel is exotic. Saturating the FESR by the resonances with the couplings obtained above, we have

$$\beta_\rho/\beta_\omega = \int \mathrm{Im}\, B(I_t = 1)\,\mathrm{d}s \Big/ \int \mathrm{Im}\, B(I_t = 0)\,\mathrm{d}s = \tfrac{5}{3}.$$

Similarly, we obtain for $\mathrm{d}A'/\mathrm{d}t$

$$\beta_\rho/\beta_\omega = \int \mathrm{Im}\,\frac{\mathrm{d}}{\mathrm{d}t} A'(I_t = 1) \Big/ \int \mathrm{Im}\,\frac{\mathrm{d}}{\mathrm{d}t} A'(I_t = 0) = \tfrac{1}{3}.$$

In other words the F/D ratios for $\mathrm{VB\bar{B}}$ couplings are

$$[F/D]_{A'} = \infty, \qquad [F/D]_B = 2/3$$

in agreement with the quark-model result. Thus we have the SU $(6)_W$ couplings for the lowest multiplets.

5.4. *Higher symmetries and duality*

It has often been said that the duality constraints lead to the result of the quark model. Indeed the exchange degeneracy for mesons leads to the nonet coupling of the quark model and it is easily incorporated in the spectrum ($\underline{36}$, all L). Furthermore it is known that a Veneziano-type model for meson–meson scattering can be constructed, which gives the results of the non-relativistic quark model (spectrum; SU (6), vertex; SU $(6)_W$), [349]. In the case of baryons, however, there are some complications.

It is well known, on the other hand, that the rich hadron spectrum is economically classified as a multiplet of the static symmetry SU (6) × O $(3)_L$. (For a recent review, see [428, 429].) In this section, we briefly summarize the higher symmetry for hadrons, and then argue whether it can be accommodated to the duality constraints.

Spectrum of hadrons

The oscillator pattern of SU (6) × O $(3)_L$ multiplets is particularly useful in a classification of baryons [232, 185, 308]. We present in fig. 45 the spectrum of baryons together with that of mesons. The multiplet on the leading baryon trajectory is what one expects in the three-quark picture of baryons. The existence of parent multiplets, $\underline{56}$, L = even; $\underline{70}$, L = odd, is well confirmed for $L \leqslant 4$,† and there is some evidence for $\underline{70}$, $L = 2$; $\underline{56}$, $L = 3$ which needs further confirmation‡ (see reviews [428, 429, 330]). For the daughter multiplets, the assignment is rather dubious. We will not discuss such daughter multiplets here, since they are less important for the argument of exchange degeneracy.

Decay symmetry (for more details, see [428])

The static SU (6), when applied to decay processes, encounters the well-known difficulties, namely it leads to $\rho \not\to \pi\pi$ and $\Delta \not\to \pi N$, for example. The SU $(6)_W$ is a relativistic generalization of

†$\underline{56}$, $L = 0$; filled up. $\underline{70}$, $L = 1$; nonstrange members are filled up.
$\underline{56}$, $L = 2$ nonstrange members are filled up. (However, $\Delta_\delta(3/2^+, 1890)$ in the Saclay analysis [24] is not yet confirmed.)
$\underline{70}$, $L = 3$; some members are known as Regge recurrences. $\underline{56}$, $L = 4$; some members are known as Regge recurrences.

‡$\underline{70}$, $L = 2$; N$(7/2^+$, 1990), which couples more strongly to $\pi\Delta$ than to πN, has been claimed as a candidate. For further evidences see [187].
$\underline{56}$, $L = 3$; $\Delta(9/2^-, \sim 2200)$ is suggested to be a candidate for this multiplet.

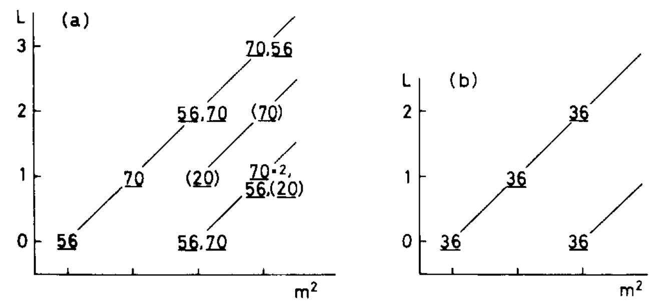

Fig. 45. Harmonic-oscillator spectrum of SU (6) × O (3)$_L$ multiplets. (a) Baryons. Multiplets in parentheses do not couple to $0^- 1/2^+$ systems. (b) Mesons.

the SU (6), in that it is invariant under the boost in the z direction (the collinear symmetry), [59, 329]. It leads to the successful F/D ratio when applied to the $B\bar{B}M$ vertex. However, the validity of the collinear symmetry for the transition matrices is not evident. Further the W-spin conservation has not been verified in any hadronic processes.

The application of the "SU $(6)_W$" to transition matrix elements stands on a firm basis when the well-defined current quark is transformed into the constituent quark by a unitary transformation [362, 363]. The SU $(6)_{W,\text{current}}$ is defined in terms of the 36 good components of the generators (we denote them as F^α), which are taken out of the 144 U(12) generators† [141]. If there exists a unitary transformation V such that $\tilde{F}^\alpha = VF^\alpha V^{-1}$ commutes with the Hamiltonian, $\tilde{F}^\alpha$ forms a *symmetry algebra* SU $(6)_{W,\text{constituents}}$ and thus hadrons are represented as its irreducible representations. Then, the mesonic transition matrix is estimated in terms of $\langle \tilde{B}|F^{5\alpha}|\tilde{A}\rangle = \langle B|VF^{5\alpha}V^{-1}|A\rangle$ with the aid of the PCAC.

One can explicitly construct such a V in the free quark model [362, 363]. For the axial current $F^{5\alpha}$, $\tilde{F}^{5\alpha}$ acquires the component which changes S_z $(\equiv W_z)$, i.e., we have $\tilde{F}^{5\alpha} = \tilde{F}^{5\alpha}_{\Delta S_z=0} + \tilde{F}^{5\alpha}_{\Delta S_z=\pm 1}$. If one assumes the transformation property of $\tilde{F}^{5\alpha}$ in the interacting case to be the same as that in the free case, the mesonic-transition amplitude is expressed in terms of two reduced matrix elements: The first component had $\Delta S_z = 0$ and corresponds exactly to the SU$(6)_W$ and the second has $\Delta S_z = \pm 1$, giving rise to a symmetry-breaking part of SU$(6)_W$. This broken SU$(6)_W$ approach preserves the successful results of the SU$(6)_W$ and further it remedies some bad prediction of the SU$(6)_W$, [255, 225].

Some results of such broken SU$(6)_W$ approach can be obtained from weaker symmetries. For example, the coplanar symmetry SU (3) × SU $(3)_{\text{copl.}}$ leads to $F/D = 2/3$ for $1/2^+, 5/2^+, \ldots$, $F/D = -1/3$ for $5/2^-, \ldots$ and $g^2_{10}(3/2^+)/g^2_8(1/2^+) = 4/25$ say [426]. (To obtain $F/D = 5/3$ for $3/2^-, \ldots$, one needs at least the $^3P_0$ model [369, 402], the matrix element of which is identical with that of the broken SU $(6)_W$ approach for mesonic decays.)

Symmetry and exchange degeneracy

As mentioned in section 3.5, many solutions of exchange degeneracy exist with more than four trajectories. We discuss here the solution when we include all the trajectories in the quark-model spectrum. It is of great theoretical interest to unify the duality approach with the quark description in order to construct a consistent picture of hadrons.

†In the free quark model these generators are given by the space integrals of 144 densities $q^\dagger\Gamma\lambda^\alpha q$ with $\Gamma \sim 16$ Dirac matrices. The 36 good components of densities are $V_0 \sim q^\dagger\lambda^\alpha q$, $A_z \sim q^\dagger\lambda^\alpha\sigma_z q$, $T_{yz} \sim q^\dagger\lambda^\alpha\beta\sigma_x q$ and $T_{zx} \sim q^\dagger\lambda^\alpha\beta\sigma_y q$.

The established baryon multiplets include $\underline{56}$ even L and $\underline{70}$ odd L. With this sequence alone, it is impossible to satisfy the constraints eq. (3.21), unless (i) we ignore the constraints imposed by exoticity in the t-channel [353, 354], or (ii) we take the constraints as approximate equations [451]. It is shown, however, in a particular model that with the spectrum

$$\begin{array}{ll} \underline{56} & L=0 \\ \underline{70} & L=1 \\ \underline{56},\ \underline{70} & L=2 \\ \underline{70},\ \underline{56} & L=3 \\ \cdot & \cdot \\ \cdot & \cdot \\ \cdot & \cdot \end{array} \tag{5.11}$$

one can satisfy the constraints in both the s and t channels [350, 427]. Furthermore it has been shown that such a solution gives resonance couplings in accordance with the broken SU $(6)_W$ and it also requires a universal dominance of either $\Delta S_z = 0$ (SU $(6)_W$-like) or $\Delta S_z = \pm 1$ (anti-SU $(6)_W$) component independent of L, [168].

Let us consider the quark diagrams (a) and (b) of fig. 46 corresponding to the (s,t) and (s,u) terms. The diagram (b) is obtained from (a) by interchanging two quarks at both the end of the upper side, so that the two diagrams are related to one another by interchanging a pair of quarks in the final state. Therefore, the even-L states in the s-channel, which are given by the sum (a) + (b), possess symmetrical multiplets $\underline{56}$ and multiplets of mixed symmetry $\underline{70}$. The odd-L states are given by their difference (a) − (b) and possess multiplets of mixed symmetry $\underline{70}$ and antisymmetric multiplets $\underline{20}$, [350]. A more detailed analysis shows that the amplitudes for MB → MB represented by diagrams (a) and (b) involve the $\underline{56}$ and $\underline{70}$ in the following proportions in the s-channel [350];

$$\begin{array}{l} \text{(a)}\ 15[\underline{56}] + 16[\underline{70}] \\ \text{(b)}\ 15[\underline{56}] - \ \ 8[\underline{70}]. \end{array} \tag{5.12}$$

These combinations, of course, have no exotics in the t- or u-channel.

Let $f(L)$ and $g(L)$ be L dependences of the s-channel baryon Regge residues in the (s,t) and (s,u) dual amplitudes, respectively. If we assume that $f(L) \neq g(L)$ and further $f(0)/g(0) = 1/2$, $f(1)/g(1) = 1$,

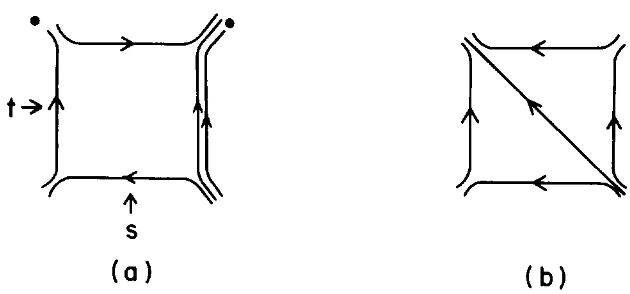

Fig. 46. The (s,t) dual (a) and the (s,u) dual (b) quark diagrams. The diagram (b) is obtained from (a) by interchanging two quarks marked by dot, followed by twisting the entire upper side.

the $\underline{70}$ and $\underline{56}$ can be eliminated at $L = 0$ and $L = 1$ respectively,† then we have the spectrum eq. (5.11) with the exchange degeneracy [427, 168],

$$
\begin{array}{ccccccccc}
L=0 & & L=1 & & L=2 & & L=3 & & \\
\underline{56} & \leftrightarrow & \underline{70} & \leftrightarrow & (\underline{56}\oplus\underline{70}) & \leftrightarrow & (\underline{70}\oplus\underline{56}) & \leftrightarrow \dots & \\
\underline{10}^4\,(3/2^+) & \leftrightarrow & \underline{8}^4_{-1/3}\,(5/2^-) & \leftrightarrow & \left\{\begin{matrix}\underline{10}^4\,(7/2^+)\\ \underline{8}^4_{-1/3}\,(7/2^+)\end{matrix}\right\} & \leftrightarrow & \left\{\begin{matrix}\underline{8}^4_{-1/3}\,(9/2^-)\\ \underline{10}^4\,(9/2^-)\end{matrix}\right\} & \leftrightarrow \dots & \\
\underline{8}^2_{2/3}\,(1/2^+) & \leftrightarrow & \left\{\begin{matrix}\underline{1}^2\,(3/2^-)\\ \underline{8}^2_{5/3}\,(3/2^-)\\ \underline{10}^2\,(3/2^-)\end{matrix}\right\} & \leftrightarrow & \left\{\begin{matrix}\underline{8}^2_{2/3}\,(5/2^+)\\ \underline{1}^2\,(5/2^+)\\ \underline{8}^2_{5/3}\,(5/2^+)\\ \underline{10}^2\,(5/2^+)\end{matrix}\right\} & \leftrightarrow & \left\{\begin{matrix}\underline{1}^2\,(7/2^-)\\ \underline{8}^2_{5/3}\,(7/2^-)\\ \underline{10}^2\,(7/2^-)\\ \underline{8}^2_{2/3}\,(7/2^-)\end{matrix}\right\} & \leftrightarrow \dots &
\end{array}
\tag{5.13}
$$

One of the most interesting tests of higher symmetry (for a review, see [428]) is the inelastic phase of $\pi N \to \pi\Delta$ in which orbital angular momentum of the final state is different from that of the initial state [186]. This phase is sensitive to the value of ΔS_z and the recent SLAC–LBL analysis indicates the $\Delta S_z = \pm 1$ dominance for the $\underline{70}$, $L = 1$ and the $\Delta S_z = 0$ dominance for the $\underline{56}$, $L = 2$ [99]. This result, if continues to hold, seems incompatible with exchange-degeneracy arguments, which require either the $\Delta S_z = 0$ or the $\Delta S_z = \pm 1$ dominance for any multiplet.

5.5. Non-degenerate parity partners

We have already mentioned in section 4.7 the possible ways to avoid parity doublets of baryon resonances. Another attempt to avoid parity doubling is to include a $\sqrt{u}$ term in the trajectory function,‡ i.e., to introduce non-degenerate parity partners [500, 272, 273].

Figure 47 shows an example of such trajectories. Here the parity partner of the $N_\alpha(940)$ is the $N_\beta(1535)$, [272]. (The parity partner of the $N_\alpha(940)$ is missing in the scheme of Barger and Cline [37, 38].) It can be seen schematically that

$$
\begin{array}{ccc}
 & \text{non-degenerate parity partner} & \\
N_\alpha(1/2^+, 940) & \longleftrightarrow & N_\beta(1/2^-, 1535) \\
 & \times \quad \text{degenerate parity partner (Barger and Cline)} & \\
N_\alpha(1/2^+, 1470) & \longleftrightarrow & N_\beta(\text{missing})
\end{array}
$$

†An example of dual amplitudes constructed using the (spinless) quark is [350].

$$B_4(s,t) = \mu \int_0^1 dx\, x^{-\alpha(s)-1}(1-x)^{-\alpha(t)-1}$$

$$B_4'(s,\mu) = \lambda \int_0^1 dx\, x^{-\alpha(s)-1}(1-x)^{-\alpha(u)-1}[1-x(1-x)]^{(s+u-M^2-\mu^2)/2}$$

corresponding to the diagrams (a) and (b), respectively. The leading power in $\alpha(t)$ at the pole $\alpha(s) = L$ behaves like

$$B_4(s,t) \to \mu[\alpha(t)]^L/L!\,\{L-\alpha(s)\},\quad B_4'(s,\mu) \to \lambda[-\alpha(t)/2]^L/L!\,\{L-\alpha(s)\}.$$

With $\lambda = 2\mu$ the conditions $f(0)/g(0) = 1/2$, $f(1)/g(1) = 1$ are satisfied.

‡This type of trajectory can easily be incorporated in the Veneziano model [500, 320].

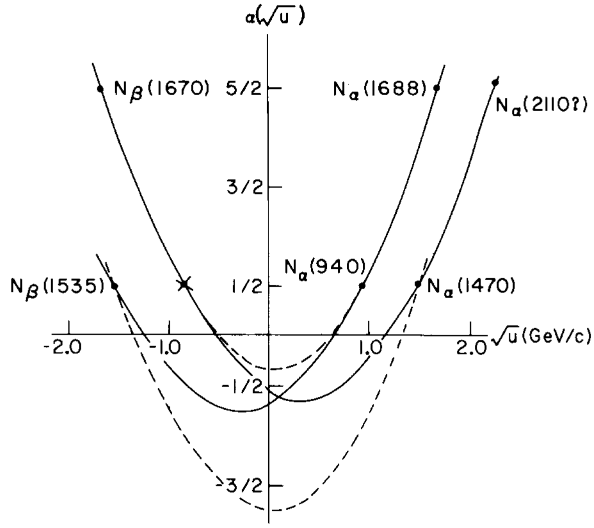

Fig. 47. An example of nucleon trajectories with non-degenerate parity partners in comparison with conventional trajectories of Barger and Cline (from Ida [272]).

In this scheme the parity doublet of the N(Λ) at $J = 5/2$ has no direct connection at all with the Gribov–MacDowell symmetry, but is a consequence of an accidental degeneracy of two nucleon (lambda) trajectories. The trajectory of $N_\alpha(940)$ appears to pass through $\alpha = -1/2$ at $u > 0$, so that the dip of $\pi^+ p \to p\pi^+$ cannot be interpreted as the wrong-signature-nonsense zero of the N_α Regge exchange. This difficulty, however, can be avoided if the so-called switching phenomenon of the two N_α trajectories occurs as in the Bethe-Salpeter model when they cross each other [273].

Based on such an interpretation, Ida classified known baryon resonances into four families of Regge trajectories $\underline{1} + \underline{8} + \underline{8}' + \underline{10}$ and their daughters.

(i) $\underline{10}_\delta - \underline{10}_{\gamma'}$, $\underline{10}_\alpha - \underline{10}_{\beta'}$, ...

(ii) $\underline{8}_\beta - \underline{8}_{\alpha'}$, $\underline{8}_\gamma - (\underline{8}_{\delta'})$, ...

(iii) $\underline{8}_\alpha - \underline{8}_{\beta'}$, $\underline{8}_\delta - \underline{8}_{\gamma'}$, ...

(iv) $\underline{1}_\gamma - (\underline{1}_{\delta'})$, $\underline{1}_\beta - (\underline{1}_{\alpha'})$, ...

The spectrum has resemblance to that of a quark model with ($\underline{56}$, L = even) ⊕ ($\underline{70}$, L = odd) as to the states of $M \lesssim 2$GeV except for the followings. The Roper resonance $N_\alpha(1/2^+, 1470)$ has a natural place in the spectrum, (ii) but there is no room in it for the $N_\gamma(3/2^-, 1700)$. In this spectrum there is also no room for the $N_\delta(7/2^+, 1990) \in (\underline{70}, L = 2)$. (These difficulties are removed by introducing another four families of trajectories [274].)

The quark model with non-degenerate parity partners

There is an attempt to unify the quark model and duality scheme by introducing the non-degenerate parity partners [283].

Assume that we have an analytic function $\alpha(\sqrt{s})$ for baryon trajectory which satisfies $\alpha(\sqrt{s}) - \alpha(\sqrt{-s}) \approx 1$ in the resonance region, and consider, for example, such a trajectory, on the positive branch of which the α–γ series appears. Then the β–δ series (non-degenerate parity partner of the α–γ series) lies on the trajectory $\alpha(-\sqrt{s})$ which is one unit below as is shown in fig. 48. In this scheme the parity partner of a baryon pole $\alpha(1/2^+)$ becomes $\beta(1/2^-)$ which is also identified as the first daughter of a parent pole $\gamma(3/2^-)$.

In order to obtain the quark-model spectrum for the quark-spin doublet say, it is sufficient to have two such trajectories which belong to $8_{2/3} \in \underline{56}$ and to $(\underline{1} \oplus \underline{8}_{5/3} \oplus \underline{10}) \in \underline{70}$. The F/D ratios of the octets as well as the ratio of $g_1^2 : g_8^2 : g_{10}^2$ in $\underline{70}$ do not vary along the trajectories for $-\infty < \sqrt{s} < \infty$. The relative weight of $\underline{56}$ and $\underline{70}$ is fixed so as to satisfy the exchange-degeneracy requirement and to eliminate $\underline{70}$ and $\underline{56}$ at $L = 0$ and $L = 1$ respectively (see eq. (5.13)).

5.6. Pomeron: duality and unitarity

The problem of pomeron is an important one, which has not been argued in this article. Here we sketch only some key points.

The most important tool for investigating the pomeron is the unitarity relation

$$\mathrm{Im}\, \langle \mathrm{f}|T|\mathrm{i}\rangle = \rho \sum_n \langle \mathrm{f}|T^\dagger|n\rangle\langle n|T|\mathrm{i}\rangle. \tag{5.14}$$

We encounter here a non-linear equation for the amplitude whereas dominant characteristics of duality are based on its linearity. The right-hand side of eq. (5.14) is dominated by multiparticle intermediate states. Equation (5.14), when we set f = i, implies $\sigma_{\mathrm{tot}} = \sigma_{\mathrm{el}} + \sigma_{\mathrm{inel}}$. Here, σ_{inel} consists of two components [505], a diffractive component yielding an energy independent n-particle cross section and a non-diffractive component such as the multi-peripheral or the multi-Regge mechanism, in which only ordinary Reggeon is exchanged in the n-particle amplitude. It is known that the non-diffractive component occupies 75 ~ 85% of the inelastic cross section† [415, 249, 192, 322].

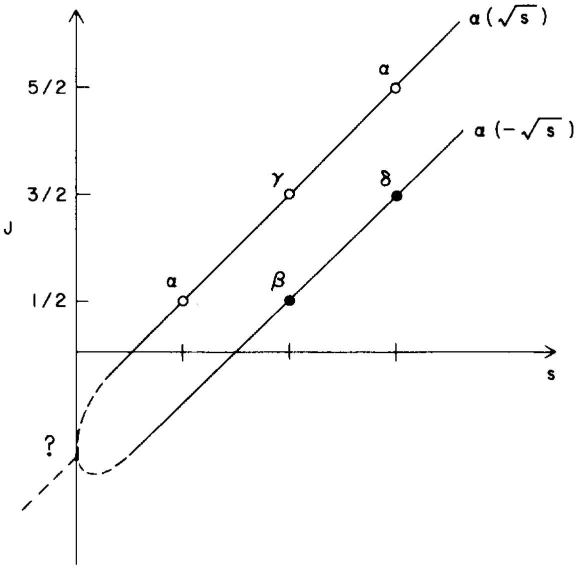

Fig. 48. A baryon trajectory which satisfies $\alpha(\sqrt{s}) - \alpha(-\sqrt{s}) \approx 1$ in the resonance region (from Igi and Shimada [283]).

†In the central region approximately 25% of the pions produced in the π^-p reaction (15% in the pp reaction) is known to come from the decay of the ρ^0 meson [e.g., 506, 472]. Hence, a considerable fraction of the pions is ascribed to the 1^-(and 2^+) meson production.

Hereafter we assume that a contribution from multiparticle states is dominated by the multi-Regge mechanism. Then, eq. (5.14) becomes an approximate relation connecting the diffractive component to the multi-Regge amplitude. We use the unitarity equation only at $t = 0$.

An n-Reggeon-exchange amplitude can be expressed as a sum of one planar amplitude and (2^n-1) non-planar amplitudes in terms of the duality diagram as is shown in fig. 49. The unitarity summation of these amplitudes leads to the diagrams in fig. 50. Here we ignore the interference between a planar and a twisted diagram and that between diagrams with twists at different positions. This is equivalent to the assumption that the production line does not include twists as is readily understandable in the duality diagram (see fig. 51). Absence of twists in production lines is equivalent to equal weight for production of particles with opposite charge conjugations, e.g., equal weight for 1^- and 2^+ resonance production (or 0^- and 1^+ production) along a multi-peripheral chain. On the contrary, inclusion of twists implies that the diagram includes exotic states when viewed

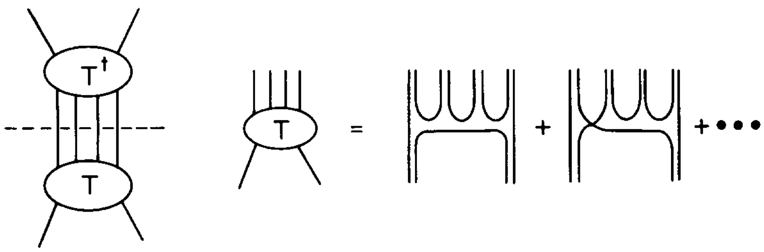

Fig. 49.

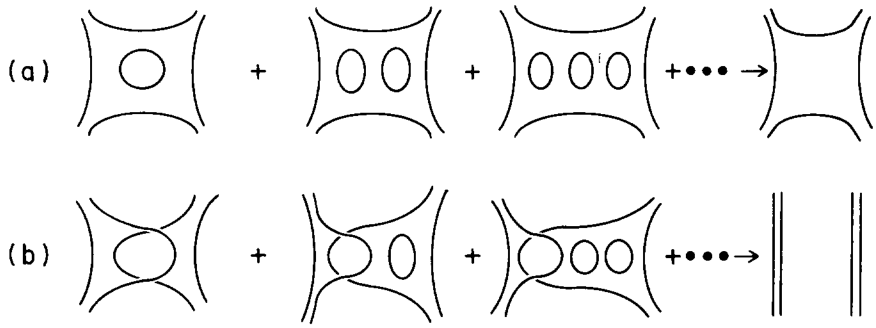

Fig. 50.

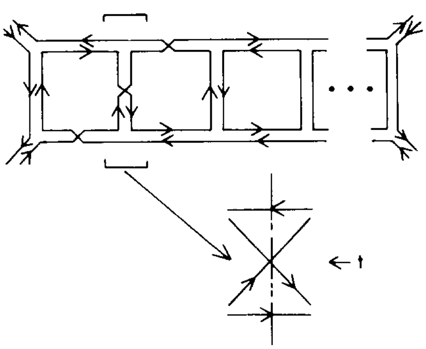

Fig. 51. Quark diagram corresponding to an overlap of two production diagrams with twists at different positions. An extra twist is inevitably required in a production line.

from the t-channel (fig. 51), so that the above assumption means that no exotic exchange should exist in the output of the unitarity summation† [454].

The unitarity summation is divided into two classes as in fig. 50. In the class (a) all the planar diagrams are summed up. They have the same topology, if closed loops are contracted, as that of the ideal-nonet meson-exchange diagram,‡ so that we equate this summation with the ideal-nonet meson-exchange amplitude. On the other hand in the class (b) all the diagrams with twists are summed. In these diagrams only the unitary singlet is allowed to be exchanged in the t-channel. This summation is thus to be equated to the pomeron-exchange amplitude [e.g., 206, 381, 327, 494, 107, 495, 109, 454]. Exotic exchanges are absent in the unitarity summation as mentioned above.

A perturbative summation of duality diagrams (the so-called KSV programme [312; see 6 for a review]) has been known as a conventional approach to satisfy the unitarity order by order in the coupling constant g^2. There is another way of summation, the so-called $1/N$ expansion, in which g^2N is fixed to be O (1) (N being the dimension of the internal symmetry SU(N)), so that the diagrams with any number of closed quark loops in it is equally important [484, 495]. (In this expansion diagrams in (b) are O ($1/N$) as compared with those in (a).) A practical approach to the loop summation is to replace a duality diagram by the square of corresponding multi-Regge amplitude and to take a sum using the multiperipheral model, as we will provide later an example.

In such a scheme, pomeron is expected to couple with external particles via Reggeons with the same quantum number as the pomeron, such as the f and the f′, [341, 96]. Then the amplitude is written as,

$$T(J,t) = \sum_{i,j=\mathrm{f},\mathrm{f}'} \frac{\gamma_i(t)}{J-\alpha_i} B_{ij}(J,t) \frac{\gamma_j(t)}{J-\alpha_j} \; . \tag{5.15}$$

Here $B_{ij}(J,t)$ represents the singularity of the pomeron (fig. 52).

The property of this (f, f′) coupled pomeron is as follows:

(i) If B_{ij} is assumed to be unitary singlet, i.e., $B_{ij} \sim (\bar{\mathrm{p}}\mathrm{p} + \bar{\mathrm{n}}\mathrm{n} + \bar{\lambda}\lambda)/\sqrt{3}$, an apparent deviation of the pomeron exchange from a unitary singlet is given through the mass breaking of f and f′. Defining $r(t) \equiv (\alpha_{\mathrm{P}}(t) - \alpha_{\mathrm{f}}(t))/(\alpha_{\mathrm{P}}(t) - \alpha_{\mathrm{f}'}(t))$ (empirically $r(0) \simeq 0.6$), we obtain, from eq. (5.15), $\sigma^{\mathrm{tot}}_{\mathrm{Kp}}/\sigma^{\mathrm{tot}}_{\pi\mathrm{p}} = (1 + r(0))/2 \simeq 0.8$, $\sigma^{\mathrm{tot}}_{\rho\mathrm{p}} = \sigma^{\mathrm{tot}}_{\omega\mathrm{p}}$, $\sigma^{\mathrm{tot}}_{\phi\mathrm{p}}/\sigma^{\mathrm{tot}}_{\rho\mathrm{p}} = r(0) \simeq 0.6$ etc. in good agreement with the experiments. Moreover, the values of $\sigma(\Lambda\mathrm{p}) \simeq 34.6 \pm 0.4$ mb [227] and $\sigma(\Sigma\mathrm{p}) \simeq 34.0 \pm 1.1$ mb [27] are consistent with the above $r(0)$ with $[F/D]_{\mathrm{TB\bar{B}}} \lesssim -5$ (see table 7).

†In a multi-peripheral model with production of only pions, e.g., in the original Chew–Pignotti model, we have $\alpha(I_t = 1) = \alpha(I_t = 2)$ in the output of the unitarity summation if the conservations of isospin and of G-parity are imposed [118]. In order to suppress the exotic exchange one needs productions of particles with opposite C-parity, the ρ meson say [454].

‡It is to be noted that

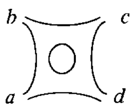

$\sim Ng^2 \times$

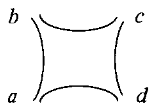

$\sim Ng^4 \, \frac{1}{4}\mathrm{Tr}\,(\lambda_a\lambda_b\lambda_c\lambda_d)$

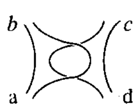

$\sim g^4 C_t \, \frac{1}{4}\mathrm{Tr}(\lambda_a\lambda_b)\mathrm{Tr}(\lambda_c\lambda_d)$,

where C_t is the C-parity of the t-channel.

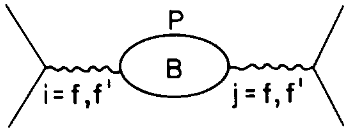

Fig. 52.

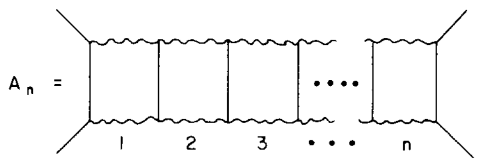

Fig. 53.

(ii) The pomeron has the same helicity structure as the f(f′). Namely, the pomeron conserves the s-channel helicity as the f does. In hyperon–nucleon scattering, however, the pomeron is predicted not to conserve the s-channel helicity at the hyperon vertex.

(iii) Factorization; the residue ratio, γ_P/γ_f, is independent of the reaction.

(iv) Equation (5.15) has a pole at $\alpha_P = \alpha_f \, (= \alpha_\rho)$. If we set $\alpha_P(t) = 1$, the pomeron coupling takes the form analogous to the electromagnetic form factor, which may validate the Wu–Yang model [509].

The (f, f′) dominated pomeron has been successfully applied to various processes such as quasi-two-body reactions [205] and inclusive reactions [e.g., 87, 510, 29, 296; see 293 for a review].

In order to argue dynamical properties of the unitarity summation, let us take the multi-peripheral model [68, 10, 118, 116, 112]. The n-Reggeon-exchange amplitude (fig. 53), in the Chew–Pignotti approximation, becomes of the form $A_n = (g\ln s)^n s^{2\alpha_M - 1}/n!$, α_M being the trajectory of exchanged Reggeons with $t \approx 0$. Hence we get

$$A_M = \sum_n \frac{(g\ln s)^n}{n!} s^{2\alpha_M - 1} = s^{2\alpha_M - 1 + g} \tag{5.16a}$$

corresponding to the summation of planar diagrams. Meanwhile the sum of $(2^n - 1)$ non-planar diagrams gives,

$$A_P = \sum_n (2^n - 1) \frac{(g\ln s)^n}{n!} s^{2\alpha_M - 1} = s^{2\alpha_M - 1 + 2g} - s^{2\alpha_M - 1 + g}. \tag{5.16b}$$

If we impose a bootstrap condition $A_M \sim s^{\alpha_M}$ on eq. (5.16a), we obtain

$$\alpha_M = 1 - g. \tag{5.17a}$$

Putting $A_P \sim s^{\alpha_P}$ for the leading term of eq. (5.16b), we have [327, 494]

$$\alpha_P = 1. \tag{5.17b}$$

This is another motivation to identify the sum of twisted diagrams with the pomeron. The similar result can be obtained by solving a multi-peripheral integral equation in the Chew–Pignotti approximation [133, 108, 109, 438, 454]. In a simple model with broken symmetry, the bootstrap condition requires ideal nonet to have equal spacing $\alpha_\rho - \alpha_{K^*} = \alpha_{K^*} - \alpha_\phi$, [158, 396].

The simple model sketched here leads to multiplicity $\langle n \rangle \approx 2g \cdot \ln s$ $(g = 1 - \alpha_M \approx 0.5)$ which is too small compared with experiments $\langle n_\pi \rangle \approx 3\langle n_{\pi^-} \rangle \simeq 3 \times 0.84 \ln(s/s_0)$, and it also gives $f_2 \equiv \langle n(n-1) \rangle - \langle n \rangle^2 = 0$. These defects, however, are overcome by identifying the produced particle as a cluster or a resonance decaying into 2.5 pions on the average.

Now the second term of eq. (5.16b) just cancels the f contribution in the output of the unitarity equation. Furthermore, by taking into account the charge conjugation, it is found that pomeron contains the $C = -$ part in the non-leading term, which denotes the ω pole and in the simple model it exactly cancels the ω contribution† [454, 438]. So far as we consider only the sum of planar diagrams, the exchange degeneracy of (ρ, A_2) and of (f, ω) is satisfied. However, if we take into account the full output in the unitarity sum, the exchange degeneracy of (f, ω) will no longer be satisfied. (The exchange degeneracy of (ρ, A_2) still holds.)

We add a remark on the pomeron in BB and $B\bar{B}$ scattering. There are $2^n/2$ non-planar diagrams with an odd number of pairs of twists in the n-Reggeon-exchange amplitude of BB scattering. On the other hand, $B\bar{B}$ amplitude has $(2^n/2 - 1)$ diagrams with an even number of pairs of twists, which also gives a secondary term that cancels the f and ω. Hence we should have $\sigma^{\text{pom}}(\text{pp}) \neq \sigma^{\text{pom}}(\text{p}\bar{\text{p}})$. A possibility to recover the equality is to take into account a contribution from the non-planar diagrams of $B\bar{B} \to$ mesons to compensate the missing piece in the $B\bar{B}$ amplitude [184]. This argument, however, brings an undesirable secondary term for the meson exchange. (The contrary argument that the $B\bar{B}$ annihilation contributes to $\sigma^{\text{tot}}(B\bar{B}) - \sigma^{\text{tot}}(BB)$ and hence builds vector mesons [e.g., 485, 229] can easily be denied by the duality-diagram argument [184].)

In this section we have given only an outline of the approach to understanding of the pomeron and Reggeons in the multi-Regge scheme combining the unitarity with the duality. Much effort has been done along this line and many interesting results have been obtained [495, 127, 108, 109, 454, 396, 72; see 22, 439, 525 for reviews]. Details of the results, however, should be deferred in another review article.

Note added: the pomeron-f identity

In the conventional theory, we have two Regge poles with the vacuum quantum number, the pomeron and f in the $I_t = 0$ channel apart from the f′. An alternative viewpoint has recently been proposed that the pomeron is just the f trajectory renormalized (and mixed with the f′ trajectory) via the cylinder correction (see fig. 17) to the planar diagram [423, 119]. The cylinder correction (C) to the planar term (R), as was given in eq. (3.32), is

$$F = R + RCR + \ldots = \frac{1}{R^{-1} - C}\,. \tag{5.18}$$

Here R has a singularity such as $R \sim 1/(J - \alpha_R)$. If C has a singularity like $C \sim 1/(J - \alpha_C)$ with $\alpha_C > \alpha_R$, we still have two singularities shifted due to the cylinder correction (see eq. (3.33)) [512, 497]. Rosenzweig and Chew assumed, however, the cylinder term has no such singularity, then the cylinder correction simply shifts α_R, and hence we have only a singularity. The situation corresponds to the cancellation of the f pole by the secondary singularity of pomeron in the full output of the unitarity summation in the multi-Regge scheme.

In the broken-SU (3) scheme one has the ideal-mixing nonet at the planar level, and the breaking of the OZI rule is introduced through the cylinder correction. Assuming the cylinder correction to be an SU (3) singlet, we take

†Planar diagrams give an equal contribution to $C_t = -$ and $C_t = +$, leading to the ω–f exchange degeneracy in the output of unitarity summation. While $(2^n/2 - 1)$ diagrams with an even number of pairs of twists contribute equally to both $C_t = -$ and $C_t = +$, $2^n/2$ diagrams with an odd number of pairs of twists give a negative contribution to $C_t = -$ and a positive one to $C_t = +$. Denoting the contribution from one diagram as $[G]$, a sum of non-planar diagrams hence gives a contribution $(2^n - 1)[G]$ to $C_t = +$ and $-[G]$ to $C_t = -$. The terms $-[G]$ in both $C_t = \pm$ states cancel the f and the ω exchanges [454].

$$R = \begin{bmatrix} \dfrac{1}{J-\alpha_0} & 0 & 0 \\ 0 & \dfrac{1}{J-\alpha_0} & 0 \\ 0 & 0 & \dfrac{1}{J-\alpha_3} \end{bmatrix} \tag{5.19}$$

and

$$C = \pm\lambda(t) \begin{bmatrix} 1 & 1 & 1 \\ 1 & 1 & 1 \\ 1 & 1 & 1 \end{bmatrix}, \tag{5.20}$$

where α_0 and α_3 denote the unrenormalized trajectories $\alpha_{f_0} = \alpha_{\omega_0} = \alpha_\rho$ and $\alpha_{f'_0} = \alpha_{\phi_0}$ respectively, and the sign of C takes $\pm$ depending upon the charge conjugation of R. Then the diagonalization of eq. (5.18) gives the f(ω) trajectory shifted upward (downward) and mixed with f'(ϕ). Figure 54 shows illustrative trajectories in this model. The mass formula of 1^- and 2^+ suggests the cylinder correction $\lambda(t)$ to be small for the time-like region such as $t \gtrsim 0.5(\mathrm{GeV}/c)^2$ (this is called the asymptotic planarity [see 120, 497]). At $t = 0$, however, there is a substantial deviation from the ideal mixing, and hence the f$-\omega$ exchange degeneracy is broken; $\alpha_f(0) = 0.81$, $\alpha_\omega(0) = 0.43$. This framework is also applied to the 0^- mesons to understand the breaking of the $\pi-\eta$ degeneracy [294].

There is an evidence that the total cross sections are well described by the nonet trajectory alone (with $\alpha_f(0) = 0.85 \sim 0.95$) up to $p_L \approx 30\mathrm{GeV}/c$, [30, 526]. Off the forward direction, however, such a one-pole description in the $I_t = 0$ channel seems not to be so successful. Especially it would be difficult to explain the disappearance of the dip with energies observed in $(\mathrm{d}\sigma/\mathrm{d}t)(\pi^- p) + (\mathrm{d}\sigma/\mathrm{d}t)(\pi^+ p)$ at $t \simeq -0.6 \sim 0.8(\mathrm{GeV}/c)^2$. Further analyses would be needed.

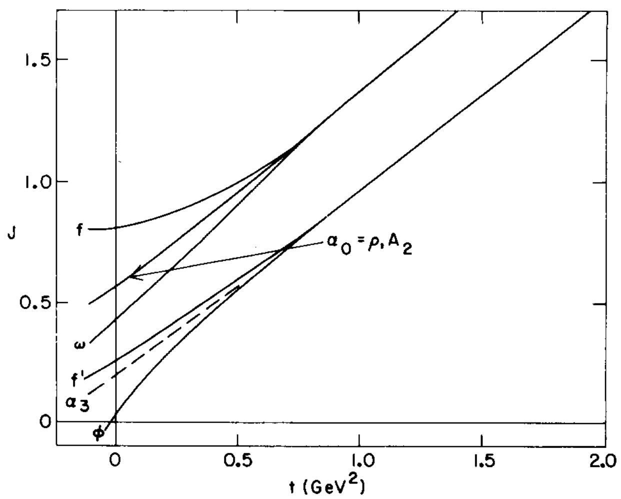

Fig. 54. The leading-trajectory pattern after the cylinder correction has displaced the $I_t = 0$ states. The scale of the splittings at $t = 0$ is fixed by the choice $\alpha_0 - \alpha_3 = 0.37$, $\alpha_0 - \alpha_\omega = 0.14$ (from Rosenzweig and Chew [423]).

Note added: violation of the OZI rule

So far we have considered only the diagrams without twists in the produced particle line (see fig. 50). Violation of the OZI rule is caused by the inclusion of such twists [527, 528]. Consider the reaction $\pi^- p \to \phi n$ (fig. 55). Writing the suppression factor of twisted produced line compared with untwisted one as ϵ, i.e., $\epsilon = \asymp / ||$, we obtain the ratio of the absorptive parts, hence that of the ρ Regge residues, $A(\pi^- p \to \phi n)/A(\pi^- p \to \omega n) = \gamma^{\rho}_{\pi\phi}/\gamma^{\rho}_{\pi\omega} \simeq \sqrt{2}\epsilon/N$ in the case of SU(N) symmetry [527]. The suppression of twisted produced line comes from the cancellation among produced particles with opposite charge conjugations. This suppression mechanism works only if the twist is in the *time-like* $q\bar{q}$ line and it does not work for the twist in the space-like $q\bar{q}$ line (|=x=|=|==|). In this picture the central production of the ϕ meson does not get the factor ϵ since it is possible to write a diagram without twists in the time-like $q\bar{q}$ line. Thus we may expect that the central production of the ϕ meson is less suppressed [529].

If we apply the above rule to the decay process [528, 530] without inquiring the validity of its application, we have the following suppression factor:

$$\phi \to \rho\pi,\ \psi \to \rho\pi : \epsilon^2/N \qquad \psi \to \phi\pi\pi \quad : \epsilon^2/N^2$$
$$\psi \to \omega\pi\pi \quad : \epsilon^2/N \qquad \psi' \to \psi\pi\pi,\ \psi' \to \psi\eta : \epsilon/N.$$

This seems to explain the tendency of the OZI rule violation in the decay process. There is another suppression due to the symmetry breaking. We ignore here the suppression for simplicity of explanation, although it becomes extremely important for the decay of the ψ particles.

It is interesting to note that the pattern of OZI rule violation depends on the varieties of reactions and their kinematical regions. In the approach given in section 3.6 the pattern of the violation is independent of them.

Besides the violation of the OZI rule, the inclusion of the twist in the produced particle line gives rise to several interesting effects; (i) exotic exchange [527] (fig. 56a); A(exotic exchange) $\sim \epsilon^2/N \cdot s^{2\alpha-1}$ and (ii) breaking of (ρ, A_2) or (K^*, K^{**}) exchange degeneracy [531–534] (fig. 56b); $\alpha_\rho(0) - \alpha_{A_2}(0) \propto \epsilon$ It has been known that the parameter ϵ obtained from analyses of these phenomena is mutually consistent.

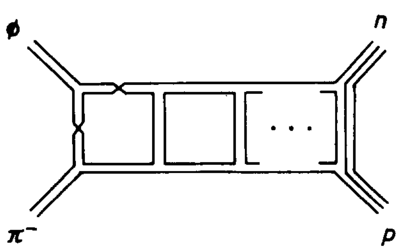

Fig. 55.

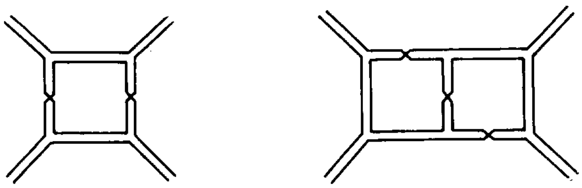

(a) (b)

Fig. 56.

Acknowledgement

The authors are grateful to Drs. T. Eguchi, T. Inami, Y. Oyanagi and S. Yazaki for helpful discussions. They would also like to thank Professor H. Sugawara, Dr. Arafune, Dr. Y. Oyanagi and Mr. S. Yada for reading the manuscript. They are also grateful for the patience of Professor M. Jacob. Finally they wish to thank Miss K. Ohtani for her patient typing of the difficult manuscript.

Appendix A: Kinematics for meson–baryon scattering

We give here the definitions of the various amplitudes referred to in the text. We consider meson–baryon scattering $M(q_1) + B(p_1) \to M(q_2) + B(p_2)$, where $q_1(q_2)$ and $p_1(p_2)$ are the four-momenta of the incident (outgoing) meson and baryon, respectively. We denote the meson mass as μ and the baryon mass as M. According to CGLN [117] the scattering amplitude is defined as follows:

$$S_{\mathrm{fi}} = \delta_{\mathrm{fi}} - (2\pi)^4 \mathrm{i}\delta^4(p_2 + q_2 - p_1 - q_1) \left(\frac{M^2}{p_1^0 p_2^0 2q_1^0 2q_2^0}\right)^{1/2} \bar{u}(p_2) T u(p_1). \tag{A.1}$$

Here, T is decomposed into the invariant amplitudes A and B,

$$T = -A - \gamma \frac{q_1 + q_2}{2} B. \tag{A.2}$$

Partial-wave analysis

By introducing the centre-of-mass variables

$$W = \sqrt{s} = \text{total energy}, \qquad E = \text{total nucleon energy} \tag{A.3}$$

the amplitudes A and B are written in terms of the usual s-channel amplitudes f_1 and f_2 as,

$$\frac{1}{4\pi} A = \frac{W+M}{E+M} f_1 - \frac{W-M}{E-M} f_2, \qquad \frac{1}{4\pi} B = \frac{1}{E+M} f_1 + \frac{1}{E-M} f_2. \tag{A.4}$$

The cross section in the centre-of-mass system is given using f_1 and f_2

$$\frac{\mathrm{d}\sigma}{\mathrm{d}\Omega} = \sum_{\mathrm{spin}} |\langle \chi_{\mathrm{f}} | f_1 + \frac{(\sigma\cdot q_2)(\sigma\cdot q_1)}{q_2 q_1} f_2 | \chi_{\mathrm{i}} \rangle|^2. \tag{A.5}$$

The s-channel amplitudes f_1 and f_2 are decomposed in the partial-wave amplitude $f_{l\pm} = (\eta_{l\pm} \exp\{2\mathrm{i}\delta_{l\pm}\} - 1)/2\mathrm{i}q$ with the total angular momentum $J = l \pm \frac{1}{2}$ and parity $(P = -(-)^l)$ as

$$f_1 = \sum_{l=0}^{\infty} f_{l+} P'_{l+1}(z) - \sum_{l=2}^{\infty} f_{l-} P'_{l-1}(z)$$

$$f_2 = \sum_{l=1}^{\infty} (f_{l-} - f_{l+}) P'_l(z) \tag{A.6}$$

with $z = \cos\theta$. Inversely, $f_{l\pm}$ is given by

$$f_{l\pm} = \tfrac{1}{2} \int_{-1}^{1} \mathrm{d}z\, (f_1 P_l(z) + f_2 P_{l\pm 1}(z)).$$

Baryon resonances are classified in four families $(\alpha, \ldots, \delta)$ according to their signature $\tau = (-)^{J-1/2}$

and parity $P = -(-)^l$:

	τ	P		
α	$+$	$+$	$J^P = 1/2^+, 5/2^+, \ldots$	f_{l-} with l = odd
β	$+$	$-$	$J^P = 1/2^-, 5/2^-, \ldots$	f_{l+} with l = even
γ	$-$	$-$	$J^P = 3/2^-, 7/2^-, \ldots$	f_{l-} with l = even
δ	$-$	$+$	$J^P = 3/2^+, 7/2^+, \ldots$	f_{l+} with l = odd.

The s-channel helicity amplitude

According to Jacob and Wick [303], the s-channel helicity amplitude is defined as

$$f_{++} = \sum_J (J+\tfrac{1}{2}) f^J_{++} d^J_{1/2\;1/2}(z) = \cos\frac{\theta}{2} \sum_J f^J_{++}(P'_{J+1/2} - P'_{J-1/2})$$

$$f_{+-} = \sum_J (J+\tfrac{1}{2}) f^J_{+-} d^J_{-1/2\;1/2}(z) = \sin\frac{\theta}{2} \sum_J f^J_{+-}(P'_{J+1/2} + P'_{J-1/2}). \tag{A.7}$$

Here we have

$$f^J_{+\pm} = f_{l+} \pm f_{(l+1)-} \tag{A.8}$$

or symbolically $f^J_{+\pm} = [\beta,\delta] \pm [\alpha,\gamma]$. The s-channel helicity amplitude is related to f_1 and f_2 as

$$f_{++} = \bar{f}_{++} \cos\frac{\theta}{2} = (f_1 + f_2)\cos\frac{\theta}{2}, \qquad f_{+-} = \bar{f}_{+-} \sin\frac{\theta}{2} = (f_1 - f_2)\sin\frac{\theta}{2}. \tag{A.9}$$

Using these amplitudes, the differential cross section and the spin parameters are given by

$$\begin{aligned} &\mathrm{d}\sigma/\mathrm{d}\Omega = |f_{++}|^2 + |f_{+-}|^2, && P\,\mathrm{d}\sigma/\mathrm{d}\Omega = 2\mathrm{Im}\, f_{++}f^*_{+-}, \\ &\tilde{R}\,\mathrm{d}\sigma/\mathrm{d}\Omega = 2\mathrm{Re}\, f_{++}f^*_{+-}, && \tilde{A}\,\mathrm{d}\sigma/\mathrm{d}\Omega = |f_{++}|^2 - |f_{+-}|^2. \end{aligned} \tag{A.10}$$

The conventional Wolfenstein parameters R and A are obtained from $\tilde{R}$ and $\tilde{A}$ by rotating the nucleon recoil angle in the laboratory system [e.g., 64],

$$\begin{bmatrix} R \\ A \end{bmatrix} = \begin{bmatrix} -\cos\theta_R & \sin\theta_R \\ \sin\theta_R & \cos\theta_R \end{bmatrix} \cdot \begin{bmatrix} \tilde{A} \\ \tilde{R} \end{bmatrix}. \tag{A.11}$$

As for the direction of the spin, we take $\boldsymbol{n} = \boldsymbol{q}_\mathrm{i} \times \boldsymbol{q}_\mathrm{f}$ according to the Basel convention.

For small-angle scattering, the impact-parameter representation gives a convenient description [e.g., 228, 1, 18]. Since the Legendre polynomial $P_l(\cos\theta)$ is approximated by $J_0([2l+1]\sin\theta/2)$ we have, by noting $P'_{l+1} - P'_l \approx lP_l$,

$$f_{++} \approx \cos\frac{\theta}{2}\, q^2 \int_0^\infty b\mathrm{d}b\, f_{++}(b) J_0(b\sqrt{-t}). \tag{A.12a}$$

Similarly using the relation $P'_l \approx lJ_1([2l+1]\sin\theta/2)/\sin\theta/2$, we get

$$f_{+-} \approx q^2 \int_0^\infty b\mathrm{d}b\, f_{+-}(b) J_1(b\sqrt{-t}). \tag{A.12b}$$

We also have similar expressions for near-backward scattering. With the help of the relation $d^J_{1/2\ 1/2}(-z) = (-1)^{J-1/2} d^J_{-1/2\ 1/2}(z)$, we have

$$f_{++} \approx q^2 \int_0^\infty b\mathrm{d}b\,(f_{++}^{l=\text{even}} - f_{++}^{l=\text{odd}}) J_1(b\sqrt{-u'})$$

$$f_{+-} \approx \sin\frac{\theta}{2} q^2 \int_0^\infty b\mathrm{d}b\,(f_{+-}^{l=\text{even}} - f_{+-}^{l=\text{odd}}) J_0(b\sqrt{-u'}). \tag{A.13}$$

The t-channel helicity amplitude and the reggeization of meson exchange

The helicity amplitude in the t-channel is simply related to that in the s-channel by the Trueman–Wick crossing operation [487], and turned out to be A' for t-channel helicity nonflip and B for t-channel helicity flip, respectively. Here A' is defined by

$$A' = A + \frac{\nu}{1 - t/4M^2} B \tag{A.14}$$

with

$$\nu = \frac{s-u}{4M} = \nu_\mathrm{L} + \frac{t}{4M} = \frac{p_t q_t}{M}\cos\theta_t \tag{A.15}$$

(ν_L = lab. energy of the meson). Using these amplitudes, the first two equations of (A.10) reduce to

$$\frac{\mathrm{d}\sigma}{\mathrm{d}t} = \frac{1}{\pi s}\left(\frac{M}{4q}\right)^2 \left(1 - \frac{t}{4M^2}\right)\left[|A'|^2 + \frac{4sq^4\sin^2\theta}{(4M^2-t)^2}|B|^2\right]$$

$$P\frac{\mathrm{d}\sigma}{\mathrm{d}t} = -\frac{1}{16\pi\sqrt{s}}\sin\theta\ \mathrm{Im}\,A'\cdot B^*. \tag{A.16}$$

The meson exchange is reggeized with the t-channel helicity amplitudes A' and B, [473] as,

$$A' = \beta_{A'}(t)\,\frac{\mp 1 - \exp\{-\mathrm{i}\pi\alpha(t)\}}{\sin\pi\alpha(t)}\left(\frac{\nu}{\nu_0}\right)^{\alpha(t)}$$

$$B = \beta_B(t)\,\frac{\mp 1 - \exp\{-\mathrm{i}\pi\alpha(t)\}}{\sin\pi\alpha(t)}\left(\frac{\nu}{\nu_0}\right)^{\alpha(t)-1}. \tag{A.17}$$

The s-channel helicity amplitude is related to A' and A for $s \to \infty$ with t fixed as

$$f_{++} \simeq \frac{M}{4\pi W}A', \qquad f_{+-} \simeq \frac{M}{4\pi W}\frac{\sqrt{-t}}{2M}A. \tag{A.18}$$

Thus the s-channel helicity amplitude corresponds to (A',A) approximately while the t-channel helicity amplitude corresponds to (A',B).

For the kinematics of unequal-mass case, see e.g., Field and Jackson [194].

The reggeization of baryon exchange

The parity-conserving helicity amplitudes in the u-channel are $f_2(\sqrt{u},s)$ and $f_1(\sqrt{u},s)$. The baryon exchange is reggeized with these amplitudes by removing the threshold singularities.† Writing them

†The reggeization is generally done with respect to the parity-conserving kinematical-singularity-free helicity amplitude [220, 240, 503, 129].

as $\tilde{F}^{\pm}$, we have†

$$\tilde{F}^{\pm}(\sqrt{u},s) = \mp(A + MB) - \sqrt{u}B. \tag{A.19}$$

(For $s \to \infty$ with u fixed it follows that $A + MB \simeq A'$.) Here $\tilde{F}^{\pm}(\sqrt{u},s)$ includes only the τP = ± Regge exchanges in the leading order in s, and is subject to the MacDowell symmetry [346]

$$\tilde{F}^{+}(\sqrt{u},s) = -\tilde{F}^{-}(-\sqrt{u},s). \tag{A.20}$$

The Regge-pole expression is given by

$$\tilde{F}^{\pm}(\sqrt{u},s) = \beta^{\pm}(\sqrt{u})\,\frac{1 + \tau\exp\{-i\pi\alpha^{\pm}(\sqrt{u})\}}{\sin\pi\alpha^{\pm}(\sqrt{u})}\left(\frac{s-t}{2s_0}\right)^{\alpha^{\pm}(\sqrt{u})} \tag{A.21}$$

for the τP = ± exchanges. Here one has the Gribov conspiracy

$$\alpha^{-}(\sqrt{u}) = \alpha^{+}(-\sqrt{u}), \qquad \beta^{-}(\sqrt{u}) = -\beta^{+}(-\sqrt{u}\,) \tag{A.22}$$

for each Regge pole [234].

In case when the trajectory is linear, it is often convenient to write the residue function as

$$\beta^{\pm}(\sqrt{u}) = \gamma^{\pm}(\sqrt{u})R(u), \qquad \gamma^{\pm}(\sqrt{u}) = \gamma^{\mathrm{even}} + \gamma^{\mathrm{odd}} \tag{A.23}$$

where γ^{even} (γ^{odd}) is an even (odd) polynomial in $\sqrt{u}$. With such polynomials, we can write

$$A'/B \simeq (A + MB)/B = \gamma^{\mathrm{even}}/\gamma^{\mathrm{odd}}. \tag{A.24}$$

The s-channel helicity amplitude behaves as

$$f_{++} \simeq \frac{\sqrt{-u'}}{8\pi}B, \qquad f_{+-} \simeq \frac{1}{8\pi}A'$$

for $s \to \infty$, with u fixed. Here $u' = u - u_{\mathrm{max}}$ ($u_{\mathrm{max}} = (M^2 - \mu^2)^2/s$ is a kinematical boundary).

Appendix B: Crossing matrix

Let us define the reaction of each channel as

$$\begin{aligned}
&(s) \qquad \mathrm{M} + \mathrm{B} \to \mathrm{M}' + \mathrm{B}' \\
&(t) \qquad \mathrm{M} + \overline{\mathrm{M}}' \to \overline{\mathrm{B}} + \mathrm{B}' \\
&(u) \qquad \overline{\mathrm{M}}' + \mathrm{B} \to \overline{\mathrm{M}} + \mathrm{B}'.
\end{aligned} \tag{B.1}$$

Then the (s,t) crossing matrices of πN and $\bar{\mathrm{K}}$N scattering are

$$\begin{bmatrix} A(I_t=0) \\ A(I_t=1) \end{bmatrix} = \begin{bmatrix} \sqrt{2/3} & 2\sqrt{2/3} \\ -2/3 & 2/3 \end{bmatrix} \begin{bmatrix} A(I_s=1/2) \\ A(I_s=3/2) \end{bmatrix} \quad \text{for } \pi\mathrm{N}$$

$$\begin{bmatrix} A(I_t=0) \\ A(I_t=1) \end{bmatrix} = \begin{bmatrix} 1/2 & 3/2 \\ 1/2 & -1/2 \end{bmatrix} \begin{bmatrix} A(I_s=0) \\ A(I_s=1) \end{bmatrix} \quad \text{for } \bar{\mathrm{K}}\mathrm{N}. \tag{B.2}$$

† $\tilde{F}^{+}(\sqrt{u},s) = \{(E_u - M)/8\pi\sqrt{u}\}f_2(\sqrt{u},s)$, $\quad \tilde{F}^{-}(\sqrt{u},s) = \{(E_u + M)/8\pi\sqrt{u}\}f_1(\sqrt{u},s)$.

The SU (3) crossing matrices of $\underline{8} \times \underline{8} \to \underline{8} \times \underline{8}$ for the SU (3) vector ($\underline{1}$, $\underline{8}_{\mathrm{As}}$, $\underline{8}_{\mathrm{sA}}$, $\underline{8}_{\mathrm{ss}}$, $\underline{8}_{\mathrm{AA}}$, $\underline{10}$, $\underline{10}^*$, $\underline{27}$) are as follows† [154, 417]:

$$X_{ts} = \begin{bmatrix} 1/8 & 0 & 0 & 1 & 1 & 5/4 & 5/4 & 27/8 \\ 0 & -1/2 & -1/2 & 0 & 0 & \sqrt{5}/4 & -\sqrt{5}/4 & 0 \\ 0 & -1/2 & -1/2 & 0 & 0 & -\sqrt{5}/4 & -\sqrt{5}/4 & 0 \\ 1/8 & 0 & 0 & -3/10 & 1/2 & -1/2 & -1/2 & 27/40 \\ 1/8 & 0 & 0 & 1/2 & 1/2 & 0 & 0 & -9/8 \\ 1/8 & 1/\sqrt{5} & -1/\sqrt{5} & -2/5 & 0 & 1/4 & 1/4 & -9/40 \\ 1/8 & -1/\sqrt{5} & 1/\sqrt{5} & -2/5 & 0 & 1/4 & 1/4 & -9/40 \\ 1/8 & 0 & 0 & 1/5 & -1/3 & -1/12 & -1/12 & 7/40 \end{bmatrix}$$

$$X_{st} = X_{ts} \tag{B.3}$$

and

$$X_{us} = \begin{bmatrix} 1/8 & 0 & 0 & 1 & -1 & -5/4 & -5/4 & 27/8 \\ 0 & -1/2 & 1/2 & 0 & 0 & -\sqrt{5}/4 & \sqrt{5}/4 & 0 \\ 0 & 1/2 & -1/2 & 0 & 0 & -\sqrt{5}/4 & \sqrt{5}/4 & 0 \\ 1/8 & 0 & 0 & -3/10 & -1/2 & 1/2 & 1/2 & 27/40 \\ -1/8 & 0 & 0 & -1/2 & 1/2 & 0 & 0 & 9/8 \\ -1/8 & -1/\sqrt{5} & -1/\sqrt{5} & 2/5 & 0 & 1/4 & 1/4 & 9/40 \\ -1/8 & 1/\sqrt{5} & 1/\sqrt{5} & 2/5 & 0 & 1/4 & 1/4 & 9/40 \\ 1/8 & 0 & 0 & 1/5 & 1/3 & 1/12 & 1/12 & 7/40 \end{bmatrix}$$

$$X_{su} = X_{us}. \tag{B.4}$$

References

[1] T. Adachi and T. Kotani, Suppl. Prog. Theor. Phys. Extra Number (1965) 316.
[2] M. Ademollo, H.R. Rubinstein, G. Veneziano and M.A. Virasoro, Phys. Rev. 176 (1968) 1904.
[3] C.W. Akerlof, P.K. Caldwell, J. Koschik, R. Kotthaus, D.I. Meyer and B. Springett, Phys. Rev. Letters 33 (1974) 119.
[4] M.G. Albrow, S. Andersson-Almehed, B. Bošnjaković, F.C. Erné, Y. Kimura, J.P. Lagnaux, J.C. Sens and F. Udo, Nucl. Phys. B29 (1971) 413.
[5] M.G. Albrow, S. Andersson-Almehed, B. Bošnjaković, C. Daum, F.C. Erné, Y. Kimura, J.P. Lagnaux, J.C. Sens, F. Udo and F. Wagner, Nucl. Phys. B30 (1971) 273.
[6] V. Alessandrini, D. Amati, M. Le Bellac and D. Olive, Phys. Reports 1C (1971) 269.
[7] S. Almehed and C. Lovelace, Nucl. Phys. B40 (1972) 157.
[8] M. Alston-Garnjost, A. Barbaro-Galtieri, S.M. Flatté, J.H. Friedman, G.R. Lynch, S.D. Protopopescu, M.S. Rabin and F.T. Solmitz, Phys. Letters 36B (1971) 152.

†The first suffix of $\underline{8}$ in the t-channel vector refers to the baryon vertex and the latter to the meson vertex.

[9] H. Alvensleben, U.J. Becker, W.K. Bertram, M. Chen, K.J. Cohen, R.T. Edwards, T.M. Knasel, R. Marshall, D.J. Quinn, M. Rohde, G.H. Sanders, H. Schubel and S.C.C. Ting, Phys. Rev. Letters 26 (1971) 273.
[10] D. Amati, A. Stanghellini and S. Fubini, Nuovo Cim. 26 (1962) 896.
[11] I. Ambats, D.S. Ayres, R. Diebold, A.F. Greene, S.L. Kramer, A. Lesnik, D.R. Rust, C.E.W. Ward, A.B. Wicklund and D.D. Yovanovitch, Phys. Rev. Letters 29 (1972) 1415.
[12] S. Andersson, C. Daum, F.C. Erné, J.P. Lagnaux, J.C. Sens, C. Schmid and F. Udo, in: Int. Conf. on High Energy Collisions Stony Brook, 1969.
[13] W.D. Apel, E. Bertolucci, S.V. Donskov, A.V. Injakin, R.P. Johnson, V.A. Kachanov, W. Kittenberger, R.N. Krasnokutsky, G. Leder, A.A. Lednev, I. Mannelli, Yu.V. Mikhailov, H. Müller, G. Pierazzini, Yu. D. Prokoshkin, D. Schinzel, H. Schneider, A. Scribano, F. Sergiampietri, R.S. Shuvalov, G. Sigurdsson, M. Steuer and M.L. Vincelli, Serpukhov preprint CAP 74-118 (1974).
[14] J. Arafune, M. Fukugita, Y. Oyanagi and H. Sugawara (1975) unpublished.
[15] F. Arbab and C.B. Chiu, Phys. Rev. 147 (1966) 1045.
[16] R. Armenteros, M. Ferro-luzzi, D.W.G.S. Leith, R. Levi-Setti, A. Minten, R.D. Tripp, H. Filthuth, V. Hepp, E. Kluge, H. Schneider, R. Barloutaud, P. Granet, J. Meyer and J.-P. Porte, Nucl. Phys. B8 (1968) 233.
[17] R.C. Arnold, Phys. Rev. Letters 14 (1965) 657.
[18] R.C. Arnold, Phys. Rev. 153 (1967) 1523.
[19] R.C. Arnold and M.L. Blackmon, Phys. Rev. 176 (1968) 2082.
[20] P. Astbury, G. Brautti, G. Finocchiaro, A. Michelini, K. Terwilliger, D. Websdale, C.H. West, P. Zanella, W. Beusch, W. Fischer, B. Gobbi, M. Pepin and E. Polgar, Phys. Letters 23 (1966) 396.
[21] P. Astbury, J. Gallivan, J. Jafar, M. Letheren, V. Steiner, J.A. Wilson, W. Beusch, M. Borghini, D. Websdale, L. Fluiri, K. Freudenreich, F.X. Gentit, W. Wetzel, P. Le Du and O. Guisan, Nucl. Phys. B99 (1975) 30.
[22] P. Aurenche, Ng S.W., J.E. Paton, Tsou S.T., Chan H.-M., A. Gula, T. Inami and R.G. Roberts, Rutherford Laboratory preprint, RL-75-084, T.121 (1975).
[23] P.R. Auvil, F. Halzen and C. Michael, Nucl. Phys. B25 (1970) 317.
[24] R. Ayed, P. Bareyre and Y. Lemoigne, Saclay preprint (1972).
[25] D.S. Ayres, R. Diebold, A.F. Greene, S.L. Kramer, J.S. Levine, A.J. Pawlicki and A.B. Wicklund, Phys. Rev. Letters 32 (1974) 1463.
[26] P. Babu, F.J. Gilman and M. Suzuki, Phys. Letters 24B (1967) 65.
[27] J. Badier, R. Bland, A. Romana, R. Vanderhagen, J.C. Chollet, D. Décamp, J.M. Gaillard, J. Lefrançois, B. Merkel, J.P. Repellin, T. Devlin, R. Meunier and G. Sauvage, Phys. Letters 41B (1972) 387.
[28] W.F. Baker, D.P. Eartly, K.P. Pretzl, S.M. Pruss, A.A. Wehmann, P. Koehler, A.J. Lennox, J.A. Poirier, C.A. Rey and O.R. Sander, Phys. Rev. Letters 32 (1974) 251.
[29] L.A.P. Balázs, Phys. Rev. D11 (1975) 1071.
[30] N.F. Bali and J.W. Dash, Phys. Rev. D10 (1974) 2102.
[31] G. Barbarino, M. Grilli, E. Iarocci, P. Spillantini, V. Valente, R. Visentin, F. Ceradini, M. Conversi, L. Paoluzi, R. Santonico, M. Nigro, L. Trasatti and G.T. Zorn, Lett. Nuovo Cim. 3 (1972) 689.
[32] A. Barbaro-Galtieri, in: Proc. 16th Int. Conf. on High Energy Physics, Chicago-Batavia, 1972, Vol. 1.
[33] V. Barger, in: Proc. 17th Int. Conf. on High Energy Physics, London, 1974.
[34] V. Barger and D. Cline, Phys. Rev. Letters 16 (1966) 913.
[35] V. Barger and D. Cline, Phys. Rev. 155 (1967) 1792.
[36] V. Barger and D. Cline, Phys. Rev. Letters 19 (1967) 1504.
[37] V. Barger and D. Cline, Phys. Letters 26B (1967) 85.
[38] V. Barger and D. Cline, Phys. Rev. Letters 20 (1968) 298.
[39] V. Barger and D. Cline, Phys. Rev. 182 (1969) 1849.
[40] V. Barger and D. Cline, Phenomenological Theories of High Energy Scattering (W.A. Benjamin Inc., New York, 1969).
[41] V. Barger and L. Durand III, Phys. Rev. Letters 19 (1967) 1295.
[42] V. Barger, K. Geer and F. Halzen, Nucl. Phys. B49 (1972) 302.
[43] V. Barger and F. Halzen, Phys. Rev. Letters 28 (1972) 194.
[44] V. Barger and F. Halzen, Phys. Rev. D6 (1972) 1918.
[45] V. Barger, F. Halzen and M.G. Olsson, Nucl. Phys. B49 (1972) 206.
[46] V. Barger, F. Halzen and R.J.N. Phillips, Nucl. Phys. B57 (1973) 401.
[47] V. Barger and A.D. Martin, Phys. Letters 39B (1972) 379.
[48] V. Barger and C. Michael, Phys. Rev. 186 (1969) 1592.
[49] V. Barger, C. Michael and R.J.N. Phillips, Phys. Rev. 185 (1969) 1852.
[50] V. Barger and M.G. Olsson, Phys. Rev. D5 (1972) 2736.
[51] V. Barger, M.G. Olsson and D.D. Reeder, Nucl. Phys. B5 (1968) 411.
[52] V. Barger, M.G. Olsson and K.V.L. Sarma, Phys. Rev. 147 (1966) 1115.
[53] V. Barger and R.J.N. Phillips, Phys. Letters 26B (1968) 730.
[54] V. Barger and R.J.N. Phillips, Phys. Rev. 187 (1969) 2210.

[55] V. Barger and R.J.N. Phillips, Nucl. Phys. B32 (1971) 93.
[56] V. Barger and R.J.N. Phillips, Nucl. Phys. B33 (1971) 22.
[57] I.S. Barker, A. Donnachie and J.K. Storrow, Nucl. Phys. B79 (1974) 431.
[58] R. Barloutaud, D. Merrill, J.C. Scheuer, A.M. Bakker, W. Hoogland, S. Focardi, A. Minguzzi-Ranzi, A.M. Rossi, B. Haber, U. Karshon, J. Goldberg, G. Lamidey and A. Rouge, Nucl. Phys. B26 (1971) 557.
[59] K.J. Barnes, P. Carruthers, F. von Hippel, Phys. Rev. Letters 14 (1965) 82.
[60] B.A. Barnett, A.T. Laasanen, P.H. Steinberg, D. Hill, S. Kato, P.F.M. Koehler, T.B. Novey, A. Yokosawa, G. Burleson, D. Eartly and K. Pretzl, Phys. Letters 34B (1971) 655.
[61] E. Barrelet, Nuovo Cim. 8A (1972) 331.
[62] D. Benaksas, G. Cosme, B. Jean-Marie, S. Jullian, F. Laplanche, J. Lefrançois, A.D. Liberman, G. Parrour, J.P. Repellin and G. Sauvage, Phys. Letters 42B (1972) 511.
[63] E.L. Berger and G.C. Fox, Phys. Rev. 188 (1969) 2120.
[64] E.L. Berger and G.C. Fox, Phys. Rev. Letters 25 (1970) 1783.
[65] E.L. Berger and G.C. Fox, Nucl. Phys. B26 (1971) 1.
[66] A. Berglund, T. Buran, P.J. Carlson, C.J.S. Damerell, I. Endo, A.R. Gillman, V. Gracco, R.J. Homer, M.J. Hotchkiss, A. Lundby, M. Macri, B.N. Ratcliff, A. Santroni, T. Tso, F. Wickens and J.A. Wilson, Phys. Letters 57B (1975) 100.
[67] L. Bertocchi, in: Proc. Heidelberg Int. Conf. on Elementary Particles, 1967 (1968).
[68] L. Bertocchi, S. Fubini and M. Tonin, Nuovo Cim. 25 (1962) 626.
[69] W. Beusch, A. Michelini, D. Websdale, W.E. Fischer, R. Frosch, P. Mühlemann, M. Pepin, E.E. Polgar, J. Codling and M.G. Green, Nucl. Phys. B19 (1970) 546.
[70] W. Beusch, A. Birman, D. Websdale and W. Wetzel, Phys. Letters 60B (1975) 101.
[71] H.H. Bingham, W.B. Fretter, W.J. Podolsky, M.S. Rabin, A.H. Rosenfeld, G. Smadja, G.P. Yost, J. Ballam, G.B. Chadwick, Y. Eisenberg, E. Kogan, K.C. Moffeit, P. Seyboth, I.O. Skillicorn, H. Spitzer and G. Wolf, Phys. Letters 41B (1972) 635.
[72] M. Bishari, Phys. Letters 59B (1975) 461.
[73] M. Biyajima, Phys. Letters 43B (1973) 197.
[74] R. Blankenbecler and M.L. Goldberger, Phys. Rev. 126 (1962) 766.
[75] J.M. Blatt and V.F. Weisskopf, Theoretical Nuclear Physics (John Wiley and Sons, New York, 1952).
[76] V.N. Bolotov, V.V. Isakov, V.A. Kachanov, C.D. Kakauridze, Yu.D. Prokoshkin and E.A. Rasuvaev, Phys. Letters 48B (1974) 280.
[77] V.N. Bolotov, V.V. Isakov, V.A. Kachanov, D.B. Kakauridze, V.M. Kutjin, Yu.D. Prokoshkin, E.A. Razuvaev, V.G. Rybakov, V.K. Semenov and V.A. Senko, Nucl. Phys. B73 (1974) 365.
[78] P. Bonamy, P. Borgeaud, M. Crozon, J.P. Guillaud, O. Guisan, P. Le Du, P. Sonderegger, J.K. Bienlein, S. Mango, L. Paul and H. Dinter, Nucl. Phys. B52 (1973) 392.
[79] N.E. Booth, Phys. Rev. Letters 21 (1968) 465.
[80] M. Borghini, L. Dick, J.C. Olivier, H. Aoi, D. Cronenberger, G. Grégoire, Z. Janout, K. Kuroda, A. Michalowicz, M. Poulet, D. Sillou, G. Bellettini, P.L. Braccini, T. Del Prete, L. Foà, P. Laurelli, G. Sanguinetti and M. Valdata, Phys. Letters 36B (1971) 493.
[81] M. Borghini, L. Dick, J.C. Olivier, H. Aoi, D. Cronenberger, G. Grégoire, Z. Janout, K. Kuroda, A. Michalowicz, M. Poulet, D. Sillou, G. Bellettini, P.L. Braccini, T. Del Prete, L. Foà, P. Laurelli, G. Sanguinetti and M. Valdata, Phys. Letters 36B (1971) 497.
[82] B.B. Brabson, R.R. Crittenden, R.M. Heinz, R.C. Kammerud, H.A. Neal, H.W. Paik and R.A. Sidwell, Phys. Rev. Letters 25 (1970) 553.
[83] G. Brandenburg, R.K. Carnegie, R.J. Cashmore, M. Davier, D.W.G.S. Leith, J. Matthews, P. Walden, S.H. Williams and F. Winkelmann, Phys. Letters 58B (1975) 367.
[84] C. Bricman, E. Pagiola and C. Schmid, Nucl. Phys. B33 (1971) 135.
[85] W.S. Brockett, G.T. Corlew, W.R. Frisken, T.L. Jenkins, A.R. Kirby, C.R. Sullivan, J.A. Todoroff and W.B. Richards, Phys. Rev. Letters 26 (1971) 527.
[86] W.S. Brockett, G.T. Corlew, W.R. Frisken, T.L. Jenkins, A.R. Kirby, W.M. Smith, A.G. Strelzoff and C.R. Sullivan, Phys. Letters 51B (1974) 390.
[87] R.C. Brower, Phys. Letters 37B (1971) 121.
[88] R.C. Brower, C.E. DeTar and J.H. Weis, Phys. Reports 14C (1974) 257.
[89] A. Browman, J. DeWire, B. Gittelman, K.M. Hanson, E. Loh and R. Lewis, Phys. Rev. Letters 32 (1974) 1067.
[90] G. Burleson, D. Hill, S. Kato, P.F.M. Koehler, T.B. Novey, A. Yokosawa, D. Eartly, K. Pretzl, B. Barnett, A. Laasanen and P. Steinberg, Phys. Rev. Letters 26 (1971) 338.
[91] N. Cabibbo, Phys. Rev. Letters 10 (1963) 531.
[92] A. Capella, Phys. Rev D8 (1973) 2047.
[93] R.H. Capps, Phys. Rev. Letters 22 (1969) 215.
[94] R.H. Capps, Phys. Rev. Letters 29 (1972) 820.
[95] R.H. Capps and V.V. Dixit, Phys. Letters 33B (1970) 596.

[96] R. Carlitz, M.B. Green and A. Zee, Phys. Rev. Letters 26 (1971) 1515; Phys. Rev. D4 (1971) 3439.
[97] R. Carlitz and M. Kislinger, Phys. Rev. Letters 24 (1970) 186.
[98] A.A. Carter, University of Cambridge preprint HEP 68-10 (1968).
[99] R.J. Cashmore, D.W.G.S. Leith, R.S. Longacre and A.H. Rosenfeld, Nucl. Phys. B92 (1975) 37.
[100] V. Chabaud, A. Eide, P. Lehmann, A. Lundby, S. Mukhin, J. Myrheim, C. Baglin, P. Briandet, P. Fleury, P. Carlson, E. Johansson, M. Davier, V. Gracco, R. Morand and D. Treille, Phys. Letters 38B (1972) 441.
[101] V. Chabaud, A. Eide, P. Lehmann, A. Lundby, S. Mukhin, J. Myrheim, C. Baglin, P. Briandet, P. Fleury, P. Carlson, E. Johansson, M. Davier, V. Gracco, R. Morand and D. Treille, Phys. Letters 38B (1972) 445.
[102] V. Chabaud, A. Eide, P. Lehmann, A. Lundby, S. Mukhin, J. Myrheim, C. Baglin, P. Briandet, P. Fleury, P. Carlson, E. Johansson, M. Davier, V. Gracco, R. Morand and D. Treille, Phys. Letters 38B (1972) 449.
[103] V. Chabaud, A. Eide, P. Lehmann, A. Lundby, S. Mukhin, J. Myrheim, C. Baglin, P. Briandet, P. Fleury, P. Carlson, E. Johansson, M. Davier, V. Gracco, R. Morand and D. Treille, Phys. Letters 41B (1972) 209.
[104] G. Chadwick, Y. Eisenberg and E. Kogan, Phys. Rev. D8 (1973) 1607.
[105] Chan H.-M., C.S. Hsue, C. Quigg and J.-M. Wang, Phys. Rev. Letters 26 (1971) 672.
[106] Chan H.-M., H.I. Miettinen and R.G. Roberts, Nucl. Phys. B54 (1973) 411.
[107] Chan H.-M. and J.E. Paton, Phys. Letters 46B (1973) 228.
[108] Chan H.-M., J.E. Paton and Tsou S.-T., Nucl. Phys. B86 (1975) 479.
[109] Chan H.-M., J.E. Paton, Tsou S.-T. and Ng S.-W., Nucl. Phys. B92 (1975) 13.
[110] Chan H.-M., R.O. Raitio, G.H. Thomas and N.A. Törnqvist, Nucl. Phys. B19 (1970) 173.
[111] G.F. Chew, Comments on Nucl. and Particle Phys. 2 (1968) 74.
[112] G.F. Chew and C.E. DeTar, Phys. Rev. 180 (1969) 1577.
[113] G.F. Chew and S.C. Frautschi, Phys. Rev. Letters 7 (1961) 394.
[114] G.F. Chew and S.C. Frautschi, Phys. Rev. Letters 8 (1962) 41.
[115] G.F. Chew, S.C. Frautschi and S. Mandelstam, Phys. Rev. 126 (1962) 1202.
[116] G.F. Chew, M.L. Goldberger and F.E. Low, Phys. Rev. Letters 22 (1969) 208.
[117] G.F. Chew, M.L. Goldberger, F.E. Low and Y. Nambu, Phys. Rev. 106 (1957) 1337.
[118] G.F. Chew and A. Pignotti, Phys. Rev. 176 (1968) 2112.
[119] G.F. Chew and C. Rosenzweig, Phys. Rev. D12 (1975) 3907.
[120] G.F. Chew and C. Rosenzweig, Nucl. Phys. B104 (1976) 290.
[121] C.B. Chiu, S.-Y. Chu and L.-L. Wang, Phys. Rev. 161 (1967) 1563.
[122] C.B. Chiu and M. der Sarkissian, Nuovo Cim. 55A (1968) 396.
[123] C.B. Chiu and J. Finkelstein, Phys. Letters 27B (1968) 510.
[124] C.B. Chiu and J. D. Stack, Phys. Rev. 153 (1967) 1575.
[125] C.B. Chiu and E. Ugaz, Phys. Letters 43B (1973) 327.
[126] S.-Y. Chu and D.P. Roy, Phys. Rev. Letters 20 (1968) 958.
[127] M. Ciafaloni, G. Marchesini and G. Veneziano, Nucl. Phys. B98 (1975) 472; 493.
[128] D. Cline, J. Matos and D.D. Reeder, Phys. Rev. Letters 23 (1969) 1318.
[129] G. Cohen-Tannoudji, A. Morel and H. Navelet, Ann. Phys. (NY) 46 (1968) 239.
[130] P.D.B. Collins, Phys. Reports 1 C (1971) 103.
[131] P.D.B. Collins and E.J. Squires, Regge Poles in Particle Physics, Springer Tracts in Modern Physics, vol. 45 (J. Springer, Berlin, 1968).
[132] P. W. Coulter, E.S. Ma and G.L. Shaw, Phys. Rev. Letters 23 (1969) 106.
[133] P.W. Coulter and D.R. Snider, Phys. Rev. D8 (1973) 4058.
[134] G. Cozzika, Y. Ducros, A. Gaidot, A. de Lesquen, J. P. Merlo and L. van Rossum, Phys. Letters 40B (1972) 281.
[135] D.J. Crennell, U. Karshon, K.W. Lai, J.S. O'Neall, J.M. Scarr, R.M. Lea, T.G. Schumann and E.M. Urvater, Phys. Rev. Letters 23 (1969) 1347.
[136] M.J. Creutz, S.D. Drell and E.A. Paschos, Phys. Rev. 178 (1969) 2300.
[137] R.R. Crittenden, R.M. Heinz, D.B. Lichtenberg and E. Predazzi, Phys. Rev. D1 (1970) 169.
[138] M. Damashek and F.J. Gilman, Phys. Rev. D1 (1970) 1319.
[139] A. Dar, M. Kugler, Y. Dothan and S. Nussinov, Phys. Rev. Letters 12 (1964) 82.
[140] A. Dar, T.L. Watts and V.F. Weisskopf, Nucl. Phys. B13 (1969) 477.
[141] R. Dashen and M. Gell-Mann, Phys. Letters 17 (1965) 142.
[142] G.V. Dass, M. Jacob and S. Papageorgiou, Nuovo Cim. 67A (1970) 429.
[143] G.V. Dass and C. Michael, Phys. Rev. Letters 20 (1968) 1066; Phys. Rev. 175 (1968) 1774.
[144] C. Daum, C. Michael and C. Schmid, Phys. Letters 31B (1970) 222.
[145] M. Davier, Phys. Letters 40B (1972) 369.
[146] M. Davier, I. Derado, D.E.C. Fries, F.F. Liu, R.F. Mozley, A. Odian, J. Park, W.P. Swanson, F. Villa and D. Yount, Nucl. Phys. B58 (1973) 31.
[147] M. Davier and H. Harari, Phys. Letters 35B (1971) 239.

[148] V. de Alfaro, S. Fubini, C. Rossetti and G. Furlan, Phys. Letters 21 (1966) 576.
[149] A.J. de Groot, W. Hoogland, B. Jongejans, J.C. Kluyver, G.G.G. Massaro, W.J. Metzger, H.G.J.M. Tiecke and J.J.M. Timmermans, Nucl. Phys. B74 (1974) 77.
[150] A. Della Selva, L. Masperi and R. Odorico, Nuovo Cim. 54A (1968) 979.
[151] A. Della-Selva, L. Masperi and R. Odorico, Nuovo Cim. 55A (1968) 602.
[152] M. Derrick, in: Topical Conf. on High-Energy Collisions of Hadrons, CERN 1968 (CERN 68-7 vol. 1).
[153] J.J. de Swart, Rev. Mod. Phys. 35 (1963) 916; 37 (1965) 326 (E).
[154] J.J. de Swart, Nuovo Cim. 31 (1964) 420.
[155] C.E. DeTar, C.E. Jones, F.E. Low, J.H. Weis, J.E. Young and C.-I. Tan, Phys. Rev. Letters 26 (1971) 675.
[156] C.E. DeTar and J.H. Weis, MIT preprint CTP-218 (1971).
[157] R.C.E. Devenish, C.D. Froggatt and B.R. Martin, DESY preprint 74/19 (1974).
[158] J. Dias de Deus and I. Uschersohn, Rutherford Laboratory preprint RL-75-042 T.112 (1975).
[159] R. Diebold, D.S. Ayres, A.F. Greene, S.L. Kramer, A.J. Pawlicki and A.B. Wicklund, Phys. Rev. Letters 32 (1974) 904.
[160] F.N. Dikmen, Phys. Rev. Letters 18 (1967) 798.
[161] P. di Vecchia, F. Drago and M.L. Paciello, Phys. Letters 26B (1968) 530.
[162] P. di Vecchia, F. Drago, C. Ferro Fontán, R. Odorico and M.L. Paciello, Phys. Letters 27B (1968) 296.
[163] R. Dolen, D. Horn and C. Schmid, Phys. Rev. Letters 19 (1967) 402.
[164] R. Dolen, D. Horn and C. Schmid, Phys. Rev. 166 (1968) 1768.
[165] C.A. Dominguez, C. Ferro Fontán and R. Suaya, Phys. Letters 31B (1970) 365.
[166] H. Ebenhöh, F. Eisele, H. Filthuth, W. Föhlisch, V. Hepp, E. Leitner, W. Presser, H. Schneider, T. Thouw and G. Zech, Zeits. f. Phys. 241 (1971) 473.
[167] T. Eguchi, Nucl. Phys. B60 (1973) 277.
[168] T. Eguchi, Nucl. Phys. B70 (1974) 390; Phys. Rev. D10 (1974) 2652.
[169] T. Eguchi, M. Fukugita and T. Shimada, Phys. Letters 43B (1973) 56.
[170] T. Eguchi, T. Shimada and M. Fukugita, Nucl. Phys. B74 (1974) 102.
[171] T. Eguchi and K. Igi, Phys. Rev. Letters 27 (1971) 1319.
[172] T. Eguchi and K. Igi, Phys. Rev. D8 (1973) 1537.
[173] A. Eide, P. Lehmann, A. Lundby, C. Baglin, P. Briandet, P. Fleury, P.J. Carlson, E. Johansson, M. Davier, V. Gracco, R. Morand, and D. Treille, Nucl. Phys. B60 (1973) 173.
[174] M.B. Einhorn, UCRL preprint UCRL-20688 (1971).
[175] M.B. Einhorn, J. Ellis and J. Finkelstein, Phys. Rev. D5 (1972) 2063.
[176] M.B. Einhorn, M.B. Green and M.A. Virasoro, Phys. Letters 37B (1971) 292.
[177] M.B. Einhorn, M.B. Green and M.A. Virasoro, Phys. Rev. D7 (1972) 102.
[178] F. Elvekjaer, T. Inami and G. Ringland, Phys. Letters 44B (1973) 91.
[179] F. Elvekjaer and B.R. Martin, CERN preprint TH-1306 (1974).
[180] F. Elvekjaer and E. Pietarinen, Nucl. Phys. B45 (1972) 621.
[181] P. Estabrooks and A.D. Martin, Phys. Letters 42B (1972) 229.
[182] P. Estabrooks and A.D. Martin, Nucl. Phys. B95 (1975) 322.
[183] R.J. Esterling, N.E. Booth, G. Conforto, J. Parry, J. Scheid, D. Sherden and A. Yokosawa, Phys. Rev. Letters 21 (1968) 1410.
[184] Y. Eylon and H. Harari, Nucl. Phys. B80 (1974) 349.
[185] D. Faiman and A.W. Hendry, Phys. Rev. 173 (1968) 1720.
[186] D. Faiman and J.L. Rosner, Phys. Letters 45B (1973) 357.
[187] D. Faiman, J.L. Rosner and J. Weyers, Nucl. Phys. B57 (1973) 45.
[188] E. Ferrari and G. Violini, Nuovo Cim. 69A (1970) 375.
[189] C. Ferro Fontán, CERN preprint TH-1490 (1972).
[190] C. Ferro Fontán, M. Lusignoli, R. Odorico, M. Restignoli and G. Violini, Nuovo Cim. 57A (1968) 442.
[191] C. Ferro Fontán, R. Odorico and L. Masperi, Nuovo Cim. 58A (1968) 534.
[192] K. Fiałkowski and H.I. Miettinen, Phys. Letters 43B (1973) 61.
[193] R.D. Field and G.C. Fox, Nucl. Phys. B80 (1974) 367.
[194] R.D. Field and J.D. Jackson, Phys. Rev. D4 (1971) 693.
[195] A. Firestone, G. Goldhaber, A. Hirata, D. Lissauer and G.H. Trilling, Phys. Rev. Letters 25 (1970) 958.
[196] A. Firestone, G. Goldhaber, D. Lissauer and G.H. Trilling, Phys. Rev. D5 (1972) 2188.
[197] K.J. Foley, R.S. Jones, S.J. Lindenbaum, W.A. Love, S. Ozaki, E.D. Platner, C.A. Quarles and E.H. Willen, Phys. Rev. Letters 19 (1967) 330.
[198] G.C. Fox, in: Phenomenology in Particle Physics 1971, California Institute of Technology.
[199] G.C. Fox and C. Quigg, Ann. Rev. Nucl. Sci. 23 (1973) 219.
[200] P.H. Frampton, Phys. Rev. D7 (1973) 3077.
[201] P.H. Frampton, Dual Resonance Models (W.A. Benjamin Inc., New York, 1974).
[202] P.H. Frampton and P.G.O. Freund, Nucl. Phys. B24 (1970) 453.

[203] S.C. Frautschi, M. Gell-Mann and F. Zachariasen, Phys. Rev. 126 (1962) 2204.
[204] P.G.O. Freund, Phys. Rev. Letters 20 (1968) 235.
[205] P.G.O. Freund, H.F. Jones and R.J. Rivers, Phys. Letters 36B (1971) 89.
[206] P.G.O. Freund and R.J. Rivers, Phys. Letters 29B (1969) 510.
[207] P.G.O. Freund, R. Walz and J.L. Rosner, Nucl. Phys. B13 (1969) 237.
[208] C.D. Froggatt and N.H. Parsons, University of Glasgow preprint, G.U. 29 (1974).
[209] J. Frøyland, F. Halzen and B. Peterson, CERN preprint, TH-1255 (1970).
[210] G. Frye and L. Susskind, Phys. Letters 31B (1970) 589.
[211] Y. Fujii and M. Fukugita, Nucl. Phys. B85 (1974) 179.
[212] M. Fukugita, University of Tokyo preprint, UT-200 (1973).
[213] M. Fukugita, (1976) in preparation.
[214] M. Fukugita and K. Igi, (1976) in preparation.
[215] M. Fukugita and T. Inami, Nucl. Phys. B44 (1972) 490.
[216] M. Fukugita and T. Inami, Nucl. Phys. B57 (1973) 543.
[217] M. Fukugita, T. Inami and Y. Kimura, Phys. Letters 36B (1971) 575.
[218] J. Gabarro and C. Pajares, Nuovo Cim. 16A (1973) 37.
[219] R. Gatto, Phys. Letters 25B (1967) 140.
[220] M. Gell-Mann, M.L. Goldberger, F.E. Low, E. Marx and F. Zachariasen, Phys. Rev. 133 (1964) B145.
[221] A. Gersten, Nucl. Phys. B12 (1969) 537.
[222] K. Ghoroku, M. Imachi, S. Otsuki and F. Toyoda, Prog. Theor. Phys. 47 (1972) 1958.
[223] K. Ghoroku, M. Imachi, S. Otsuki and F. Toyoda, in: Proc. Int. Symp. on High Energy Physics, Tokyo, 1973.
[224] F.J. Gilman, H. Harari and Y. Zarmi, Phys. Rev. Letters 21 (1968) 323.
[225] F.J. Gilman, M. Kugler and S. Meshkov, Phys. Rev. D9 (1974) 715.
[226] F.J. Gilman, J. Pumplin, A. Schwimmer and L. Stodolsky, Phys. Letters 31B (1970) 387.
[227] S. Gjesdal, G. Presser, P. Steffen, J. Steinberger, F. Vannucci, H. Wahl, K. Kleinknecht, V. Lüth and G. Zech, Phys. Letters 40B (1972) 152.
[228] R.J. Glauber, Lectures in Theoretical Physics, vol. 1 (Interscience, New York, 1959).
[229] H. Goldberg, Phys. Rev. D6 (1972) 2542.
[230] H.A. Gordon, K.W. Lai and F.E. Paige, Phys. Rev. D5 (1972) 1113.
[231] K. Gottfried and J.D. Jackson, Nuovo Cim. 34 (1964) 735.
[232] O.W. Greenberg, Phys. Rev. Letters 13 (1964) 598.
[233] V.N. Gribov, Zh. Eksp. Teor. Fiz. 41 (1961) 667 [Sov. Phys. JETP 14 (1962) 478].
[234] V.N. Gribov, Zh. Eksp. Teor. Fiz. 43 (1962) 1529 [Sov. Phys. JETP 16 (1963) 1080].
[235] V.N. Gribov, Zh. Eksp. Teor. Fiz. 53 (1967) 654 [Sov. Phys. JETP 26 (1968) 414].
[236] D.J. Gross, Phys. Rev. Letters 19 (1967) 1303.
[237] D.J. Gross, A. Neveu, J. Scherk and J.H. Schwarz, Phys. Rev. D2 (1970) 697.
[238] M. Haguenauer, P. Miné, U. Nguyen-Khac, K. Bjørnenak, A. Haatuft, J.M. Olsen, R. Arnold, B. Escoubes, A. Lloret, M. Paty, J.L. Riester, S. de Unamuno, L. Ferrer, P.L. de Guevara and R. Llosa, Phys. Letters 37B (1971) 538.
[239] F. Halzen and C. Michael, Phys. Letters 36B (1971) 367.
[240] Y. Hara, Phys. Rev. 136 (1964) 507.
[241] Y. Hara, Suppl. Prog. Theor. Phys. 51 (1972) 96.
[242] Y. Hara and T. Kuroda, Prog. Theor. Phys. 55 (1976) 1169.
[243] Y. Hara, T. Kuroda and Y. Takaiwa, Prog. Theor. Phys. 51 (1974) 840.
[244] H. Harari, Phys. Rev. Letters 20 (1968) 1395.
[245] H. Harari, Phys. Rev. Letters 22 (1969) 562.
[246] H. Harari, in: Proc. 4th Int. Symp. on Electron and Photon Interactions at High Energy, Liverpool, 1969.
[247] H. Harari, Ann. Phys. (N.Y.) 63 (1971) 432.
[248] H. Harari, Phys. Rev. Letters 26 (1971) 1400.
[249] H. Harari and E. Rabinovici, Phys. Letters 43B (1973) 49.
[250] H. Harari and Y. Zarmi, Phys. Rev. 187 (1969) 2230.
[251] H. Harari and Y. Zarmi, Phys. Letters 32B (1970) 291.
[252] E.H. Harvey, E. Marquit, E.A. Peterson, T.G. Rhoades, H. Romer, K. Ruddick and J.K. Randolph, Phys. Rev. Letters 27 (1971) 885.
[253] F. Hayot and A. Morel, Phys. Rev. D8 (1973) 223.
[254] F. Henyey, G.L. Kane, J. Pumplin and M. Ross, Phys. Rev. Letters 21 (1968) 946.
[255] A.J.G. Hey, J.L. Rosner and J. Weyers, Nucl. Phys. B61 (1973) 205.
[256] K. Hidaka, Lett. Nuovo Cim. 11 (1974) 503.
[257] K. Hidaka, Lett. Nuovo Cim. 12 (1975) 273.

[258] D. Hill, P.F.M. Koehler, T.B. Novey, B. Sandler, H. Spinka, A. Yokosawa, D. Eartly, K. Pretzl, G. Burleson and H. Davis, Phys. Rev. Letters 27 (1971) 1241.
[259] D. Hill, P. Koehler, T. Novey, P. Rynes, B. Sandler, H. Spinka, A. Yokosawa, D. Eartly, K. Pretzl, G. Burleson, G. Hicks, C. Wilson and W. Risk, Phys. Rev. Letters 30 (1973) 239.
[260] A.C. Hirshfeld, Phys. Letters 39B (1972) 233.
[261] H. Högaasen and C. Michael, Nucl. Phys. B44 (1972) 214.
[262] G. Höhler, J. Baacke and G. Eisenbeiss, Phys. Letters 22 (1966) 203.
[263] G. Höhler, J. Baacke, H. Schlaile and P. Sonderegger, Phys. Letters 20 (1966) 79.
[264] G. Höhler and H.P. Jakob, Universität Karlsruhe preprint TKP 23/72 (1972).
[265] G. Höhler and H.P. Jakob, Universität Karlsruhe preprint TKP 9/74 (1974).
[266] G. Höhler and R. Strauss, Zeits. f. Phys. 232 (1970) 205.
[267] P. Hoyer, in: Proc. 17th Int. Conf. on High Energy Physics, London, 1974.
[268] P. Hoyer, R.G. Roberts and D.P. Roy, Nucl. Phys. B56 (1973) 173.
[269] P. Hoyer, R.G. Roberts and D.P. Roy, Phys. Letters 44B (1973) 258.
[270] B. Hyams, C. Jones, P. Weilhammer, W. Blum, H. Dietl, G. Grayer, W. Koch, E. Lorenz, G. Lütjens, W. Männer, J. Meissburger, W. Ochs, U. Stierlin and F. Wagner, Nucl. Phys. B64 (1973) 134.
[271] B. Hyams, C. Jones, P. Weilhammer, W. Blum, H. Dietl, G. Grayer, W. Koch, E. Lorenz, G. Lütjens, W. Männer, J. Meissburger, W. Ochs and U. Stierlin, Nucl. Phys. B100 (1975) 205.
[272] M. Ida, Lett. Nuovo Cim. 4 (1972) 707; Prog. Theor. Phys. 48 (1972) 2346.
[273] M. Ida, Prog. Theor. Phys. 49 (1973) 1259.
[274] M. Ida, T. Tajima and K. Yamawaki, Prog. Theor. Phys. 52 (1974) 1583.
[275] K. Igi, Phys. Rev. Letters 9 (1962) 76.
[276] K. Igi, Phys. Rev. 130 (1963) 820.
[277] K. Igi, Phys. Letters 28B (1968) 330.
[278] K. Igi, in: Proc. Int. Symp. on High Energy Physics, Tokyo, 1973.
[279] K. Igi and T. Eguchi, Phys. Letters 42B (1972) 449.
[280] K. Igi and S. Matsuda, Phys. Rev. Letters 18 (1967) 625; 822(E).
[281] K. Igi and S. Matsuda, Phys. Rev. 163 (1967) 1622.
[282] K. Igi, S. Matsuda, Y. Oyanagi and H. Sato, Phys. Rev. Letters 21 (1968) 580.
[283] K. Igi and T. Shimada, Lett. Nuovo Cim. 12 (1975) 193; Prog. Theor. Phys. 53 (1975) 1731.
[284] K. Igi and J.K. Storrow, Nuovo Cim. 62A (1969) 972.
[285] J. Iizuka, Suppl. Prog. Theor. Phys. 37–38 (1966) 21.
[286] J. Iizuka, K. Okada and O. Shito, Prog. Theor. Phys. 35 (1966) 1061.
[287] M. Imachi, Prog. Theor. Phys. 47 (1972) 1445.
[288] M. Imachi, T. Matsuoka, K. Ninomiya and S. Sawada, Prog. Theor. Phys. 40 (1968) 353.
[289] M. Imachi, T. Oroguchi, S. Otsuki and F. Toyoda, Prog. Theor. Phys. 45 (1971) 1849.
[290] M. Imachi, S. Otsuki and F. Toyoda, Prog. Theor. Phys. 43 (1970) 1105.
[291] T. Inami, Nuovo Cim. 63A (1969) 987.
[292] T. Inami, Prog. Theor. Phys. 45 (1971) 1903.
[293] T. Inami, in: Proc. Palermo Int. Conf. on Elementary Particles, 1975.
[294] T. Inami, K. Kawarabayashi and S. Kitakado, Phys. Letters 61B (1976) 60; Prog. Theor. Phys. 56 (1976) 1570.
[295] T. Inami and H.I. Miettinen, Phys. Letters 49B (1974) 67.
[296] T. Inami and R.G. Roberts, Nucl. Phys. B93 (1975) 497.
[297] A.C. Irving, A.D. Martin and C. Michael, Nucl. Phys. B32 (1971) 1.
[298] A.C. Irving and L.G.F. Vanryckeghem, Nucl. Phys. B93 (1975) 324.
[299] J.D. Jackson, in: Proc. Lund Int. Conf. on Elementary Particles, 1969.
[300] J.D. Jackson, in: Proc. Int. Conf. on Duality and Symmetry in Hadron Physics, Tel Aviv, 1971.
[301] J.D. Jackson and C. Quigg, Phys. Letters 29B (1969) 236.
[302] M. Jacob, in: Proc. Lund Int. Conf. on Elementary Particles, 1969.
[303] M. Jacob and G.C. Wick, Ann. Phys. (N.Y.) 7 (1959) 404.
[304] C.L. Jen, K. Kang, P. Shen and C.-I. Tan, Phys. Rev. Letters 27 (1971) 754.
[305] K. Johnson and S. Treiman, Phys. Rev. Letters 14 (1965) 189.
[306] W.B. Johnson, D.W.G.S. Leith, J.S. Loos, G.J. Luste, K. Moriyasu, W.M. Smart, F.C. Winkelmann and R.J. Yamartino, Phys. Rev. Letters 26 (1971) 1053.
[307] G. Kaiser, Nucl. Phys. B43 (1972) 345.
[308] G. Karl and E. Obryk, Nucl. Phys. B8 (1968) 609.
[309] K. Kawarabayashi, S. Kitakado and H. Yabuki, Phys. Letters 28B (1969) 432.
[310] B. Kayser, Phys. Rev. D1 (1970) 306.
[311] N.N. Khuri and T. Kinoshita, Phys. Rev. 137B (1965) 720.

[312] K. Kikkawa, B. Sakita and M.A. Virasoro, Phys. Rev. 184 (1969) 1701.
[313] I. Kimel and H. Miyazawa, Prog. Theor. Phys. 40 (1968) 124.
[314] M.J. King and K.C. Wali, Phys. Rev. Letters 24 (1970) 1460.
[315] A.R. Kirby, W.S. Brockett, G.T. Corlew, W.R. Frisken, T.L. Jenkins, C.R. Sullivan, J.A. Todoroff and W.B. Richards, Bull. Am. Phys. Soc. 16 (1971) 634; in: Gidal, LBL preprint LBL-352 (1971).
[316] V. Kistiakowsky, F.A. Triantis, R.K. Yamamoto, R.D. Klem, P. Marcato, I.A. Pless, I. Spirn, E.F. Anelli, C.N. DeMarzo, A. Romano, D.G. Crabb, A.C. Meyers III and J.R. O'Fallon, Phys. Rev. Letters 26 (1971) 1498.
[317] K. Kleinknecht, in: Proc. 17th Int. Conf. on High Energy Physics, London, 1974.
[318] T. Kondo, Y. Shimizu and H. Sugawara, University of Tokyo (INS) preprint (1972).
[319] A. Kotlewski, W. Lee, M. Suzuki and J. Thaler, Phys. Rev. D8 (1973) 348.
[320] M. Kuroda and M. Ida, Kyoto University (RIFP) preprint RIFP-176 (1973).
[321] J. Kwieciński, Lett. Nuovo Cim. 3 (1972) 619.
[322] J. Lach and E. Malamud, Phys. Letters 44B (1973) 474.
[323] K.W. Lai and J. Louie, Nucl. Phys. B19 (1970) 205.
[324] P.V. Landshoff, Nucl. Phys. B15 (1968) 284.
[325] T.A. Lasinski, Nucl. Phys. B29 (1971) 125.
[326] P. Lauscher, G. Otter, H. Wieczorek, E. Matthäus, H.J. Schreiber, V.T. Cocconi, M.J. Counihan, J.D. Hansen, G. Kellner, A. Kotànski, D.R.O. Morrison, P. Schmid, D. Sotiriou, J.E. Allen, P.J. Dornan, P.R. Thornton, D.J. Kocher, M. Markytan and J. Strauss, Nucl. Phys. B86 (1975) 189.
[327] Huan Lee, Phys. Rev. Letters 30 (1973) 719.
[328] R. Levi Setti, in: Proc. Lund Int. Conf. on Elementary Particles, 1969.
[329] H.J. Lipkin and S. Meshkov, Phys. Rev. Letters 14 (1965) 670.
[330] P.J. Litchfield, in: Proc. 17th Int. Conf. on High Energy Physics, London, 1974.
[331] P.J. Litchfield, T.C. Bacon, I. Butterworth, J.R. Smith, E. Lesquoy, R. Strub, A. Berthon, J. Vrana, J. Meyer, E. Pauli, B. Tallini and J. Zatz, Nucl. Phys. B30 (1971) 125.
[332] Y.C. Liu and I.J. McGee, Phys. Rev. D3 (1970) 183.
[333] Y.C. Liu and S. Okubo, Phys. Rev. Letters 19 (1967) 190.
[334] R. Logan, Phys. Rev. Letters 14 (1965) 414.
[335] A.A. Logunov, L.D. Soloviev and A.N. Tavkhelidze, Phys. Letters 24B (1967) 181.
[336] J.S. Loos and J.A.J. Matthews, Phys. Rev. D6 (1972) 2463.
[337] C. Lovelace, Phys. Letters 28B (1968) 264.
[338] C. Lovelace, Nucl. Phys. B12 (1969) 253.
[339] C. Lovelace, in: Proc. Conf. on $\pi\pi$ and $K\pi$ Interactions, Argonne, 1969.
[340] C. Lovelace, Proc. Roy. Soc. (London) A318 (1970) 321.
[341] C. Lovelace, Phys. Letters 34B (1971) 500.
[342] M.D. Lyberg, Nucl. Phys. B55 (1973) 573.
[343] M.D. Lyberg, NORDITA preprint (1974).
[344] E.S. Ma and G.L. Shaw, Phys. Rev. D3 (1971) 1264.
[345] E.S. Ma and G.L. Shaw, SLAC preprint PUB-1512 (1974).
[346] S.W. MacDowell, Phys. Rev. 116 (1959) 774.
[347] S. Mandelstam, Phys. Rev. 166 (1968) 1539.
[348] S. Mandelstam, Phys. Rev. Letters 21 (1968) 1724.
[349] S. Mandelstam, Phys. Rev. 184 (1969) 1625.
[350] S. Mandelstam, Phys. Rev. D1 (1970) 1734.
[351] S. Mandelstam, Phys. Reports C13 (1974) 259.
[352] J. Mandula, C. Rebbi, R. Slansky, J. Weyers and G. Zweig, Phys. Rev. Letters 22 (1969) 1147.
[353] J. Mandula, J. Weyers and G. Zweig, Phys. Rev. Letters 23 (1969) 266.
[354] J. Mandula, J. Weyers and G. Zweig, Ann. Rev. Nucl. Sci. 20 (1970) 289.
[355] A.D. Martin and C. Michael, Phys. Letters 32B (1970) 297.
[356] A.D. Martin and C. Michael, Phys. Letters 37B (1971) 513.
[357] A.D. Martin, C. Michael and R.J.N. Phillips, Nucl. Phys. B43 (1972) 13.
[358] M.J. Matison, A. Barbaro-Galtieri, M. Alston-Garnjost, S.M. Flatté, J.H. Friedman, G.R. Lynch, M.S. Rabin and F.T. Solmitz Phys. Rev. D9 (1974) 1872.
[359] S. Matsuda, Nucl. Phys. B9 (1969) 113.
[360] S. Matsuda and K. Igi, Phys. Rev. Letters 19 (1967) 928; 20 (1967) 781 (E).
[361] Y. Matsumoto, T. Muta, H. Nakajima, A. Niegawa, Y. Okumura and T. Uematsu, Phys. Letters 39B (1972) 258.
[362] H.J. Melosh, California Institute of Technology preprint (thesis), (1973).
[363] H.J. Melosh, Phys. Rev. D9 (1974) 1095.
[364] J. Meyer and D.E. Plane, Nucl. Phys. B25 (1971) 428.

[365] C. Michael, Phys. Letters 29B (1969) 230.
[366] C. Michael, Springer Tracts in Modern Physics, vol. 55 (1970) p. 174.
[367] C. Michael and R. Odorico, Phys. Letters 34B (1971) 422.
[368] W. Michael, G.S. Abrams, M. Alston-Garnjost, A. Barbaro-Galtieri, B.Y. Daugeras, G. Gidal, A.D. Johnson, G.R. Lynch, F.T. Solmitz and F.C. Winkelmann, Phys. Rev. Letters 35 (1975) 193.
[369] L. Micu, Nucl. Phys. B10 (1969) 521.
[370] P. Minkowski, Lett. Nuovo Cim. 3 (1970) 503; Nucl. Phys. B48 (1972) 247.
[371] M.N. Misheloff, Phys. Rev. 184 (1969) 1732.
[372] O. Miyamura and F. Takagi, Prog. Theor. Phys. 39 (1968) 858.
[373] O. Miyamura and F. Takagi, Prog. Theor. Phys. 39 (1968) 1000.
[374] D. Morgan, Rutherford Laboratory preprint, RL-75-133 T.133 (1975).
[375] L. Moscoso, J.R. Hubbard, A. Rouge and H. Videau, Phys. Letters 40B (1972) 285.
[376] A.H. Mueller, Phys. Rev. D2 (1970) 2963.
[377] N. Nakanishi, Prog. Theor. Phys. 48 (1972) 355.
[378] Y. Nambu, in: Symmetries and Quark Models (Gordon and Breach, New York, 1970).
[379] Y. Nambu, in: Proc Int. Symp. on High Energy Physics, Tokyo, 1973.
[380] A. Neveu and J.H. Schwarz, Nucl. Phys. B31 (1971) 86.
[381] H. Noda and K. Kinoshita, Prog. Theor. Phys. 30 (1972) 819.
[382] H. Noda and F. Toyoda, Prog. Theor. Phys. 45 (1971) 1634.
[383] R. Odorico, Phys. Letters 34B (1971) 65.
[384] R. Odorico, Nucl. Phys. B37 (1972) 509.
[385] R. Odorico, Phys. Letters 38B (1972) 37.
[386] R. Odorico, Phys. Letters 38B (1972) 411.
[387] R. Odorico, Phys. Letters 41B (1972) 339.
[388] R. Odorico, Phys. Rev. D8 (1973) 3952.
[389] R. Odorico, A. Garcia and C.A. Garcia-Canal, Phys. Letters 32B (1970) 375.
[390] S. Okubo, Phys. Letters 5 (1963) 165.
[391] P. Olesen, CERN preprint TH-1376 (1971).
[392] D. Olive, in: Proc. 17th Int. Conf. on High Energy Physics, London, 1974.
[393] M.G. Olsson, Phys. Letters 26B (1968) 310.
[394] M.G. Olsson, Nuovo Cim. 57A (1968) 420.
[395] K. Paler, S.N. Tovey, T.P. Shah, J.J. Phelan, R.J. Miller, M. Spiro, R. Barloutaud, M. Bardadin-Otwinowska, A. Borg, B. Chaurand, B. Drévillon, J.M. Gago and R.A. Salmeron, Nucl. Phys. B96 (1975) 1.
[396] N. Papadopoulos, C. Schmid, C. Sorensen and D.M. Webber, Nucl. Phys. B101 (1975) 189.
[397] Particle Data Group (PDG), Phys. Letters 50B (1974) 1.
[398] J.E. Paton and Chan H.-M., Nucl. Phys. B10 (1969) 516.
[399] R. Patton, W.A. Barletta, R. Ehrlich, A. Etkin, P.A. Souder, M.E. Zeller, M. Mishina and D.M. Lazarus, Phys. Rev. Letters 34 (1975) 975.
[400] M.R. Pennington and S.D. Protopopescu, Phys. Letters 40B (1972) 105.
[401] M.R. Pennington and C. Schmid, Phys. Rev. D7 (1973) 2213.
[402] W.P. Petersen and J.L. Rosner, Phys. Rev. D6 (1972) 820.
[403] B. Peterson and N.A. Törnqvist, Nucl. Phys. B13 (1969) 629.
[404] C. Peterson and L. Sollin, University of Lund preprint (1974).
[405] R.J.N. Phillips, in: Proc. Amsterdam Conf. on Elementary Particles, 1971.
[406] R.J.N. Phillips, Nucl. Phys. B72 (1974) 481.
[407] R.J.N. Phillips and W. Rarita, Phys. Rev. 139 (1965) B1336.
[408] R.J.N. Phillips and W. Rarita, Phys. Rev. Letters 15 (1965) 807.
[409] R.J.N. Phillips and G.A. Ringland, Nucl. Phys. B32 (1971) 131.
[410] H. Pilkuhn, W. Schmidt, A.D. Martin, C. Michael, F. Steiner, B.R. Martin, M.M. Nagels and J.J. de Swart, Nucl. Phys. B65 (1973) 460.
[411] D.E. Plane, P. Baillon, C. Bricman, M. Ferro-Luzzi, J. Meyer, E. Pagiola, N. Schmitz, E. Burkhardt, H. Filthuth, E. Kluge, H. Oberlack, R. Barloutaud, P. Granet, J.P. Porte and J. Prevost, Nucl. Phys. B22 (1970) 93.
[412] K. Pretzl and K. Igi, Nuovo Cim. 63A (1969) 609.
[413] N.M. Queen, M. Restignoli and G. Violini, Forts. d. Phys. 17 (1969) 467.
[414] C. Quigg, Nucl. Phys. B34 (1971) 77.
[415] C. Quigg and J.D. Jackson, NAL preprint, THY-93 (1972).
[416] C. Rebbi, Phys. Reports C12 (1974) 1.
[417] C. Rebbi and R. Slansky, Rev. Mod. Phys. 42 (1970) 68.
[418] B. Renner, Phys. Letters 33B (1970) 599.

[419] M. Restignoli, L. Sertorio and M. Toller, Phys. Rev. 150 (1966) 1389.
[420] C.A. Rey, A.J. Lennox, J. Poirier and K.P. Pretzl, Phys. Rev. Letters 32 (1974) 908; 33 (1974) 250 (E).
[421] M. Rimpault and Ph. Salin, Nucl. Phys. B22 (1970) 235.
[422] G.A. Ringland and D.P. Roy, Phys. Letters 36B (1971) 110.
[423] C. Rosenzweig and G.F. Chew, Phys. Letters 58B (1975) 93.
[424] J.L. Rosner, Phys. Rev. Letters 21 (1968) 950; 1468 (E).
[425] J.L. Rosner, Phys. Rev. Letters 22 (1969) 689.
[426] J.L. Rosner, Phys. Rev. D6 (1972) 1781.
[427] J.L. Rosner, Phys. Rev. D7 (1973) 172.
[428] J.L. Rosner, Phys. Reports 11C (1974) 189.
[429] J.L. Rosner, in: Proc. 17th Int. Conf. on High Energy Physics, London, 1974.
[430] J.L. Rosner, C. Rebbi and R. Slansky, Phys. Rev. 188 (1969) 2367.
[431] M. Ross, F. Henyey and G.L. Kane, Nucl. Phys. B23 (1970) 269.
[432] R.E. Rothschild, T. Bowen, P.K. Caldwell, D. Davidson, E.W. Jenkins, R.M. Kalbach, D.V. Petersen and A.E. Pifer, Phys. Rev. D5 (1972) 499.
[433] D.P. Roy and R.G. Roberts, Nucl. Phys. B77 (1974) 240.
[434] D.P. Roy, R.G. Roberts, R.J.N. Phillips and H.I. Miettinen, Phys. Rev. D6 (1972) 1317.
[435] D.P. Roy and M. Suzuki, Phys. Letters 28B (1969) 558.
[436] H.R. Rubinstein, A. Schwimmer, G. Veneziano and M.A. Virasoro, Phys. Rev. Letters 21 (1968) 491.
[437] D.R. Rust, P.N. Kirk, R.A. Lundby, C.E.W. Ward, D.D. Yovanovitch, S.M. Pruss, C.W. Akerlof, K.S. Han, D.I. Meyer and P. Schmueser, Phys. Rev. Letters 24 (1970) 1361.
[438] N. Sakai, Nucl. Phys. B99 (1975) 167,
[439] N. Sakai, in: Proc. Palermo Int. Conf. on Elementary Particles, 1975.
[440] N.P. Samios, M. Goldberg and B.T. Meadows, Rev. Mod. Phys. 46 (1974) 49.
[441] A.I. Sanda, Phys. Rev. D6 (1972) 280.
[442] J.J.G. Scanio, Phys. Rev. 152 (1966) 1337.
[443] J. Scherk, Nucl. Phys. B31 (1971) 222.
[444] J.C. Scheuer, R. Barloutaud, D. Merrill, A.M. Bakker, A.J. de Groot, W. Hoogland, G.G.G. Massaro, G. Giacomelli, P. Lugaresi-Serra, A. Minguzzi-Ranzi, A.M. Rossi, G. Alexander, Y. Eisenberg, U. Karshon, A. Shapira, J. Goldberg, G. Lamidey and A. Rouge, Nucl. Phys. B33 (1972) 61.
[445] C. Schmid, Phys. Rev. Letters 20 (1968) 628.
[446] C. Schmid, Phys. Rev. Letters 20 (1968) 689.
[447] C. Schmid, Lett. Nuovo Cim. 1 (1969) 165.
[448] C. Schmid, Nuovo Cim. 61A (1969) 289.
[449] C. Schmid, Proc. Roy. Soc. (London) A318 (1970) 257.
[450] C. Schmid, in: Phenomenology in Particle Physics 1971, California Institute of Technology.
[451] C. Schmid, in: Proc. Amsterdam Conf. on Elementary Particles, 1971.
[452] C. Schmid, in: Proc. Int. Conf. on Duality and Symmetry in Hadron Physics, Tel Aviv, 1971 (in Panel Discussion).
[453] C. Schmid, in: Proc. 16th Int. Conf. on High Energy Physics, Chicago-Batavia, 1972, vol. 1.
[454] C. Schmid and C. Sorensen, Nucl. Phys. B96 (1975) 209.
[455] C. Schmid and J.K. Storrow, Nucl. Phys. B29 (1971) 219.
[456] C. Schmid and J.K. Storrow, Nucl. Phys. B44 (1972) 269.
[457] C. Schmid and J. Yellin, Phys. Letters 27B (1968) 19.
[458] C. Schmid and J. Yellin, Phys. Rev. 182 (1969) 1449.
[459] F.H. Schmidt, C. Baglin, P.J. Carlson, A. Eide, V. Gracco, E. Johansson and A. Lundby, Phys. Letters 45B (1973) 157.
[460] M.G. Schmidt, Nucl. Phys. B15 (1970) 157.
[461] B. Schrempp and F. Schrempp, Nucl. Phys. B54 (1973) 525.
[462] B. Schrempp and F. Schrempp, Nucl. Phys. B60 (1973) 110.
[463] B. Schrempp and F. Schrempp, in: Proc. 9th Rencontre de Moriond, 1974.
[464] J.H. Schwarz, Phys. Rev. 159 (1967) 1269.
[465] J.H. Schwarz, Phys. Reports 8C (1973) 269.
[466] A. Schwimmer, Phys. Rev. 184 (1969) 1508.
[467] L. Sertorio and L.-L. Wang, Phys. Rev. 178 (1969) 2462.
[468] J.A. Shapiro, Phys. Rev. 179 (1969) 1345.
[469] J.A. Shapiro and J. Yellin, UCRL preprint UCRL-18500 (1968).
[470] T. Shimada, Nucl. Phys. B100 (1975) 225.
[471] R.A. Sidwell, R.R. Crittenden, K.F. Galloway, R.M. Heinz and H.A. Neal, Phys. Rev. D3 (1971) 1523.

[472] R. Singer, T.H. Fields, L.G. Hyman, R. Engelmann, T. Kafka, M. Pratap, L. Voyvodic, R. Walker and J. Whitmore, Phys. Letters 60B (1976) 385.
[473] V. Singh, Phys. Rev. 129 (1963) 1889.
[474] D. Sivers and J. Yellin, UCRL preprint UCRL-18665 (1969), Ann. Phys. (N.Y.) 55 (1969) 107.
[475] A. Sommerfeld, Partielle Differentialgleichungen der Physik, Vorlesungen über theoretische Physik, Bd. 6 (Dieterich'sche Verlagsbuchhandlung, Wiesbaden, 1947) S.282 [Partial Differential Equation in Physics (Academic Press Inc., New York, 1949) p. 282].
[476] N.J. Sopkovich, Nuovo Cim. 26 (1962) 186.
[477] H.P. Stapp, Phys. Rev. D3 (1971) 3177.
[478] J.K. Storrow, Nucl. Phys. B47 (1972) 174.
[479] J.K. Storrow and G.A. Winbow, Nucl. Phys. B54 (1973) 560.
[480] H. Sugawara and F. von Hippel, Phys. Rev. 145 (1966) 1331.
[481] K. Sundermeyer, DESY preprint 70/55 (1970).
[482] L. Susskind, Nuovo Cim. 69A (1970) 457.
[483] Y. Takahashi and Y. Kohsaka, Prog. Theor. Phys. 50 (1973) 1334.
[484] G. 't Hooft, Nucl. Phys. B72 (1974) 461.
[485] R.D. Ting, Phys. Rev. 181 (1969) 1942.
[486] R.D. Tripp, in: Proc. 14th Int. Conf. on High Energy Physics, Vienna, 1968.
[487] T.L. Trueman and G.C. Wick, Ann. Phys. (N.Y.) 26 (1964) 322.
[488] S.-H.H. Tye and G. Veneziano, Phys. Letters 38B (1972) 30; Phys. Rev. D6 (1972) 1675.
[489] A. Ukawa, Y. Oyanagi and M. Fukugita, Nucl. Phys. B72 (1974) 474.
[490] L.G.F. Vanryckeghem, Nucl. Phys. B90 (1975) 161.
[491] K.V. Vasavada and K. Raman, Phys. Rev. Letters 21 (1968) 577.
[492] G. Veneziano, Nuovo Cim. 57A (1968) 190.
[493] G. Veneziano, Lett. Nuovo Cim. 1 (1971) 681.
[494] G. Veneziano, Phys. Letters 43B (1973) 413.
[495] G. Veneziano, Nucl. Phys. B74 (1974) 365; Phys. Letters 52B (1974) 220.
[496] G. Veneziano, Phys. Reports 9C (1974) 199.
[497] G. Veneziano, Nucl. Phys. B108 (1976) 285.
[498] M.A. Virasoro, Phys. Rev. 177 (1969) 2309.
[499] M.A. Virasoro, Phys. Rev. D1 (1970) 2933.
[500] D.V. Volkov and V.V. Radchenko, Phys. Letters 36B (1971) 83.
[501] G. von Dardel, D. Dekkers, R. Mermod, M. Vivargent, G. Weber and K. Winter, Phys. Rev. Letters 8 (1962) 173.
[502] F. Wagner and C. Lovelace, Nucl. Phys. B25 (1971) 411.
[503] L.-L.C. Wang, Phys. Rev. 142 (1966) 1187.
[504] C.E.W. Ward, W.T. Meyer and D.R. Rust, ANL preprint HEP-7425 (1974).
[505] K.G. Wilson, Cornell University preprint CLNS-131 (1970).
[506] F.C. Winkelmann, H. H. Bingham, D.M. Chew, B.Y. Daugeras, W.B. Fretter, G. Goldhaber, W.R. Graves, A.D. Johnson, J.A. Kadyk, L. Stutte, C.H. Trilling, G.P. Yost, D. Bogert, R. Hanft, F.R. Huson, S. Kahn, D. Ljung, C. Pascaud, S. Pruss and W.M. Smart, Phys. Letters 56B (1975) 101.
[507] R. Worden, Nucl. Phys. B37 (1972) 253.
[508] R. Worden, Nucl. Phys. B58 (1973) 205.
[509] T.T. Wu and C.N. Yang, Phys. Rev. 137 (1965) B708.
[510] S. Yazaki, Phys. Letters 43B (1973) 225.
[511] S. Yazaki, unpublished (1974).
[512] S. Yazaki, in: University of Tokyo preprint UT-247 (1975).
[513] J. Yellin, UCRL preprint UCRL-18637 (1968).
[514] J. Yellin, UCRL preprint UCRL-18664 (1969).
[515] A. Yokosawa, in: Phenomenology in Particle Physics 1971, California Institute of Technology.
[516] T. Yoneya, Prog. Theor. Phys. 48 (1972) 2044.
[517] H. Yuta, R. Engelmann, B. Musgrave, B. Forman, N. Gelfand and H. Schulz, Nucl. Phys. B52 (1973) 70.
[518] G. Zweig, CERN preprint TH-412 (1964).
[519] M.R. Pennington, Ann. Phys. (N.Y.) 92 (1975) 164.
[520] A.V. Barnes, D.J. Mellema, A.V. Tollestrup, R.L. Walker, O.I. Dahl, R.A. Johnson, R.W. Kenney and M. Pripstein, Phys. Rev. Letters 37 (1976) 76.
[521] O.I. Dahl, R.A. Johnson, R.W. Kenney, M. Pripstein, A.V. Barnes, D.J. Mellema, A.V. Tollestrup and R.L. Walker, Phys. Rev. Letters 37 (1976) 80.
[522] G. Cosme, A. Courau, B. Dudelzak, B. Grelaud, B. Jean-Marie, S. Jullian, D. Lalanne, F. Laplanche, G. Parrour, R. Riskalla, P. Roy and G. Szklarz, Phys. Letters 63B (1976) 352.

[523] A.J. Pawlicki, D.S. Ayres, D. Cohen, R. Diebold, S.L. Kramer and A.B. Wicklund, Phys. Rev. Letters 37 (1976) 971.
[524] V.N. Bolotov, V.V. Isakov, D.B. Kakauridze, Yu.D. Prokoshkin, S.A. Sadovski and G.V. Khaustov, Serpukhov preprint IHEP 75-148 (1975).
[525] Chan H.-M. and Tsou S.-T., Rutherford Laboratory preprint RL-76-080 T.165 (1976).
[526] P.R. Stevens, G.F. Chew and C. Rosenzweig, California Institute of Technology preprint CALT-68-541 (1976).
[527] C. Schmid, D.M. Webber and C. Sorensen, Nucl. Phys. B111 (1976) 317.
[528] Chan H.-M., J. Kwiecinski and R.G. Roberts, Phys. Letters 60B (1976) 367.
[529] S. Yazaki, M. Fukugita, T. Inami and N. Sakai, University of Tokyo preprint UT-281 (1977).
[530] Chan H.-M., K. Konishi, J. Kwiecinski and R.G. Roberts, Phys. Letters 60B (1976) 469.
[531] Chan H.-M., K. Konishi, J. Kwiecinski and R.G. Roberts, Phys. Letters 63B (1976) 441.
[532] M. Fukugita, T. Inami, N. Sakai and S. Yazaki, University of Tokyo preprint UT-265 (1976); University of Tokyo, Komaba preprint UT-Komaba 76-9 (1976).
[533] J. Uschersohn, Nucl. Phys. B104 (1976) 137.
[534] Y. Eylon, Nucl. Phys. B118 (1977) 119.